1977

Investigation of metal hydrides using multiple wavelength neutron powder diffraction and the crystal structure determinations of the 2,4-dinitrophenylhydrazone derivative of 5-bromomethylidenecyclononanone and the 1-hydroxy-6-acetoxy-10[alpha]-bromo-bicyclo [4.3.1] deca-3-ene

Patrick William DeHaven
Iowa State University

INFORMATION TO USERS

This material was produced from a microfilm copy of the original document. While the most advanced technological means to photograph and reproduce this document have been used, the quality is heavily dependent upon the quality of the original submitted.

The following explanation of techniques is provided to help you understand markings or patterns which may appear on this reproduction.

1. The sign or "target" for pages apparently lacking from the document photographed is "Missing Page(s)". If it was possible to obtain the missing page(s) or section, they are spliced into the film along with adjacent pages. This may have necessitated cutting thru an image and duplicating adjacent pages to insure you complete continuity.

2. When an image on the film is obliterated with a large round black mark, it is an indication that the photographer suspected that the copy may have moved during exposure and thus cause a blurred image. You will find a good image of the page in the adjacent frame.

3. When a map, drawing or chart, etc., was part of the material being photographed the photographer followed a definite method in "sectioning" the material. It is customary to begin photoing at the upper left hand corner of a large sheet and to continue photoing from left to right in equal sections with a small overlap. If necessary, sectioning is continued again — beginning below the first row and continuing on until complete.

4. The majority of users indicate that the textual content is of greatest value, however, a somewhat higher quality reproduction could be made from "photographs" if essential to the understanding of the dissertation. Silver prints of "photographs" may be ordered at additional charge by writing the Order Department, giving the catalog number, title, author and specific pages you wish reproduced.

5. PLEASE NOTE: Some pages may have indistinct print. Filmed as received.

University Microfilms International
300 North Zeeb Road
Ann Arbor, Michigan 48106 USA
St. John's Road, Tyler's Green
High Wycombe, Bucks, England HP10 8HR

77-16,953

DeHAVEN, Patrick William, 1949-
INVESTIGATION OF METAL HYDRIDES USING MULTIPLE WAVELENGTH NEUTRON POWDER DIFFRACTION AND THE CRYSTAL STRUCTURE DETERMINATIONS OF THE 2,4-DINITROPHENYLHYDRAZONE DERIVATIVE OF 5-BROMOMETHYLIDENECYCLONONANONE AND THE 1-HYDROXY-6-ACETOXY-10α-BROMO-BICYCLO-[4.3.1]DECA-3-ENE.

Iowa State University, Ph.D., 1977
Chemistry, physical

Investigation of metal hydrides using multiple wavelength neutron powder diffraction and the crystal structure determinations of the 2,4-dinitrophenylhydrazone derivative of 5-bromomethylidenecyclononanone and the 1-hydroxy-6-acetoxy-10α-bromo-bicyclo[4.3.1]deca-3-ene

by

Patrick William DeHaven

A Dissertation Submitted to the
Graduate Faculty in Partial Fulfillment of
The Requirements for the Degree of
DOCTOR OF PHILOSOPHY

Department: Chemistry
Major: Physical Chemistry

Approved:

Signature was redacted for privacy.

In Charge of Major Work

Signature was redacted for privacy.

For the Major Department

Signature was redacted for privacy.

For the Graduate College

Iowa State University
Ames, Iowa

1977

TABLE OF CONTENTS

A NEW NEUTRON DIFFRACTION TECHNIQUE UTILIZING MULTIPLE WAVELENGTHS

Introduction

The problem of low neutron flux has been a major limitation in the study of both single crystals and powders by neutron diffraction. In general, for a conventional two-axis diffractometer the intensity of the neutron beam incident upon the sample is approximately three orders of magnitude less than the intensity of a typical X-ray beam used for diffraction studies. Consequently, a number of undesirable steps must be taken in order to offset the low incident beam intensity. These include enlarging the sample size (with a corresponding enlargement of the beam size), lowering the degree of collimation used (which leads to poorer resolution), and either increasing the counting time or running several scans in order to improve counting statistics.

One of the main reasons for the low neutron flux lies in the design of the experimental apparatus. Most neutron diffraction experiments are based on those originally developed for X-ray diffraction in that they utilize a monochromatic neutron beam. However, unlike X-rays which have an intense characteristic wavelength in their spectrum (the Kα peak), the neutron spectrum emerging from the

reactor is described by a Maxwellian curve

$$(1) \qquad \Phi_{incident}(\lambda) \;\alpha\; \frac{e^{-P1/\lambda^2}}{\lambda^5}$$

where Φ_{incid} is the neutron flux emerging from the reactor, P1 is related to the moderator temperature, and λ is the wavelength. This spectrum is illustrated diagramatically for a typical research reactor in Figure 1. As a result, any experiment which involves the use of a monochromatic neutron beam will utilize only a small fraction of the available neutrons.

In order to overcome this handicap, there have been several attempts to carry out diffraction experiments utilizing the entire neutron spectrum (the so-called "white" neutron beam). Lowde[1] proposed the use of the Laue method to obtain diffraction data from the "white" neutron beam. Hubbard, Quicksall and Jacobson[2] were able to develop a technique, based on Lowde's work, for refining single crystal structures using data obtained from a white radiation experiment. While this method allowed reduction in the sample size (and beam size) required, and significantly improved data collection rates, several problems resulted. The method required precise determination of the incident neutron spectrum, as well as the exact wavelength dependence of absorption, extinction, and thermal diffuse scattering.

Figure 1. Intensity versus wavelength distribution for the neutron beam emerging from a typical research reactor. The shaded area represents the wavelength band selected by a particular monochromator.

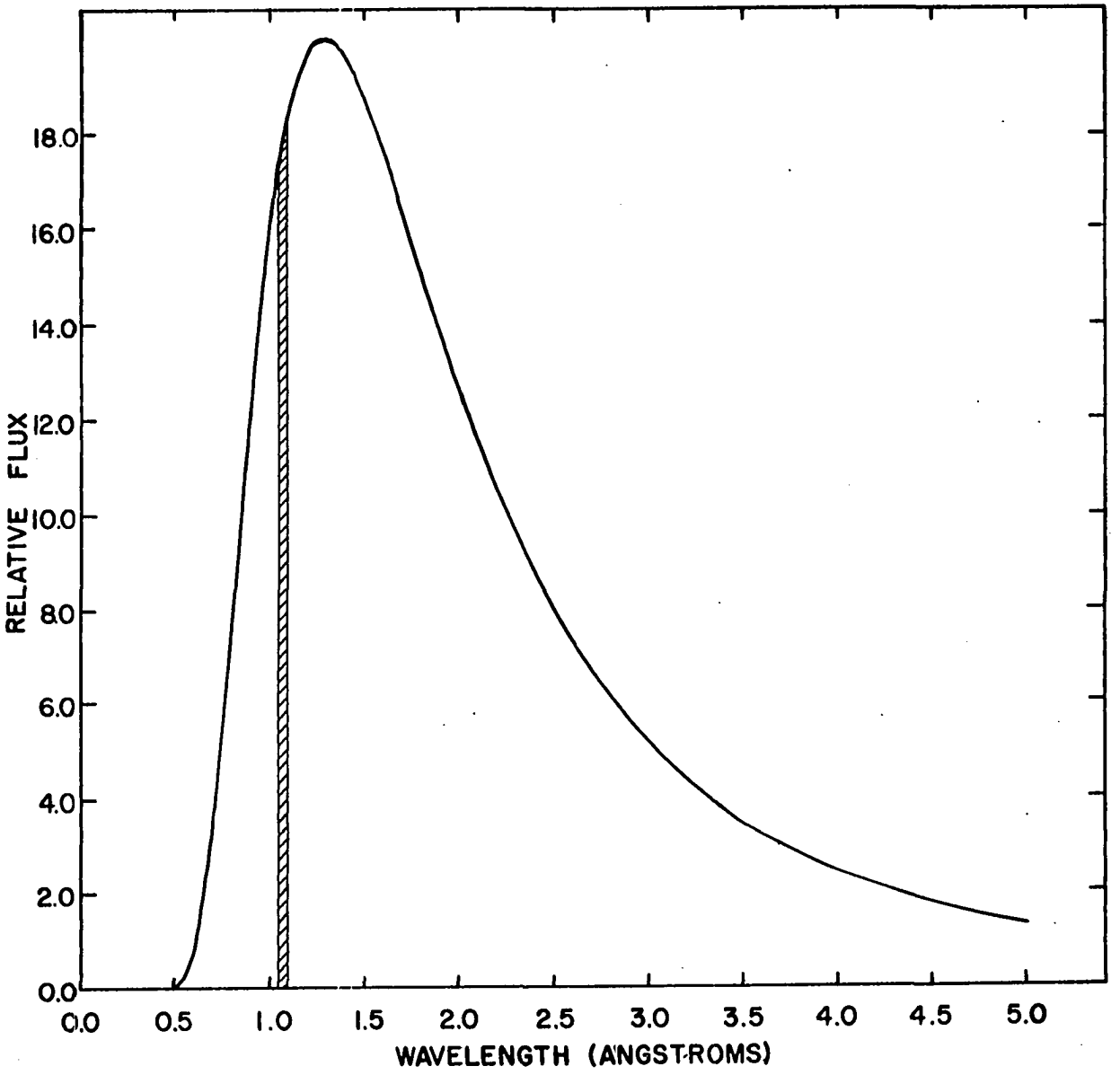
RELATIVE FLUX
18.0
16.0
14.0
12.0
10.0
8.0
6.0
4.0
2.0
0.0
0.0
0.5
1.0
1.5
2.0
2.5
3.0
3.5
4.0
4.5
5.0
WAVELENGTH (ANGSTROMS)

In addition, the use of the entire neutron spectrum as opposed to a single wavelength resulted in a sharp increase in the background due to incoherent scattering (it must be remembered that while elastic scattering occurs for only a few selected wavelengths, incoherent scattering will occur over the entire neutron spectrum). Time-of-flight diffractometry, as discussed by Turberfield[3], shows the most promise as a means of utilizing the entire neutron spectrum. However, in order to be efficient, time-of-flight techniques require the existence of pulsed neutron sources. And, as with the Laue method, there is a need to calibrate the incident beam spectrum and to apply wavelength dependent absorption and extinction corrections.

We present here a method which, while not utilizing the entire neutron spectrum, can significantly increase the incident neutron flux without extensive equipment modifications (as would be required for time-of-flight techniques), and without any increase in beam size or decrease of resolution. The method can be applied to both single crystal and powder studies; however the description given on the following pages will apply only to the case of neutron powder diffraction. The discussion will be restricted further to the case of elastic scattering.

The Multiple Wavelength Technique

Multiple Bragg scattering

The diffraction of waves (X-ray, neutron, electron) by crystalline solids is described mathematically by the Laue equation:

$$(2) \qquad \vec{h} = \frac{\vec{k} - \vec{k}_o}{\lambda}$$

Here $\vec{k}$ and $\vec{k}_o$ are unit vectors describing the direction of the incident and scattered waves, λ is the wavelength, and $\vec{h}$ is a vector, normal to the reflecting plane, whose magnitude is equal to 1/d, where d is the interplanar spacing. A vectorial representation of the Laue equation for the case of a monochromatic beam is shown in Figure 2a. The Laue equation can be expressed in scalar form

$$(2a) \qquad |\vec{h}| = \frac{|\vec{k} - \vec{k}_o|}{\lambda}$$

from which the familiar Bragg relation can be derived:

$$(3) \qquad \lambda = 2d\sin\theta$$

The multiple wavelength effect arises from the observation that for a given scattering angle θ, higher order reflections will diffract at successively lower wavelengths. This can be seen by inspection of the Laue equation. If we multiply both sides of equation (2a) by some integer n, we get the following result:

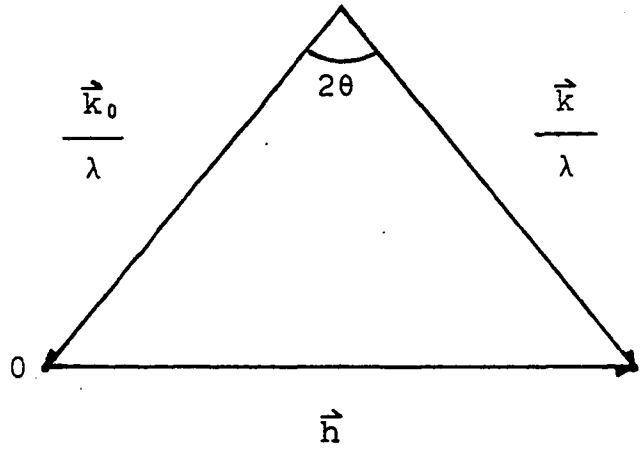

Figure 2a. Reciprocal space diagram illustrating Bragg reflection of 'white' beam. 0 is the origin of reciprocal space(from Turberfield[3]).

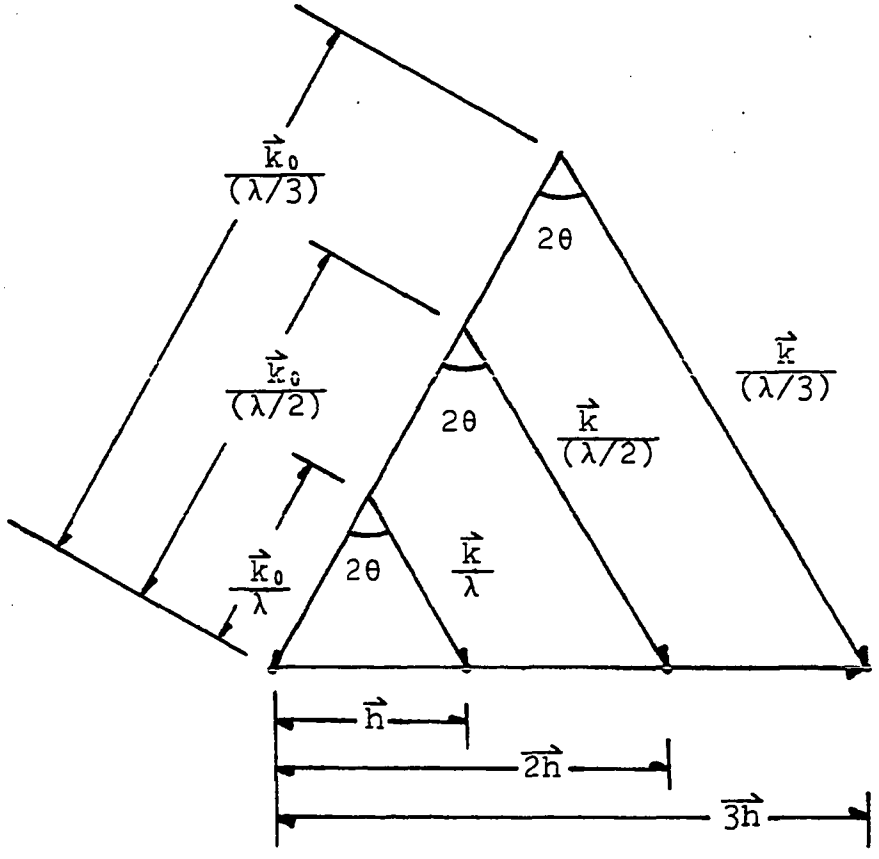

Figure 2b. Reciprocal space diagram illustrating Bragg reflection of 'white' beam by higher orders of fundamental reflection.

$$n|\vec{h}| = n \left| \frac{\vec{k} - \vec{k}_o}{\lambda} \right| = \frac{|\vec{k} - \vec{k}_o|}{(\lambda/n)}.$$

Thus if we have a set of reflecting planes with interplanar spacing $d \equiv \frac{1}{|\vec{h}|}$ which diffract a given wavelength λ at some angle θ, if there exists a set of planes with interplanar spacing d/n, then these planes will simultaneously diffract at θ with the characteristic wavelength λ/n. The effect is illustrated in Figure 2b. Expressing the reflecting planes in terms of Miller indices, the multiple wavelength effect can be described in the following general form:

> For a given set of planes (hkℓ) which diffract a given wavelength λ at some fixed angle $\theta_{hk\ell}$, a set of planes (nh,nk,nℓ) where n is an integer, will also diffract at $\theta_{hk\ell}$ with the characteristic wavelength λ/n. In general, any set of planes $\left(\frac{n}{m} h, \frac{n}{m} k, \frac{n}{m} \ell\right)$ such that n, m, and $\left(\frac{n}{m} h\right)$, $\left(\frac{n}{m} k\right)$, $\left(\frac{n}{m} \ell\right)$ are all integral values, will diffract with characteristic wavelength $\frac{m}{n} \lambda$.

In a conventional two-axis diffractometer the monochromating crystal (generally Pb, Cu, Be, or graphite) is aligned so as to reflect a narrow wavelength band from the neutron spectrum emerging from the reactor (Figure 1). The width of this band will be dependent on the mosaic spread of the crystal and the degree of collimation of the

incident beam; in general the wavelength spread will be approximately $2\delta\lambda$ where $\delta\lambda = 2\beta d\cos\theta$. Here β is the collimator angle, d the interplanar spacing, and θ the Bragg angle. As a result of the multiple wavelength effect, this diffracted beam will contain contributions from higher and lower order reflecting planes. For example, for a lead crystal aligned so that the (111) planes diffract a monochromatic beam at 1.5 Å, a simultaneous contribution will arise from diffraction by the (222) planes at 3/4 Å. Due to the nature of the incident neutron spectrum these contributions can be significant, and special steps must be taken in order to obtain a monochromatic beam with negligible contamination. These steps include:

(a) Alignment of the monochromator so as to intersect the spectrum at a wavelength lower than at maximum beam intensity. This results in a sharp decrease in intensity of the $\lambda/2$, $\lambda/3$, etc. contributions due to the rapid decrease in intensity at wavelengths below the peak of the neutron spectrum (Figure 1).

(b) Use of a plutonium filter. Plutonium has an absorption resonance at 0.533 Å. Therefore, by alignment of the monochromator so as to intersect the spectrum at 1.066 Å, and passing the diffracted beam through a plutonium foil of appropriate

thickness, a hundredfold reduction in the $\lambda/2$ component can be obtained at the expense of a twofold reduction in the intensity of the fundamental wavelength.

(c) Use of a monochromating crystal whose structure is such that scattering from the second order planes (2h, 2k, 2ℓ) is extinct or nearly so.

The major disadvantage of methods (a) and (b) is that both result in a decrease in the diffracted beam intensity. In the case of (b) this decrease is substantial. For method (c), most monochromating crystals in use today whose second order component is systematically extinct or nearly so (i.e. germanium) in general have a lower reflectivity (hence lower diffracted beam intensity) than the more commonly used monochromators.

Instead of treating the multiple wavelength (or more appropriately, multiple Bragg scattering) effect as a source of unwanted contamination, we felt it should be possible to utilize the effect to increase the intensity of the diffracted beam. By a suitable alignment of the monochromating crystal, a diffracted beam can be obtained which consists of two or more strong contributions from different wavelengths. The major problem arising from the use of such a treatment lies in the interpretation of the resulting

diffraction data. For the case of powders, the diffraction pattern resulting from the scattering of such a multiple wavelength beam will be a superposition of the separate patterns which would result from the use of each of the contributing wavelength beams alone. Consequently any attempt to obtain structural information by standard methods (i.e. by use of integrated intensities) would require deconvolution of the separate patterns, a difficult if not impossible task. However, as will be shown in the next section, structural information can be obtained directly by means of the profile refinement technique.

Data analysis

In order to obtain structural information from a powder pattern produced by a multiple wavelength neutron beam, a modification of the Rietveld profile analysis procedure[4,5] is used. The profile analysis method provides a means for refining structural parameters using neutron powder data for cases where it is impossible to obtain integrated intensities for the contributing reflections due to overlap by adjacent diffraction peaks. The method is based on the experimental observation that, given a particular set of planes k which diffract at a Bragg angle θ_k, the distribution of intensity about θ_k is essentially Gaussian in shape. We can therefore write the following expression for the

intensity at any point θ_i[†] in a scan through reflection k.

$$y_{i,k} = tF_k^2 j_k L_k \frac{2\sqrt{\ell n 2}}{H_k\sqrt{\pi}} \exp\left(-2Q\frac{\sin^2\theta_k}{\lambda^2}\right) \quad (5)$$
$$*\exp\left[-4\ell n 2\left(\frac{(2\theta_i - 2\theta_k)}{H_k}\right)^2\right]$$

where t is the stepwidth of the counter, F_k^2 is the nuclear structure factor, j_k is the multiplicity of the reflection, L_k is the Lorentz factor, $2\theta_k$ is the calculated position of the Bragg peak corrected for the zeropoint shift of the counter, $\exp\left(-2Q\frac{\sin^2\theta_k}{\lambda^2}\right)$ is a correction for overall thermal motion, and H_k is the full-width at half-height of the peak. For a powder scan, the intensity at each point along the scan will be the resultant of contributions from all reflections within range of that point (because of the rapid drop-off in intensity from peak maximum as a result of the nature of the Gaussian curve, the contribution for each reflection is arbitrarily cut off at $1.5*H_k$ on either side of $2\theta_k$). Consequently we can write an expression for the intensity at any point along a neutron powder scan.

[†]In a conventional two-axis diffractometer, the incident beam position is fixed with respect to the samples so that the angle measured by the detector is 2θ as opposed to θ.

$$y_i = \Sigma_k t F_k^2 j_k L_k \frac{2\sqrt{\ell n 2}}{H_k\sqrt{\pi}} * \exp\left(-2Q\frac{\sin^2\theta_k}{\lambda^2}\right) * \exp\left(-G\alpha_k^2\right)$$

(6)

$$*\exp\left[-4\ell n 2\left(\frac{(2\theta_i - 2\theta_k)}{H_k}\right)^2\right] * \left[1-P(2\theta_i - 2\theta_k)^2 \cdot \frac{S}{\tan\theta_k}\right].$$

The term $\exp(-G\alpha_k^2)$ is a correction for preferred orientation in the crystallites, while $\left[1-P(2\theta_i - 2\theta_k)^2 \frac{S}{\tan\theta_k}\right]$ is a correction for peak asymmetry at low 2θ values. These two terms will be explained in detail in a later section.

Equation (6) allows one to obtain a set of intensity values $y_i(\text{calc})$, given a particular model structure and appropriate experimental parameters. These calculated intensities can be used with the actual observed data points $y_i(\text{obs})$ from the powder pattern in a least-squares treatment similar to that used to refine structural parameters using integrated intensities. The quantity minimized is

$$(7) \quad M = \Sigma_i \omega_i \{y_i(\text{obs}) - \frac{1}{c} y_i(\text{calc})\}^2$$

where the sum is over all independent observations, c is a scale factor, and ω_i is the weight of each observation, which can be shown to be proportional to $1/\sigma_i^2 \approx 1/y_i(\text{obs})$ [6]. Refinement is carried out over both structural (positional coordinates, temperature factors, etc.) and experimental (half-width, zero-point, etc.) parameters. As with refine-

ment involving integrated intensities, a set of agreement factors have been developed in order to measure the goodness of fit between observed and calculated data. The first of these, $R_{profile}$, provides a comparison between the observed and calculated powder patterns as follows:

$$(8a) \quad R_{profile} = 100 * \frac{\sum_i |y_i(obs) - \frac{1}{c} y_i(calc)|}{\sum_i |y_i(obs)|} .$$

In order to provide a qualitative comparison with the results obtained by least-squares methods involving integrated intensities, the factor $R_{nuclear}$ has been developed. While experimental integrated intensities ($I_k(obs)$) cannot be obtained from most neutron powder patterns analyzed by the Rietveld method, a fair approximation to $I_k(obs)$ can be made,

$$I_k(obs) = \sum_j \chi_{j,k} F_k^2(calc) \frac{y_j(obs)}{y_j(calc)} .$$

Here the sum is over all data points which can theoretically contribute to the integrated intensity $I_k(obs)$ and

$$\chi_{j,k} = t_{jk} L_k \frac{2\sqrt{\ell n 2}}{H_k \sqrt{\pi}} * \exp\left(-4 \ell n 2 \left[\frac{(2\theta_i - 2\theta_k)}{H_k} \right]^2 \right)$$

$$* \exp\left(-G\alpha_k^2\right) * \exp\left(-2Q \frac{\sin^2\theta_k}{\lambda^2} \right)$$

$$* \left[1 - P(2\theta_i - 2\theta_k)^2 \cdot \frac{S}{\tan\theta_k} \right] .$$

With this definition of the experimental integrated intensity, a nuclear agreement factor $R_{nuclear}$ can be written,

$$(8b) \quad R_{nuclear} = 100 * \frac{\sum_k |I_k(obs) - \frac{1}{c} I_k(calc)|}{\sum_k I_k(obs)} .$$

Rietveld has also developed an idealized agreement factor which can be used as a measure of the appropriateness of a particular structural model. The expression is

$$(8c) \quad R_{expected} = 100 * \left(\frac{(N - P + C)}{\sum_i \omega_i (y_i(obs))^2} \right)^{\frac{1}{2}}$$

where N is the number of statistically independent observations, P the number of least-squares parameters, C the number of constraint functions, and N - P + C is the number of degrees of freedom.

We therefore set out to explore the feasibility of extending the profile refinement technique to allow the analysis of powder data obtained from a multiple wavelength neutron experiment. As mentioned previously, for the conventional case (monochromatic beam), the intensity y_i at each point along the powder scan can be considered to be the resultant of contributions from all reflections within range of that point (the range of each reflection being previously defined). For a multiple wavelength beam a given set of atomic planes will scatter each of the contributing wavelengths at a different 2θ angle. Consequently the intensity

y_i at each point will be the resultant of all reflections due to each wavelength which are within range of y_i. This summation can be stated mathematically by an expression similar to equation (5). However, before an accurate expression can be obtained, the wavelength dependence of the experimental and structural parameters must be derived.

Halfwidth Caglioti[7] has shown that for a standard two-axis diffractometer, the full-width at half-maximum for each reflection k can be expressed as a function of the degree of collimation, the scattering angle θ_k, and the mosaic spread of the monochromating crystal, β_1. The exact dependence is given by

$$(9) \qquad \text{fwhm} = \frac{N}{(\alpha_1^2 + \alpha_2^2 + 4\beta_1^2)^{\frac{1}{2}}}$$

where $$N = \Big[\alpha_1^2\alpha_2^2 + \alpha_1^2\alpha_3^2 + 4\beta_1^2(\alpha_2^2 + \alpha_3^2) - 4\sigma\alpha_2^2(\alpha_1^2 + 2\beta_1^2) + 4\sigma^2(\alpha_1^2\alpha_2^2 + \alpha_1^2\beta_1^2 + \alpha_2^2\beta_1^2)\Big]^{\frac{1}{2}},$$

α_i is the angular divergence of the ith collimator, and σ a parameter known as the dispersion parameter. The dispersion parameter is a measure of the relative dispersion undergone by the twice-reflected neutron beam for a given wavelength spread of the beam coming off the monochromator.

Mathematically,

$$\sigma \equiv \frac{(d\lambda/d\theta)_{monochromator}}{(d\lambda/d\theta)_{sample}} .$$

By differentiating Bragg's law this becomes

$$\sigma = \frac{\tan\theta_k}{\tan\theta_{monochromator}} .$$

The values of α_i, β_1, and $\theta_{monochromator}$ are fixed for a given experimental configuration, while σ is simply a function of the scattering angle θ_k. Consequently H_k is dependent only on θ_k, and has no explicit wavelength dependence. A good approximation to equation (9) is given by Rietveld;

$$(9a) \quad (fwhm)^2 = H_k^2 = U \tan^2\theta_k + V \tan\theta_k + W,$$

where θ_k is the scattering angle and U,V,W are wavelength independent parameters which can be determined experimentally.

Lorentz factor For normal beam equatorial geometry the Lorentz factor L_k for powders is given by

$$L_k = \frac{1}{\sin 2\theta_k \sin\theta_k}$$

As with the halfwidth, the Lorentz factor is a function only of the scattering angle θ_k.

Asymmetry correction As a result of the finite sample height and finite detector aperture, there will be a certain degree of vertical divergence in the diffracted

neutron beam[8]. The extent of this vertical divergence will depend on the wavelength spread of the monochromatic neutron beam, the sample height, the shape of the detector aperture, and the scattering angle θ_k (the vertical divergence is zero at $2\theta = 90^\circ$ but increases with decreasing angle, becoming significant below $2\theta = 30^\circ$). The effect of vertical divergence is to introduce a degree of asymmetry in the intensity distribution about the Bragg angle θ_k, with the peak maximum being shifted to lower angles. The intensity of a particular diffraction peak is not affected; however for a profile analysis type of refinement it must be accounted for. Rietveld uses the semi-empirical relation

$$(11) \quad \frac{1 - P(2\theta_i - 2\theta_k) \cdot S}{\tan\theta_k}$$

where P is a variable (the asymmetry parameter), and S = +1, 0, or -1, depending on whether $(2\theta_i - 2\theta_k)$ is positive, zero, or negative. The only wavelength dependence, if any, in this expression must reside in P. However Sayer and Cooper[9] have derived detailed analytical expressions for the shape of the predicted diffraction peaks on the basis of the resolution function of the instrument. The peak shift is expressed as a function of the horizontal and vertical divergence angles (wavelength independent), and the scattering angle θ_k. Consideration of the form of equation (11) along with the arguments of Sayer and Cooper leads us to

conclude that P can effectively be considered wavelength independent.

Preferred orientation correction Normally the orientation of the crystallites in a powder sample can be considered random. However for the case where the sample is contained in a cylindrical holder, plate-like crystallites often tend to align their normals along the vertical axis of the holder. If this effect is not too pronounced the intensity can be corrected for preferred orientation using the relation

$$(12) \quad I_{corr} = I_{obs} \exp(-G\alpha_k^2)$$

where G is a variable parameter which is a measure of the halfwidth of the assumed Gaussian distribution of the normals about the preferred orientation direction (wavelength independent), and α_k is the acute angle between the scattering vector $\vec{h}$ (defined previously) and the normal to the crystallites. As the scattering vector $\vec{h}$ is dependent only on the particular set of scattering planes which give rise to the diffraction peak k, the value of α_k as well as G is wavelength independent.

Structure factor The nuclear structure factor for a particular reflection k is given by

$$(13) \quad F_k^2 = A_k^2 + B_k^2$$

where

$$A_k = \sum_i n_i b_i \exp(-B_i \sin^2\theta_{k/\lambda 2}) \sum_r \cos 2\pi(hx_{i,r} + ky_{i,r} + \ell z_{i,r}),$$

and

$$B_k = \sum_i n_i b_i \exp(-B_i \sin^2\theta_{k/\lambda 2}) \sum_r \sin 2\pi(hx_{i,r} + ky_{i,r} + \ell z_{i,r}).$$

$\sum_i$ is the summation over all atoms in the asymmetric unit, $\sum_r$ the summation over the equivalent positions, b_i the nuclear scattering length, B_i the isotropic temperature factor for each atom, n_i the site occupation number, $x_{i,r}$, $y_{i,r}$, $z_{i,r}$ the fractional coordinates of the ith atom in the rth equivalent position, and h,k,ℓ the crystallographic indices pertaining to reflection k. With the exception of the temperature factor B_i, it should be obvious that all the above parameters are wavelength independent. The wavelength dependence (if any) of B_i will be considered in the next section. If one recalls that $\frac{\sin^2\theta_k}{\lambda^2} = \frac{1}{4d_k^2}$ (wavelength independent), we can conclude that the structure factor is wavelength independent, provided B_i has no explicit wavelength dependence.

Temperature factors Using the Debye model for crystal vibrations, Weinstock[10] has shown that, in the case of elastic scattering by a monatomic cubic crystal, the nuclear scattering length is reduced by a factor $\exp(-B\sin^2\theta/\lambda^2)$ where

$$(14) \quad B = \frac{6h^2}{m_a k\theta}\left(\frac{\phi(\chi)}{\chi} + 1/4\right).$$

Here h is Plank's constant, m_a is the nuclear mass, k is the Boltzmann constant, θ is the Debye temperature of the crystal, χ is given by θ/T, T being the absolute temperature of measurement, and $\phi(\chi)$ is a function of χ defined by

$$(14a) \quad \phi(\chi) = \frac{1}{\chi}\int_0^{\chi} \frac{\xi d\xi}{(\xi^2-1)}.$$

All the parameters in the above expression are wavelength independent, so that B can be considered to be wavelength independent. However, Weinstock's treatment is applicable only to a limited number of systems. The thermal parameters for the general case are obtained in the following manner. Using orthogonal axes and assuming that the atoms move isotropically, it can be shown[11] that the result of thermal motion is a reduction in the nuclear scattering length by the factor

$$(15) \quad \exp\left(-2\pi^2\left[h^2(\overline{\Delta x})^2 + k^2(\overline{\Delta y})^2 + \ell^2(\overline{\Delta z})^2\right]\right)$$

where $(\overline{\Delta x})^2$, $(\overline{\Delta y})^2$, and $(\overline{\Delta z})^2$ are the mean square displacements along the orthogonal x, y, and z axes. For anisotropic motion this factor becomes

$$(15a) \quad \exp\left(-\left[\beta_{11}h^2 + \beta_{22}k^2 + \beta_{33}\ell^2 + \beta_{12}hk + \beta_{13}h\ell + \beta_{23}k\ell\right]\right)$$

where β_{ij} are constants to be determined empirically.

The isotropic temperature factors B_i and Q may be obtained by defining the mean square amplitude of vibration $\mu^2 = a^2(\overline{\Delta x})^2 = b^2(\overline{\Delta y})^2 = c^2(\overline{\Delta z})^2$. Remembering that $d = (h^2/a^2 + k^2/b^2 + \ell^2/c^2)^{\frac{1}{2}} = \lambda/2\sin\theta$ we can rewrite equation (15) in the following form

(15b) $\exp(-B\sin^2\theta/\lambda^2)$

where $B = 8\pi^2\mu^2$. As expected, this is the same form as derived by Weinstock for the monatomic cubic crystal. Since the mean square displacements $(\overline{\Delta x})^2$, $(\overline{\Delta y})^2$, and $(\overline{\Delta z})^2$ are not dependent upon the wavelength of the neutron beam for the case of elastic scattering, the temperature factor can be considered wavelength independent for the general case.

Several corrections are considered insignificant and are not included in the profile refinement algorithm. In the case of absorption, there is, for nearly all elements, a wavelength dependence in which the absorption correction μ_{obs} varies linearly with the wavelength. However, usually the absorption of neutrons by the sample is negligibly small. Thermal diffuse scattering (TDS) can sometimes lead to appreciable errors. Accurate corrections for TDS are highly complex and can be applied only to high symmetry systems. It has been shown[12] that the ratio of the true integrated intensity to that measured assuming a linear background under the Bragg reflection is of the form exp (-2W) where

$$W = \text{constant} * \frac{\sin^2\theta}{\lambda^2} .$$

Thus good agreement between observed and calculated intensities can be obtained by introducing an artificial change in the Debye-Waller factor[13]. Finally, for the case of powders, extinction effects are negligible, so no correction for extinction need be made.

Having determined the wavelength dependence of the experimental and structural parameters, one can write the following expression for the intensity at any point along a multiple wavelength scan:

$$y_i = \sum_{\ell} c_\ell \sum_k t F_k^2 j_k L_{k,\ell} \frac{2\sqrt{\ell n 2}}{\sqrt{\pi}\, H_{k,\ell}} * \exp\left(-G\alpha_k^2\right)$$

$$* \exp\left(-4\ell n 2 \left[\frac{(2\theta_i - 2\theta_{k,\ell})}{H_{k,\ell}}\right]^2\right) * \exp\left(-2Q\frac{\sin^2\theta_{k,\ell}}{\lambda_\ell^2}\right) \tag{16}$$

$$* \left[1 - P(2\theta_i - 2\theta_{k,\ell})^2 \cdot \frac{S}{\tan\theta_{k,\ell}}\right] .$$

Here $\sum_{\ell}$ is the summation over the contributing wavelengths, $\sum_k$ the summation over those reflections k scattering at wavelength ℓ which contribute to y_i, and c_ℓ the scale factor for wavelength ℓ. Each wavelength requires a different scale factor, as the relative fluxes of the different wavelength contributions will vary. All other parameters have been described previously (equation (6)). A double subscript is

used for both the Bragg angle and those parameters which are explicitly dependent on the Bragg angle. This is to indicate that the scattering angle is determined by both the particular set of reflecting planes, k, and the wavelength ℓ, as can be seen by inspection of equation (3):

$$\theta_{k,\ell} = \sin^{-1}\left(\frac{\lambda_\ell}{2d_k}\right).$$

Equation (16) can be simplified by making use of the observation that the ratios of the relative beam fluxes for the different wavelength contributions will be constant for a given experimental configuration. Consequently the ratio of the scale factors will be constant. We can therefore designate r_ℓ such that

$$r_1 = \frac{c_1}{c_1} = 1, \quad r_2 = \frac{c_2}{c_1}, \quad r_3 = \frac{c_3}{c_1}, \text{ etc.}$$

Equation (16) can then be rewritten as

$$y_i = \sum_\ell r_\ell \sum_k t F_k^2 j_k L_{k,\ell} \frac{2\sqrt{\ell n 2}}{H_{k,\ell}\sqrt{\pi}}$$

$$* \left[1 - P(2\theta_i - 2\theta_{k,\ell})^2 \cdot \frac{S}{\tan\theta_{k,\ell}}\right] \tag{16a}$$

$$* \exp\left(-4\ell n 2\left[\frac{(2\theta_i - 2\theta_{k,\ell})}{H_{k,\ell}}\right]^2\right) * \exp\left(-2Q\frac{\sin^2\theta_{k,\ell}}{\lambda_\ell^2}\right)$$

$$* \exp\left(-G\alpha_k^2\right)$$

with the minimization function becoming

$$(17) \quad M = \sum_i \omega_i \{ y_i(obs) - c_1 y_i(calc) \}^2$$

The form of equation (17) is essentially identical to the single wavelength case (equation (7)).

The agreement factors $R_{profile}$ and $R_{expected}$ are identical to those of the single wavelength case (equations (8a) and (8c)). The expression for $R_{nuclear}$ takes on a somewhat different form. We define $I_k^{obs}(\lambda_\ell)$ such that

$$I_k^{obs}(\lambda_\ell) = \sum_i \chi_{j,k}(\lambda_\ell) F_k^2(calc) y_j(obs)/y_j(calc)$$

where $\chi_{j,k}(\lambda_\ell) = t_{j_k} L_{k,\ell} \dfrac{2\sqrt{\ell n 2}}{H_{k,\ell}\sqrt{\pi}}$

$$(18) \quad * \exp\left(-4\ell n 2 \left[\frac{(2\theta_i - 2\theta_{k,\ell})}{H_{k,\ell}} \right]^2 \right)$$

$$* \left[1 - P(2\theta_i - 2\theta_{k,\ell})^2 \cdot \frac{S}{\tan\theta_{k,\ell}} \right] * \exp\left(-2Q \frac{\sin^2\theta_{k,\ell}}{\lambda_\ell^2} \right)$$

$$* \exp\left(-G\alpha_k^2 \right)$$

and as with the single wavelength case, the summation is over all data points which can theoretically contribute to the integrated intensity. The expression for $R_{nuclear}$ then becomes

$$(18a)\quad R_{nuclear} = \frac{\sum_{\ell k} |I_k^{obs}(\lambda_\ell) - c_\ell I_k^{calc}(\lambda_\ell)|}{\sum_{\ell k} I_k^{obs}(\lambda_\ell)}.$$

Here $\sum_{\ell}$ is the summation over the various wavelength contributions, and $\sum_{k}$ is the summation over those reflections scattering at wavelength ℓ which contribute to the resulting powder pattern.

Experimental

To test the validity of the multiple wavelength technique, a series of modifications were carried out on a conventional two-axis diffractometer located at the 5MW Ames Laboratory Research Reactor. The initial design and installation of the experimental apparatus has been detailed in a previous report[14]. For the multiple wavelength study, an oriented graphite crystal was chosen for the monochromator. Oriented graphite, also known as pyrolytic graphite, was chosen because of its high reflectivity (it has been shown[15] that the reflectivity of pyrolytic graphite is superior to all other commonly used neutron monochromators). High reflectivity is essential not only in order to maximize the intensity of the scattered neutron beam, but also to allow the use of thin crystals, with subsequent reduction in background due to incoherent scattering by the monochromator. A UCAR pyrolytic graphite monochromator, grade ZYD, fwhm(002)

$1.0^{\circ} \pm 0.2^{\circ}$, with dimensions 2" by 3½" by 1/16", was obtained from the Union Carbide Corporation. The flight path was modified so that the angle between the incident and diffracted beam would be 34°. As the monochromator table was located inside the reactor face, a somewhat extensive modification of the original experimental configuration between the monochromator and diffractometer was required. The current configuration is shown in Figure 3. The flight path from the monochromator to the diffractometer table is a concrete-lined steel tube, 1" by 1" square. As the apparatus was originally designed for single crystal studies, there are presently no means for introducing extensive collimation into this flight tube (work is underway to rectify this problem). Some collimation is provided by a circular cadmium aperture approximately 1.4 cm in diameter at the reactor face, as well as a cadmium slit 0.8 cm wide in front of the BF_3 detector. Alignment of the monochromator and diffractometer followed the methods described in the previous report. The monochromating crystal was aligned such that the (004) planes intersect the white neutron beam at 1 Å. In this orientation the (002) planes give a strong contribution at 2 Å. Analysis of data from a standard NaCl single crystal showed the 2 Å contribution to be approximately seven times as intense as the 1 Å beam. The only other significant contribution occurs from scattering by the (006) planes, resulting in a contribution at 2/3 Å whose intensity is approximately 3% that of

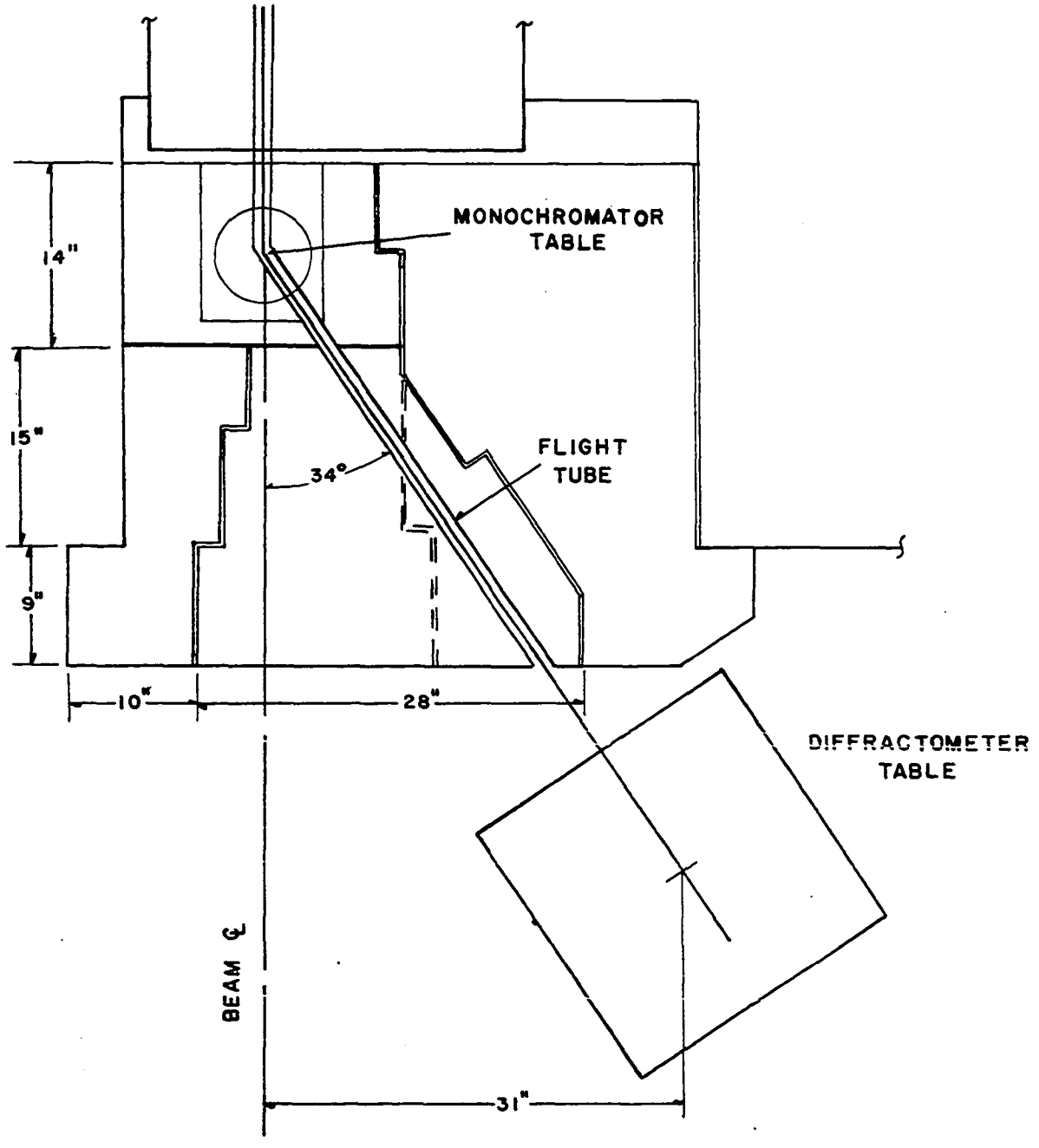

Figure 3. Schematic illustration of the current experimental configuration of the multiple wavelength neutron diffractometer.

the 1 Å beam. A very small contribution from scattering at ½ Å by the (008) planes was detected; however the intensity is so weak that it is practically indistinguishable from background. We shall henceforth not consider the ½ Å contribution in our discussion.

In order to carry out the data analysis, a copy of the Rietveld profile refinement program, modified by Hewat[6] to allow the refinement of anisotropic thermal vibrations, was obtained from Dr. John C. Taylor, Chemical Technology Division, Australian Atomic Energy Commission. The program was modified to allow refinement of multiple wavelength data, based on equations (16a) and (17). There are two parts to the program, a preliminary data preparation routine and the actual profile refinement algorithm. The data preparation routine (MPREP) takes the raw data from a neutron powder scan, corrects for background by means of linear interpolation, determines which reflections will contribute to the intensity at each point along the scan, and creates a dataset containing this information, which can then be input into the profile refinement program (MPROR). MPROR carries out the actual least-squares refinement. Input consists of intensity data (from MPREP) and the initial values of the experimental and structural parameters. Output consisting of the new values of the least-squares parameters, their shifts, and their standard deviation, as well as the agreement factors, is

given after each cycle. A listing of the observed and calculated intensities, y_i(obs) and y_i(calc), can be obtained after the last cycle. In addition, MPROR has been further modified to create a plot of the observed and calculated powder patterns, using the automatic plotting routine SIMPLOTTER[16].

Results: nickel

Nickel was chosen to initially test the validity of the multiple wavelength profile refinement technique as it has a small number of reflections which contribute to the scan. A sample of nickel powder, reagent grade, was placed in a cylindrical vanadium holder, 4.5 cm high and 1 cm in diameter, and covered with a tantalum cap. A series of four scans were run from $2\theta = 24^\circ$ to $2\theta = 110^\circ$ in increments of 0.1° 2θ. The data were averaged, and a plot of the resulting averaged scan is shown in Figure 4. The scan is comprised of 860 data points containing 12 independent reflections. The qualitative difference between this multiple wavelength scan and a scan involving a monochromatic neutron beam can be seen by comparing these results with a nickel scan taken by Atoji[17] on a conventional neutron diffractometer located at Argonne National Laboratory (Figure 5).

The raw data were input into MPREP, and a suitable data-set created for input into MPROR. As nickel metal has a face-centered cubic structure with the nickel atoms at

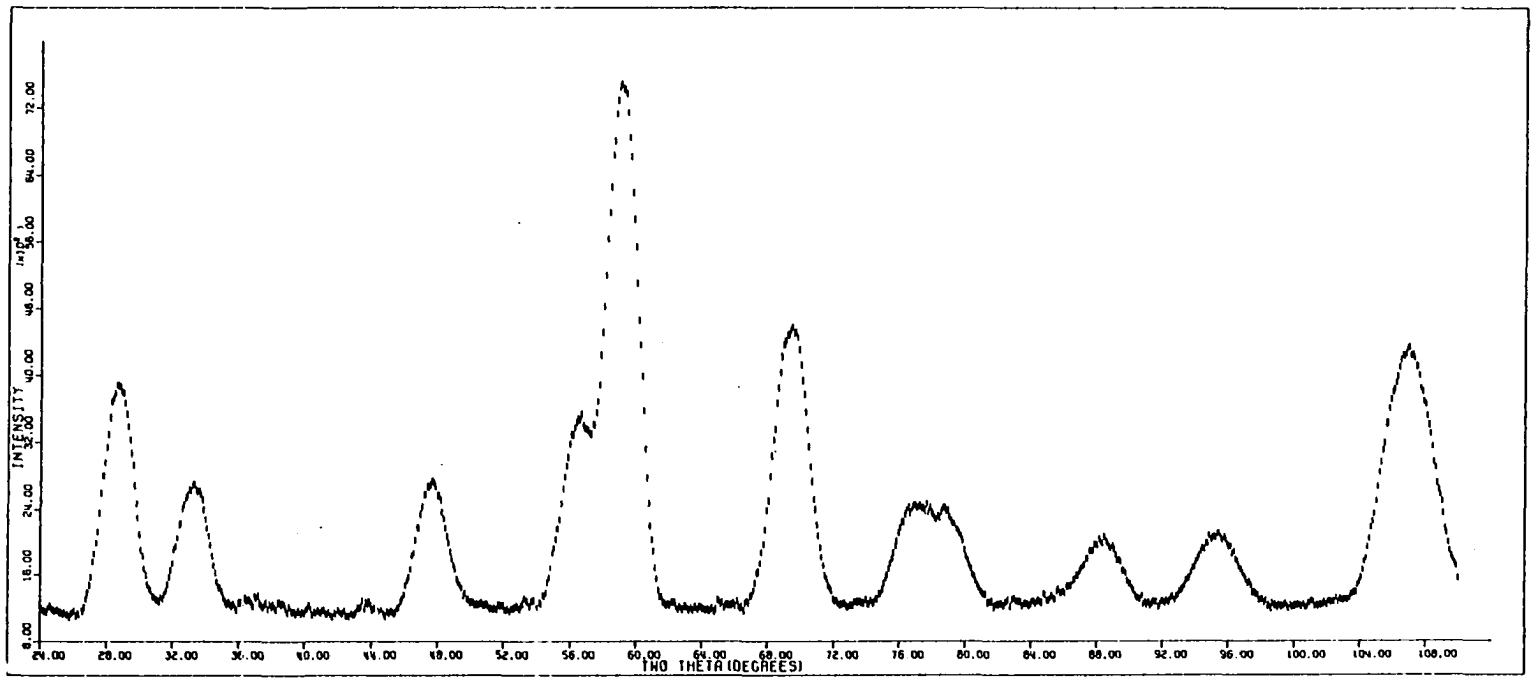

Figure 4. Neutron diffraction pattern of nickel powder obtained from the multiple wavelength neutron diffractometer at ALRR.

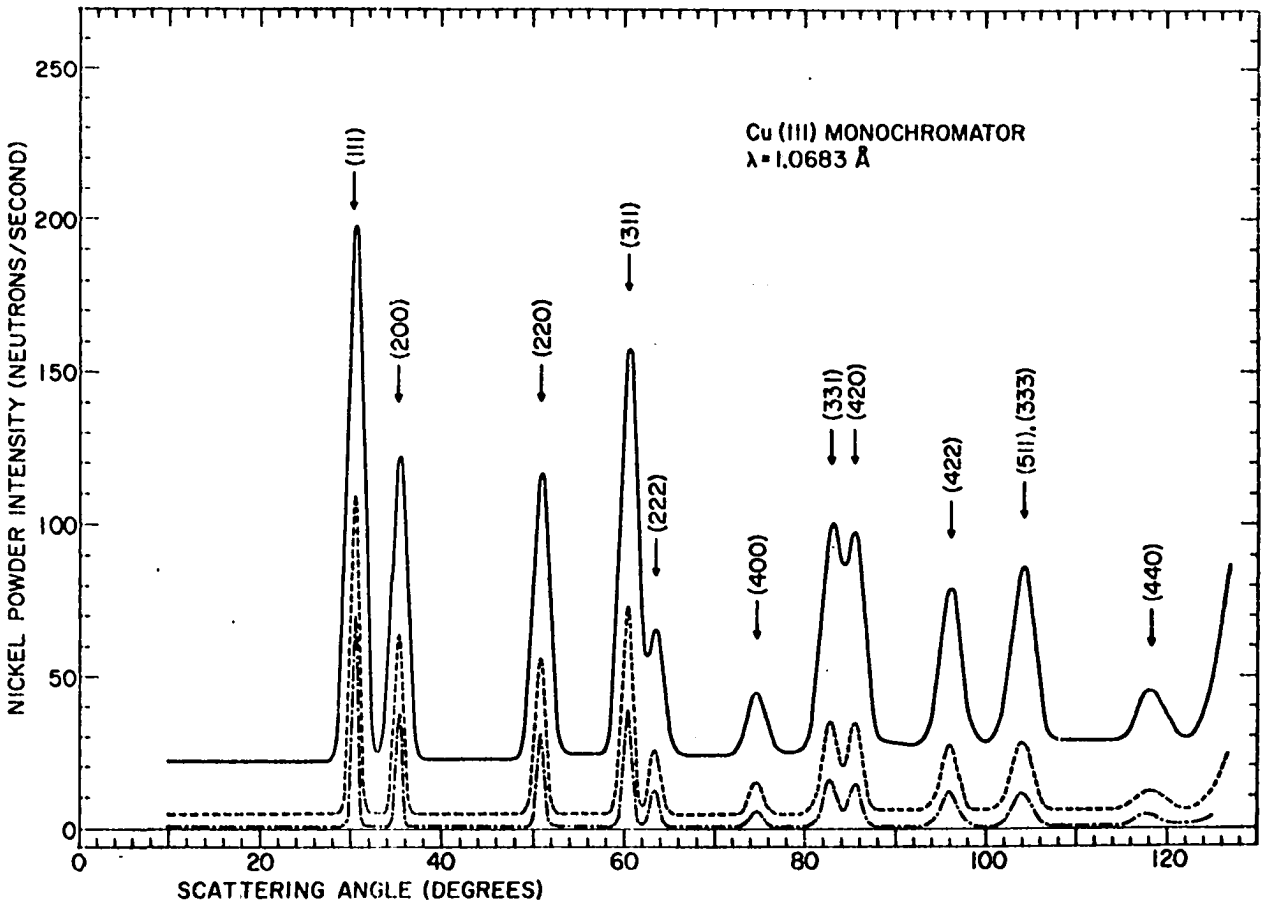

Figure 5. Neutron diffraction pattern of nickel powder obtained from a conventional two-axis diffractometer located at the Argonne National Laboratory. The solid, dotted, and broken curves were obtained with the counter collimations, no Soller, and 6-in. and 12-in. Soller collimators, respectively(from Atoji[17]).

(0,0,0), (½,½,0), (½,0,½), (0,½,½), the only structural parameters that can be varied are the cell length a_o and the isotropic temperature factor B_{ni}. Initial values for these parameters were obtained from the International Tables for X-ray Crystallography[18,19]. The nuclear scattering factor for nickel was obtained from Bacon[20]. The initial experimental parameters were obtained as follows:

Scale Factor: An approximate value for the scale factor was obtained by use of the program YCALC. YCALC was written to allow calculation, on the basis of equation (16), of the neutron powder pattern resulting from a given model system. For the case of nickel, the structural and experimental parameters were input and the scale factor varied until the peak intensity of the calculated pattern roughly matched that of the observed pattern.

Halfwidth parameters: A set of full-width at half-maximum (fwhm) versus two theta values were obtained from the resolvable peaks in the powder pattern; U,V,W values were than obtained by a least-squares fit to equation (9a) using the above data. A plot of the halfwidth curve is shown in Figure 6.

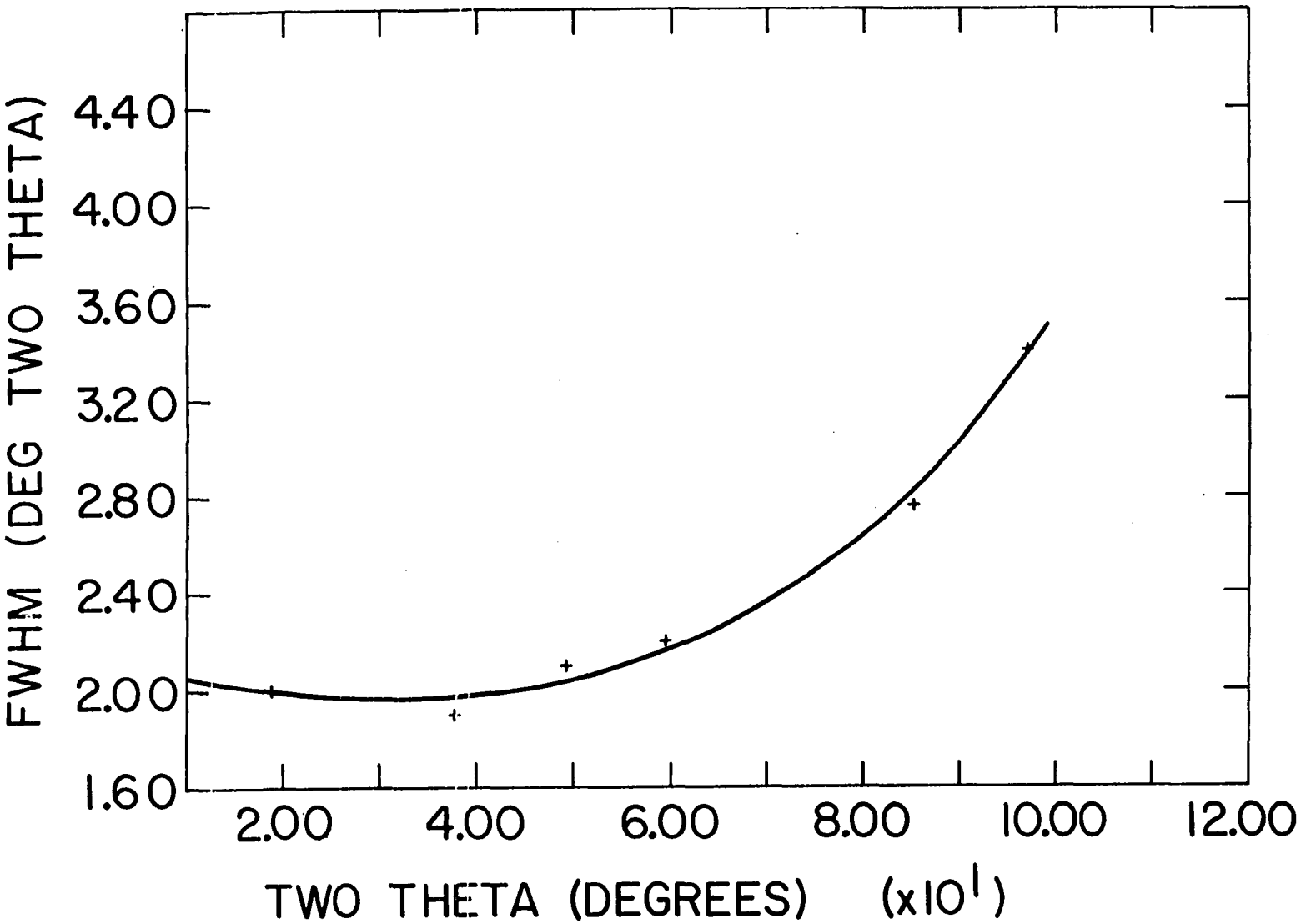

Figure 6. Variation of full-width at half-maximum with scattering angle for nickel.

\+ measured values —— calculated curve

Counter zeropoint: An approximate value for the zeropoint was obtained by running scans through the low angle region on both the positive and negative sides of the diffractometer. The peak positions on each side were then compared in order to determine the zeropoint.

Asymmetry parameter: Arbitrarily set to zero.

Preferred orientation correction: It was not necessary to correct for preferred orientation in the case of nickel.

The above data were input into MPROR and a total of six cycles run. Only the 1 Å and 2 Å contributions were included in the refinement. The parameters varied were the halfwidth parameters U,V, and W, the counter zeropoint, the asymmetry parameter P, the cell length a_o, and the isotropic temperature factor for nickel B_{ni}. The results of the refinement are shown in Table 1. Figure 7 gives a plot of the observed and calculated powder patterns. Both the values obtained for the cell length and the isotropic temperature factor are in excellent agreement with those calculated from single crystal X-ray intensity measurements (a_o = 3.524, B_{ni} = 0.42). The agreement factors, especially $R_{nuclear}$, are either superior to or comparable with values obtained from conventional (monochromatic beam) patterns. Though the value of $R_{profile}$

Table 1. Profile refinement results for nickel

Space Group: Fm3m

Ni at (0,0,0), (½,½,0), (½,0,½), (0,½,½)

a	=	3.524(1) Å
B_{Ni}	=	0.44(1)
$R_{nuclear}$	=	3.7%
$R_{profile}$	=	6.1%
$R_{expected}$	=	4.2%

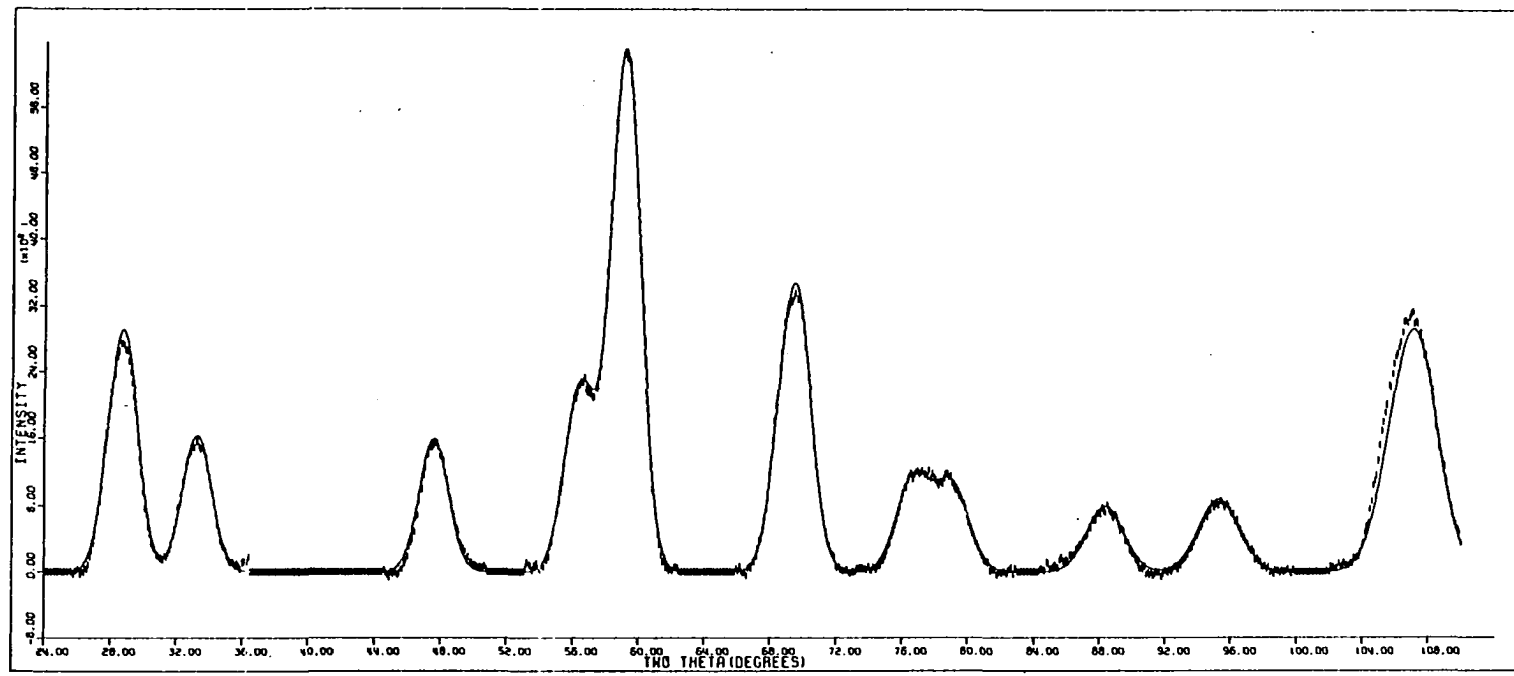

Figure 7. Comparison of observed and calculated neutron powder patterns for nickel. The broken line represents the observed pattern, while the solid line represents the calculated profile.

may be considered a bit high, inspection of Figure 7 shows an almost perfect fit between the observed and calculated patterns, except at very high angles ($2\theta > 100^{o}$). The poor fit in this region is the result of instrumental difficulties. Due to the weight of the BF_3 counter and its associated shielding, the detector has a tendency to drop below the true horizontal plane at very high scattering angles. This results in a distortion of the resulting diffraction peaks in this region. If, in the case of nickel, we carry out the refinement neglecting all data above 2θ equal to 100^{o}, we find a marked improvement in the agreement factors, with $R_{nuclear} = 2.2\%$ and $R_{profile} = 5.0\%$.

It has been mentioned previously that the 2/3 Å wavelength contribution to the incident beam was ignored in the refinement. Any attempt to incorporate the 2/3 Å contribution into the refinement must deal with the fact that the intensity of the 2/3 Å beam is only several per cent that of the 1 Å beam. As a result the contribution due to the 2/3 Å beam will be noticeable above background only for the most intense peaks. Direct inclusion of the 2/3 Å contribution into the profile refinement algorithm would mean not only extensive modification of the program, but also the addition of a degree of arbitrariness (choice of contributing peaks) into the refinement. Therefore the following algorithm is used to deal with the 2/3 Å contribution:

(a) Data is refined using only the 1 Å and 2 Å contributions.

(b) Using the structural and experimental parameters obtained in (a), the program YCALC is used to calculate the 2/3 Å contribution to the raw data.

(c) The 2/3 Å contribution obtained in (b) is subtracted from the raw data.

(d) The corrected data is rerun through the profile refinement routine.

This algorithm was tested with the nickel data using a variety of scale factor ratios. Best results were obtained using a value of .01 for the ratio c(2/3 Å)/c(1 Å). Three refinement cycles were run on the corrected data. The resulting agreement factors were $R_{nuclear}$ = 3.4% and $R_{profile}$ = 5.8% for a complete scan, and $R_{nuclear}$ = 2.0%, $R_{profile}$ = 4.8% for the short scan (high angle data deleted). Comparison with refinement results using the uncorrected data shows that while there is a slight improvement in the agreement factors, the difference is marginal. Consequently for most structures it is not necessary to correct the data for the 2/3 Å contribution. However there are some cases where the 2/3 Å contribution will be an important consideration. The most obvious of these is any compound whose structure is such as to give rise to weak superstructure reflections

in the powder pattern. The correction for the 2/3 Å contribution must be made here so as not to confuse the 2/3 Å peaks with possible superstructure peaks.

A NEUTRON POWDER STUDY OF NIOBIUM HYDRIDE, $NbH_{.73}$, UTILIZING THE MULTIPLE WAVELENGTH EFFECT

Introduction

In order to determine the effectiveness of the multiple wavelength technique on a structure of moderate complexity, a neutron powder diffraction study was carried out on the β-hydride of niobium. Attention has recently been focused on the niobium-hydrogen system, as niobium, because of its resistance to hydrogen embrittlement, is under consideration as a first wall material in a controlled thermonuclear reactor[21]. The niobium-hydrogen system has been fairly well characterized; Siegel and Libowitz provide a thorough review of the work done prior to 1968[22]. The phase diagram of the niobium-hydrogen system (Figure 8) consists of two major phases, the α and β phases, and a number of minor phases. Their structures are described below:

α-phase The α-phase consists of a solid solution of hydrogen in the body-centered cubic metal structure. X-ray powder studies[23,24] indicate that an isotropic expansion of the metal lattice occurs upon addition of hydrogen, the expansion being linearly related to the hydrogen concentration. While no neutron diffraction study has been carried out on the α-phase, deuteron channeling experiments[25]

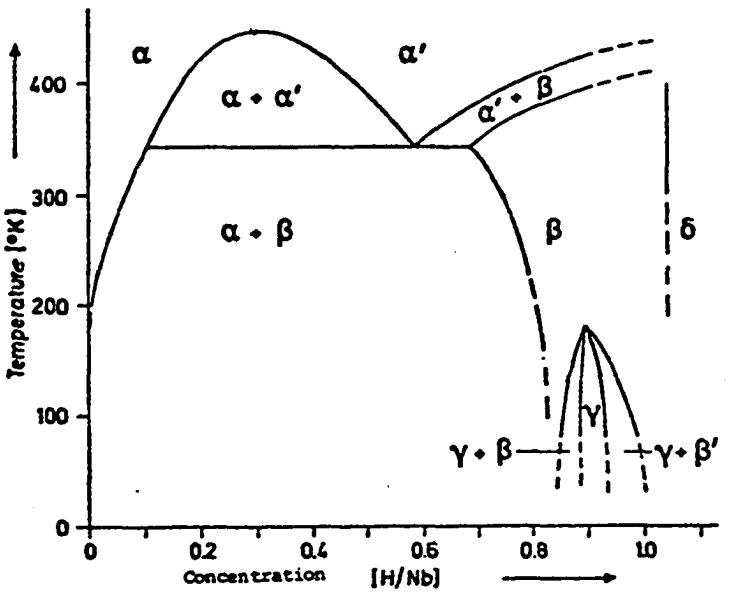

Figure 8. Phase diagram of the niobium-hydrogen system (from Pick[23]).

indicate that the hydrogen atoms are statistically distributed among the tetrahedral sites in the niobium lattice.

β or hydride phase The β-phase is characterized by a distortion of the niobium metal lattice. A large number of X-ray powder diffraction studies have been carried out on this phase; the best agreement between observed and calculated patterns has been obtained[26,27,28] by indexing the pattern on the basis of a face-centered orthorhombic cell (Figure 9). As with the α-phase, the hydrogen atoms occupy the tetrahedral interstices in the lattice, but in an ordered fashion, so that only half the available tetrahedral sites are occupied. This unique structural feature has been well characterized by neutron diffraction[23,29] and electron microscopy[30]. At elevated temperatures the metal lattice reverts to its original body-centered cubic cell (α'-phase). High-temperature neutron powder diffraction studies[29] indicate that the ordering of the hydrogen in the tetrahedral sites breaks down in this phase, with the hydrogen resuming a statistical distribution over all the tetrahedral sites in the lattice.

Figure 9. A f.c.o. cell(heavy lines) derived from a b.c.c. cell showing the f.c.o. unit vectors $\bar{A}$, $\bar{B}$, and $\bar{C}$(from Rashid and Scott[28]).

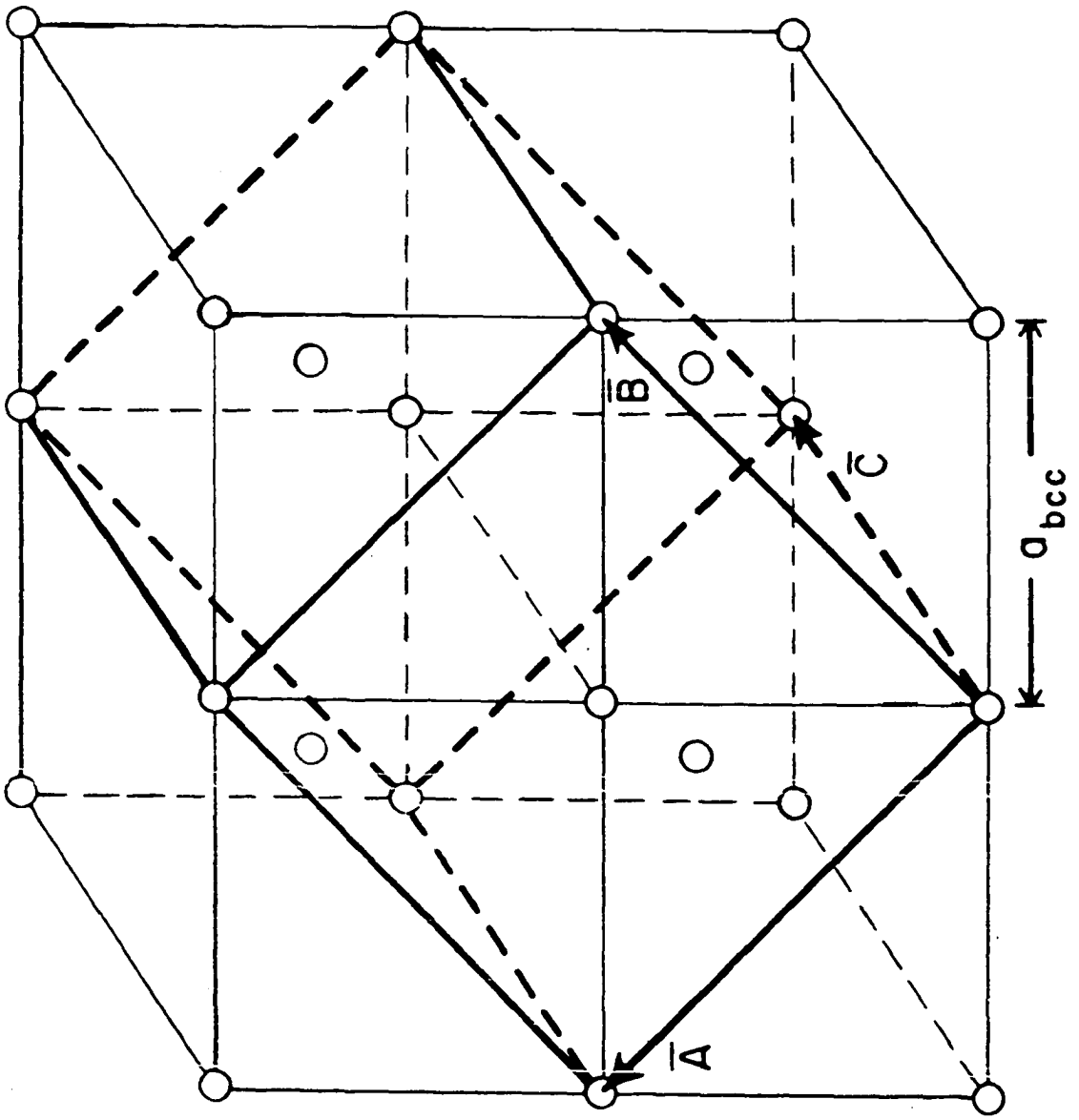
B
C
A
a_{bcc}

γ, β', and δ phases The structures of these phases have not been well characterized, and will not be considered further.

Several factors influenced the choice of niobium hydride as a test case for the modified profile refinement algorithm. The structure of the β-phase is relatively complex, with 78 independent reflections in the range 16° - 102° 2θ (for λ~1 Å). However the distortion from cubic symmetry is slight, resulting in extensive peak overlap. Previous investigators[23,29] were unable to resolve this overlap. They attempted to circumvent the problem by obtaining a set of integrated intensities I_{obs} (each I_{obs} containing contributions from one or more independent reflections) for those peaks in the pattern which could be resolved. These values were then compared to a set of I_{theor} values calculated from the appropriate structural model. The above treatment suffers from two major drawbacks. Because of increasing complexity in the neutron powder pattern with increasing scattering angle, the angular range of data that can be analyzed by this method is limited ($2\theta < 60^{\circ}$ for the case of niobium hydride). A more serious problem results from the limited amount of intensity data available (each of the two previous studies were based on only 8 values of I_{obs}). A least-squares type of refinement is impossible with so few points; consequently the structural parameters (lattice constants,

temperature factors, etc.) must remain fixed in any comparison of I_{obs} and I_{theor}; only the scale factor can be allowed to vary. As a result accurate values of the structural parameters must be obtained, either by alternate experimental techniques, such as X-ray diffraction, or from theoretical considerations. As the profile refinement technique suffers from neither of these limitations, one should be able not only to utilize a greater range in the scattering angle, but also obtain accurate structural information on niobium hydride directly from the neutron powder pattern.

Experimental

A sample of niobium hydride, composition $NbH_{.731}$, was kindly supplied by Dr. David T. Peterson. This composition was chosen because it lies near a phase boundary (see Figure 8). The two previous investigations[23,29], on the other hand, used samples with a composition close to NbH (H/Nb ratio > 0.9). Somenkov *et al.*[31], have carried out a neutron powder diffraction study on a niobium deuteride of similar composition at various temperatures (including room temperature); however the only result reported from the room temperature study was the appearance of the superstructure reflections found in the NbH_{χ} ($\chi > 0.9$) patterns. It was felt that a more extensive diffraction study in this concentration region would be useful in the characterization of the properties of the β-phase hydrides.

The sample was sealed in a thin-wall (~5 mil) cylindrical sample holder, 1 cm in diameter and 4 cm in height. A series of five scans were run at room temperature on the sample from 16° to 102° 2θ in increments of 0.1° 2θ. The resulting data were averaged; a correction for scattering by the aluminum sample holder was made by running a scan of the empty holder and subtracting the resulting intensity pattern from the original intensity data. The corrected powder scan is shown in Figure 10. A further correction for additional background effects, such as hydrogen incoherent scattering, was made by use of the profile preparation routine MPREP (see page 29). The superstructure reflections appear as weak shoulders at approximately 21° and 32° 2θ. Their identification is hampered by poor resolution in the pattern. An additional series of scans were run in the low angle region of the diffraction pattern to try and improve the resolution. The result, shown in Figure 11, clearly shows the existence of the superstructure reflections.

Choice and Refinement of the Model System

The structural model used for refinement was the one initially proposed by Somenkov *et al.*[29];

P_{nnn}

Nb at 4f (0,0,0) (0,½,½) (½,0,½) (½,½,0)

H at 2a (¼,¼,¼) (3/4,3/4,3/4)

2b (3/4,¼,¼) (¼,3/4,3/4) .

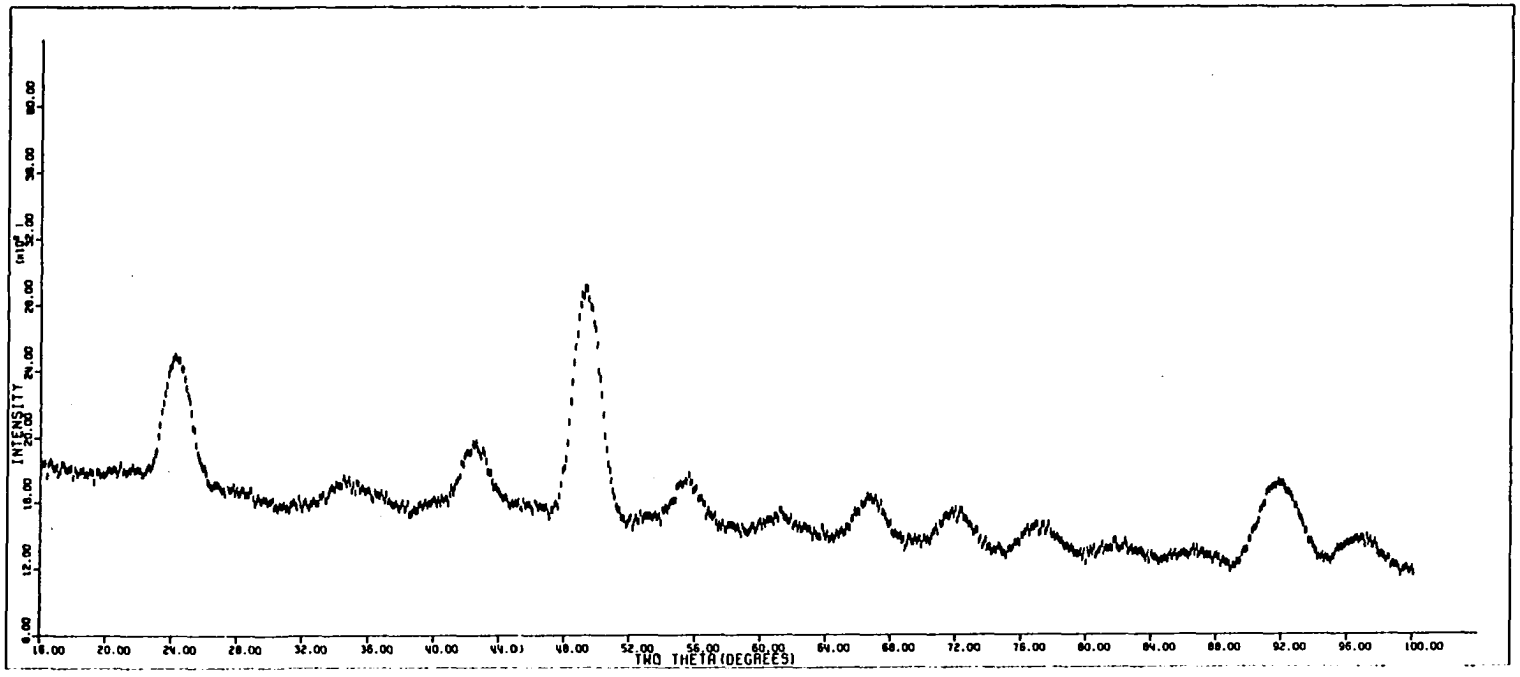

Figure 10. Neutron diffraction pattern of $NbH_{.73}$ powder.

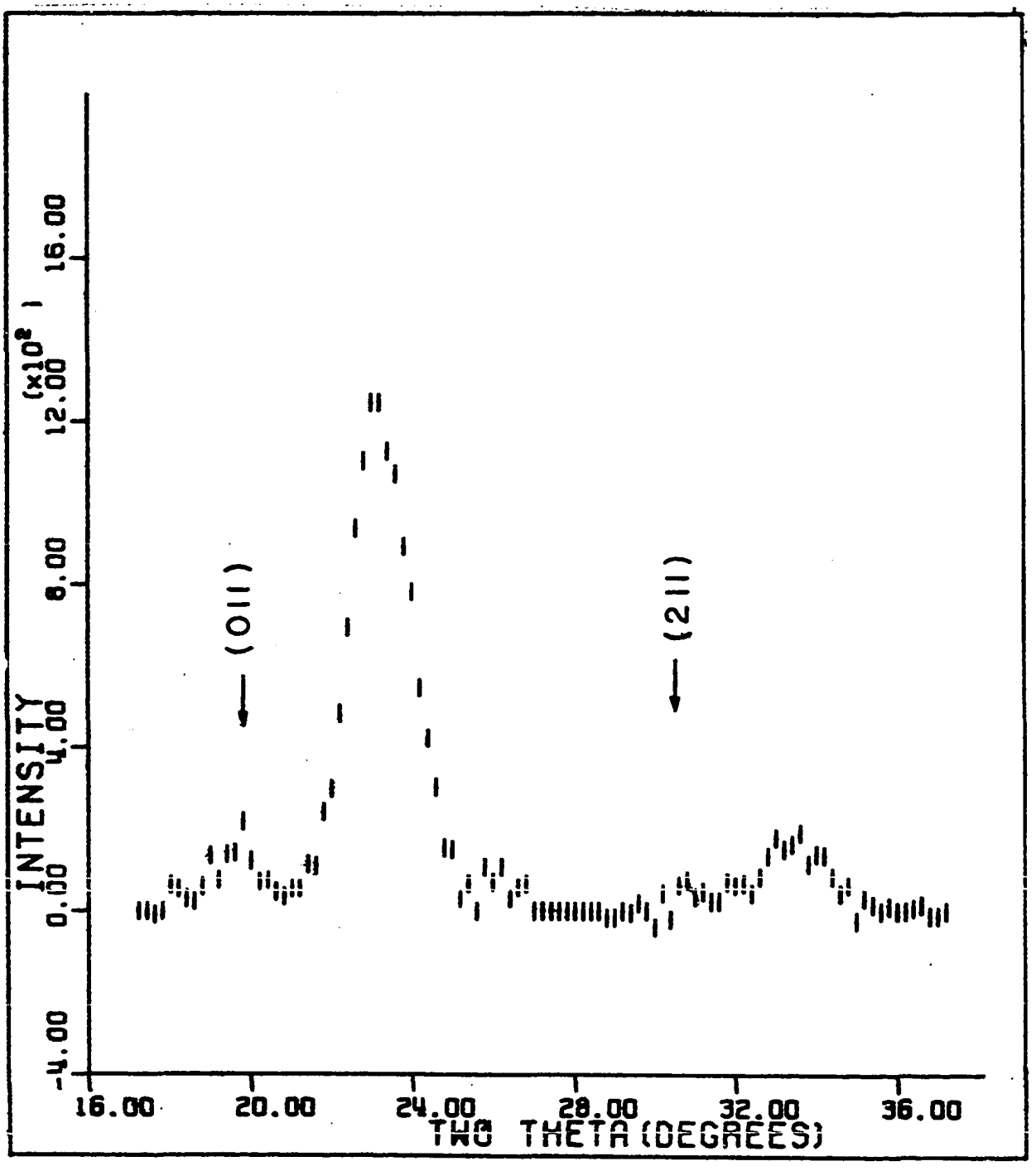

Figure 11. Low-angle neutron diffraction pattern of $NbH_{.73}$ powder, showing the existence of the (011) and (211) superstructure reflections.

The neutron powder patterns resulting from a variety of possible structures were calculated using the program YCALC. Examination of these patterns confirmed Somenkov's model as the only reasonable structure capable of explaining the existence of the superstructure reflections. It was also shown through the use of YCALC that the satellite peaks observed at 21° and 32° 2θ were superstructure reflections, and not caused by scattering of the 2/3 $\mathring{A}$ contribution to the incident neutron beam.

The nuclear scattering factors were obtained from Bacon[20]. Debye-Waller factors were determined in the following manner. For niobium a value (.31) taken from the low end of the range of values given for the pure metal (.31 - .46)[19] was used. The lower value for B_{Nb} was selected as it was felt that the niobium-hydrogen interaction in the hydride might lower the degree of thermal vibration by niobium with respect to that of the pure metal. For hydrogen, the value of the Debye-Waller factor obtained by Pick[23] was used. Pick calculates B_H by assuming the atoms to be independent Einstein oscillators. Using vibrational frequencies obtained by inelastic neutron scattering studies on $NbH_{.85}$ [32] and $NbH_{.95}$ [33], Pick was able to obtain a value of $B_H = 0.8$ for niobium hydride.

A starting set of lattice constants could not be obtained directly from the powder pattern because of peak

overlap. However, use was made of the fact that the deviation from cubic symmetry in the β-hydride is slight. Consequently, to a good approximation, the peaks in the scan could be indexed on a cubic cell, and a resultant set of (h,k,ℓ) and $2\theta_{hk\ell}$ values obtained. These values were input into a general lattice constant refinement program[34], which produced a value of $a_o = 3.420(2)$. The cubic lattice was then transformed into the face-centered orthorhombic cell (see Figure 9), with the resulting lattice parameters $a_o = b_o = 4.837$, $c_o = 3.420$.

The experimental parameters required by the profile refinement algorithm were obtained as follows:

Halfwidth parameters — A treatment similar to that used to obtain a starting set of lattice constants was used to determine an initial set of full-width at half-maximum (H_k) values. As with the case of nickel, the values of U,V, and W were obtained by a least-squares fit to the H_k's and their corresponding $2\theta_k$'s.

Scale factor — The initial scale factor was determined in a manner similar to that of nickel, through the use of the program YCALC.

Asymmetry parameter — The asymmetry parameter was initially set to zero.

Counter zeropoint For a given experimental configuration, the counter zeropoint should be independent of the sample used, provided the samples are properly aligned. Consequently the counter zeropoint obtained from the nickel refinement was used for the niobium hydride data.

Preferred orientation No correction for preferred orientation was required.

The above experimental and structural parameters were input along with the corrected intensity data (from MPREP) into the modified profile refinement routine MPROR. Four cycles of refinement with fixed temperature factors reduced the agreement factors to $R_{nuclear} = 0.148$ and $R_{profile} = 0.168$. The thermal parameters were allowed to vary; three more cycles of refinement reduced the agreement factors to $R_{nuclear} = 0.145$ and $R_{profile} = 0.166$. Further refinement did not lead to any lowering of these values.

Results and Discussion

A plot of the observed and calculated profiles is given in Figure 12. The resulting structural parameters are listed in Table 2. Also listed are the pertinent interatomic distances; these values were calculated from the positional parameters, and the lattice constants and their estimated standard deviations, using a program written at this

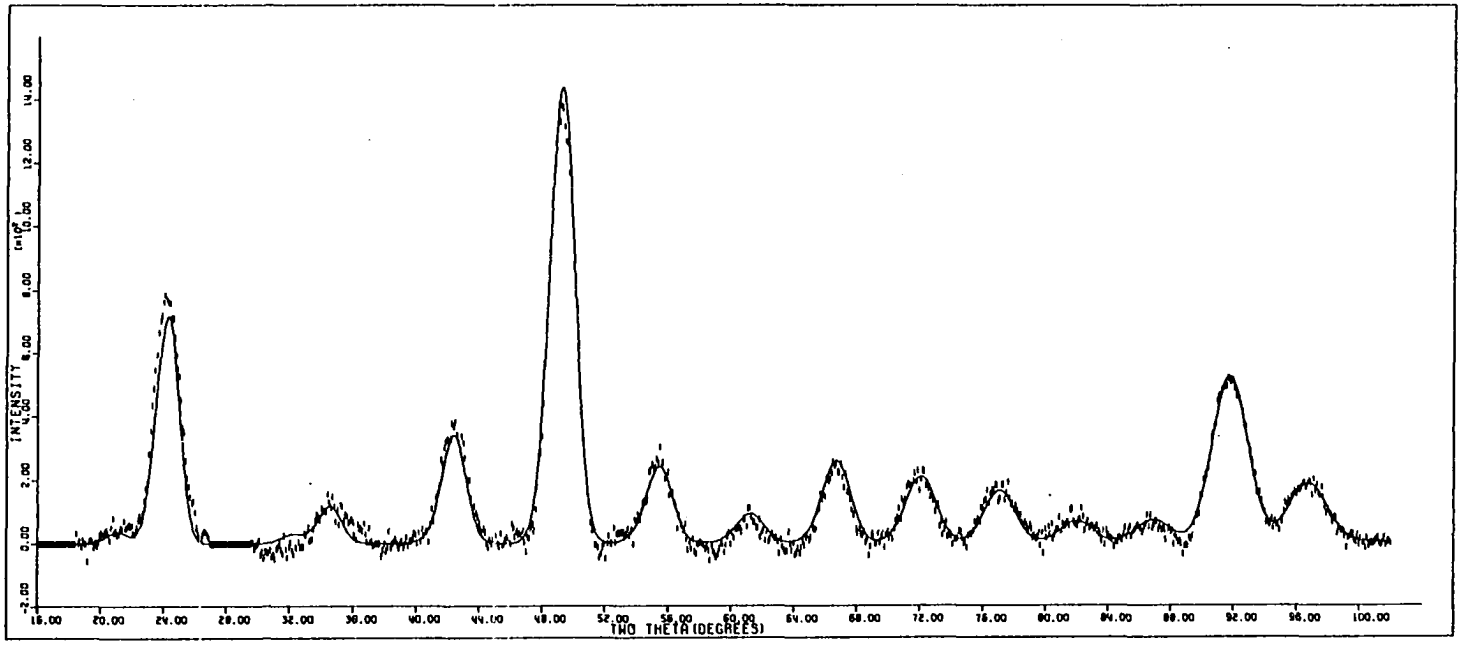

Figure 12. Comparison of the observed and calculated neutron powder patterns for $NbH_{.73}$. The broken line represents the observed pattern, while the solid line represents the calculated profile.

Table 2. Refined structural parameters and pertinent interatomic distances[a] for $NbH_{.73}$

Space group: P_{nnn}

Nb at 4f (0,0,0), (0,½,½), (½,0,½), (½,½,0)
H at 2a (¼,¼,¼), (3/4,3/4,3/4)
2b (3/4,¼,¼), (¼,3/4,3/4)

a = 4.841(10) Å b = 4.852(10) Å c = 3.405(1) Å

B_{Nb} = 0.35 B_H = 1.07

$R_{nuclear}$ = 14.5% $R_{profile}$ = 16.6% $R_{expected}$ = 19.1%

Interatomic Distances (Å):

Nb-H	1.915(2)
Nb-Nb(min)	2.966(4)
Nb-H(min)	2.422(4)

---

[a]For the lattice constants and interatomic distances, the numbers given in parentheses are the estimated standard deviations for the least significant figures.

laboratory[35]. There is good agreement between the interatomic distances obtained in this study and those obtained by Somenkov et al.[29], (d_{Nb-H} = 1.92 Å, $d_{H-H(min)}$ = 2.42 Å). The existence of the β-phase hydride at the composition $NbH_{.73}$ appears to contradict the ^{93}Nb magnetic resonance work of Barnes, et al.[36], which predicts the phase boundary between the α + β and β regions must pass between $NbH_{.78}$ and $NbH_{.82}$ at 300°K.

As can be seen by inspection of the R factors, the agreement between the observed and calculated diffraction profiles of $NbH_{.73}$ is poorer than that of nickel. This is probably a result of the high degree of peak overlap in the niobium hydride pattern. A better measure of the goodness of fit can be made by comparing the results of the niobium hydride study with a profile refinement study on a system of similar complexity. The only other study of this type was done by Kuijpers and Loopstra[37] on a series of RCo_5 (R = La, Ce, Pr, Nd) deuterides. These compounds are similar in complexity to $NbH_{.73}$, crystallizing in either orthorhombic or hexagonal cells. In addition, since their investigation employed a single wavelength profile refinement technique, a comparison can be made between multiple wavelength and conventional single wavelength methods. The agreement factors obtained by Kuijpers and Loopstra were found to range from $R_{nuclear}$ = 0.053 for $PrCo_5D_{3.6}$ (orthorhombic) to $R_{nuclear}$ =

0.110 for $NdCo_5D_{2.8}$ (orthorhombic), and from $R_{profile} = 0.055$ for $PrCo_5D_{3.6}$ to $R_{profile} = 0.115$ for $NdCo_5D_{2.8}$. While this agreement is still better than in $NbH_{.73}$, the difference is now approximately what one would expect when factors such as incoherent scattering and low degree of collimation are taken into account. The diffraction studies of Kuijpers and Loopstra were done on deuterides, thus avoiding problems of hydrogen incoherent scattering. In addition, the instrumental resolution obtained by Kuijpers and Loopstra was markedly better, with an average H_k value of approximately 1° 2θ as opposed to approximately 2° 2θ for the multiple wavelength diffractometer. It might also be noted that the values $R_{nuclear}$ and $R_{profile}$ obtained for the $NbH_{.73}$ pattern are lower than the predicted value ($R_{expected} = 0.191$). Therefore one can reasonably conclude that the profile refinement technique is capable of producing refined structural models using multiple wavelength diffraction data with an accuracy comparable to that obtained by conventional (monochromatic beam) techniques.

Unfortunately, a direct comparison of the lattice parameters obtained for $NbH_{.73}$ from profile refinement with those obtained by X-ray powder diffraction cannot be made since the only X-ray study done on a hydride of similar composition, $NbH_{.70}$ [38], was indexed on the basis of a body-centered cubic cell. However, an indirect comparison can be

made, based on Pick's[23] observation that the lattice expansion in the β-phase hydride should be linearly related to concentration. The lattice parameters of a number of β-phase niobium hydrides of varying composition, obtained from Rashid and Scott[28], were input along with the parameters obtained for $NbH_{.73}$ into a routine which fit these values to a straight line using least squares. The results are plotted in Figure 13. Inspection of this figure shows agreement between observed and calculated values to be good for all three cell lengths of $NbH_{.73}$. It should be noted that there is a slight disagreement between the results shown in Figure 13 and those obtained by Pick. Pick predicts a slight increase in a_o with increasing concentration; Figure 13 shows a slight decrease in a_o with increasing concentration. However, this difference is not significant, as the two curves differ by less than the experimental error.

The Debye-Waller factor obtained for niobium (0.34) is essentially identical to that found for the pure metal. This seems to indicate that any constraint imposed on the vibrational freedom of niobium by niobium-hydrogen interactions is at least partially offset by lattice expansion. The hydrogen also appears to be less constrained than expected; the value of B_H = 1.07 obtained from the profile refinement is substantially higher than the theoretical value (B_H = 0.8) obtained by Pick[23] (Somenkov et al.[29], do not give an explicit

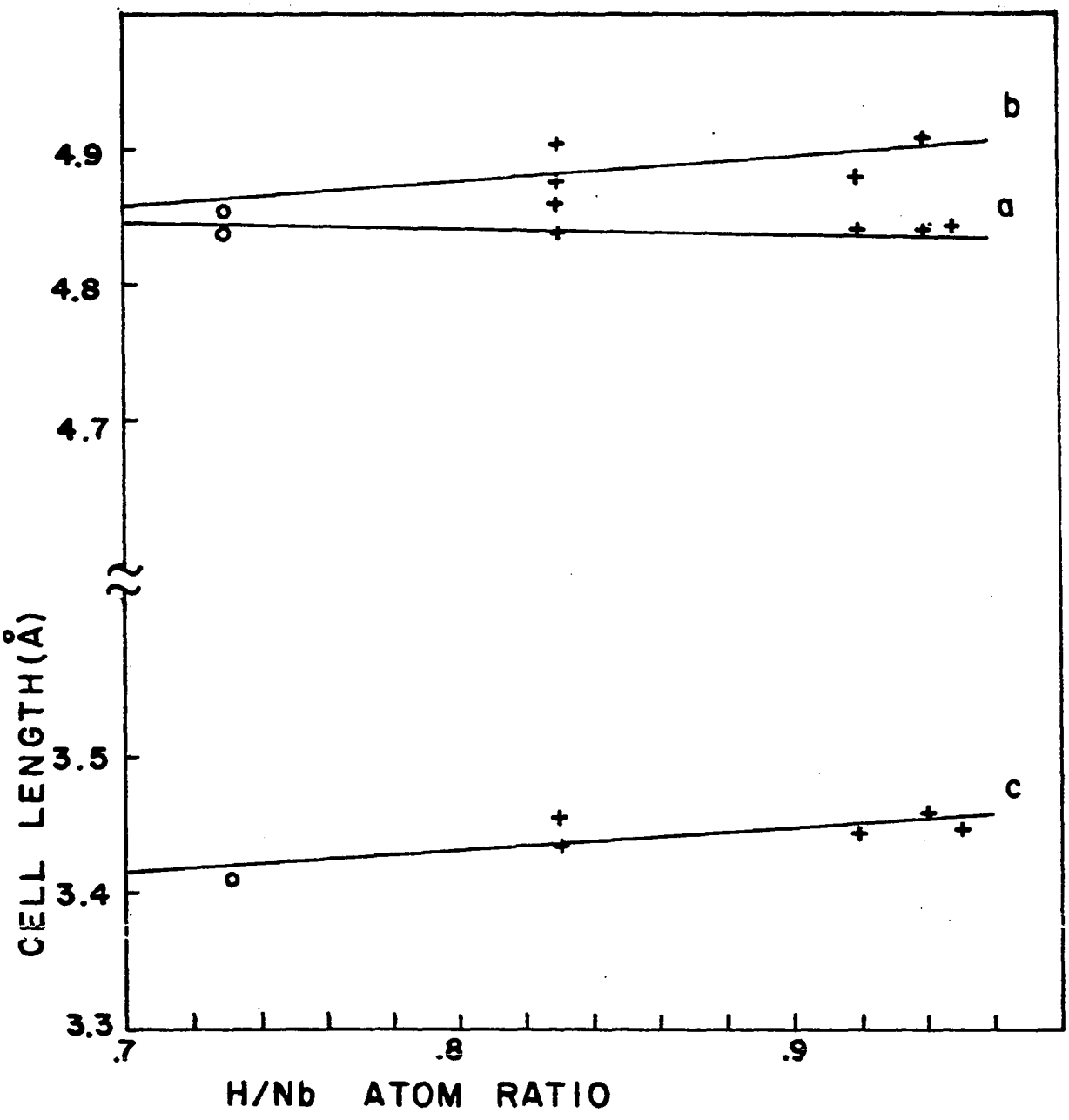

Figure 13. Concentration dependence of lattice parameters in β-phase niobium hydride.

o experimental lattice constants(this study)

\+ experimental lattice constants(Rashid and Scott[28])

— calculated values

value of B_H). Inspection of the correlation matrix showed no significant correlation between the thermal motion of the niobium and that of hydrogen. However the thermal parameters for the non-equivalent hydrogens could not be varied independently, indicating a strong correlation between these atoms. A closer inspection of the cell showed that while the two sets of occupied interstitial sites are crystallographically non-equivalent in this space group, it is possible to select a space group of higher orthorhombic symmetry in which the hydrogen atom sites are all equivalent. The space group and corresponding atom sites are listed below:

Space Group: C_{ccm}

Nb at 4e	(¼,¼,0)	(¼,3/4,½)	(3/4,3/4,0)	(3/4,¼,½)
H at 4a	(0,0,¼)	(0,0,3/4)	(½,½,¼)	(½,½,3/4)

As was discussed previously, Caglioti[7] has shown that for a conventional two-axis diffractometer the full-width at half-maximum (H_k) should be a function only of the scattering angle θ_k and the experimental configuration, both of which are independent of sample composition. Consequently, the half-width curves for nickel and niobium hydride should be identical. A comparison of these two curves, obtained using the U,V,W values from the least least-squares refinement cycles of nickel and $NbH_{.73}$, is shown in Figure 14. The standard deviation in the two curves can be calculated using the relation

Figure 14. Comparison of calculated half-width curves for nickel and $NbH_{.73}$.

+++ nickel

—— $NbH_{.73}$

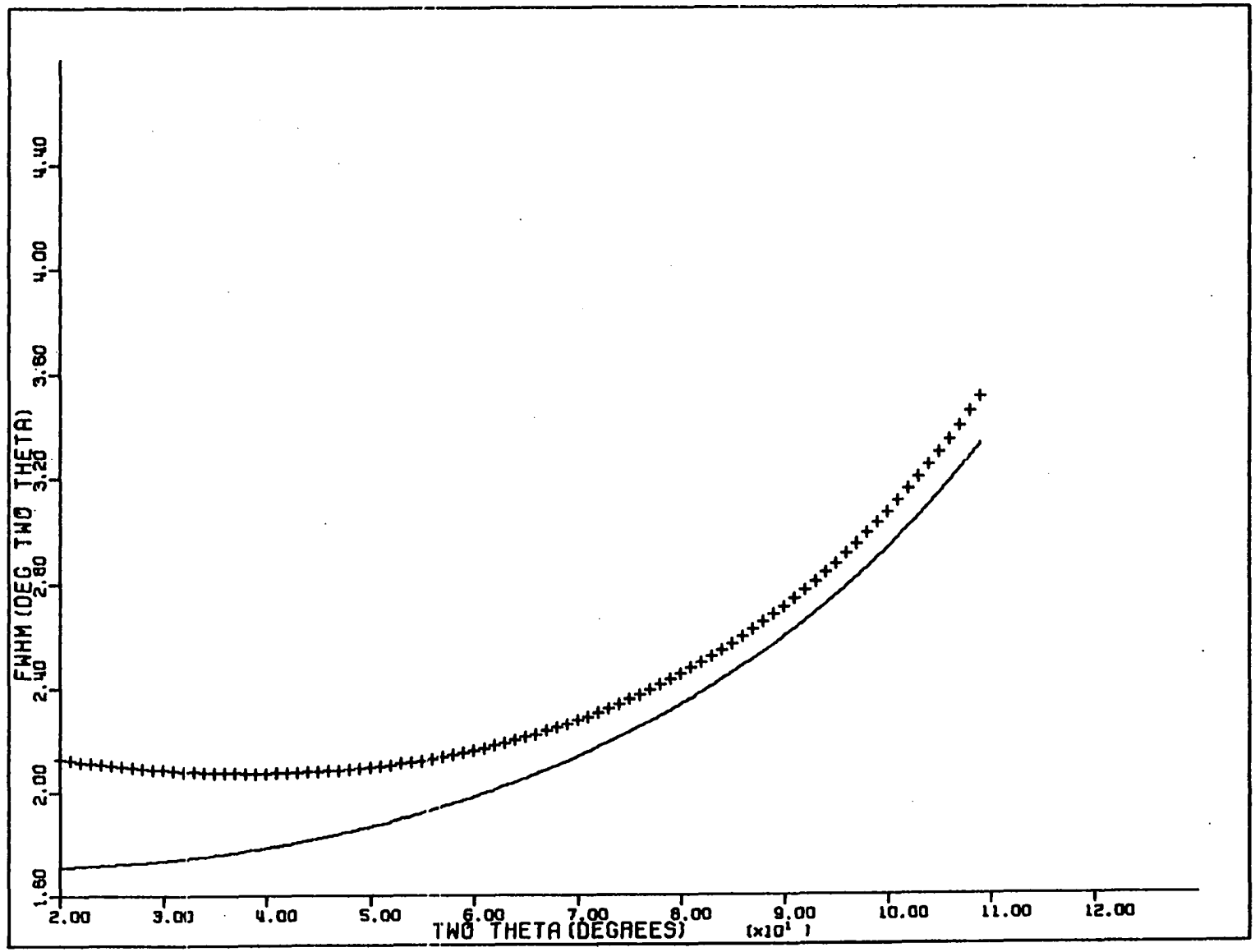
FWHM (DEG TWO THETA)
1.60
2.00
2.40
2.80
3.20
3.60
4.00
4.40
2.00
3.00
4.00
5.00
6.00
7.00
8.00
9.00
10.00
11.00
12.00
TWO THETA (DEGREES)
(x10¹)

$$\sigma^2(H_k) = \left(\frac{\partial H_k}{\partial U}\right)^2_{V,W} \sigma^2(U) + \left(\frac{\partial H_k}{\partial V}\right)^2_{U,W} \sigma^2(V) + \left(\frac{\partial H_k}{\partial W}\right)^2_{U,V} \sigma^2(W) \quad (19)$$

where $\sigma^2(U)$, $\sigma^2(V)$, and $\sigma^2(W)$ are obtained from the profile refinement algorithm MPROR. Input of the appropriate values into equation (19) produced the results shown in Table 3. These results clearly demonstrate that the two halfwidth curves agree within the estimated standard deviation, thus verifying Caglioti's calculations.

The most interesting aspect of β-phase niobium hydride is the ordering of the hydrogen atoms in the niobium metal lattice. A number of theoretical studies have been previously carried out on the ordering of solvent atoms in interstitial solid solutions. Zener[39] developed a method for evaluating the strain energy (energy resulting from forces exerted by a solute atom on the metal lattice) interaction of solute atoms in a b.c.c. or f.c.c. lattice, and concluded that in certain cases this interaction could result in a self-induced preferential distribution of solute atoms among available sites. Khachaturyan[40] extended Zener's work to account for the effect of anisotropy, the discrete crystal structure of the metal lattice, and the dependence of the interaction energy on the atomic configuration of the solute atoms.

Table 3. Comparison of selected halfwidth values and their standard deviations for nickel and niobium hydride

	Ni		$NbH_{.73}$	
$2\theta(^{o})$	$H_k(^{o}2\theta)$	$\sigma(H_k)$	$H_k(^{o}2\theta)$	$\sigma(H_k)$
20	2.13	.49	1.72	.57
30	2.09	.54	1.74	.60
40	2.07	.60	1.79	.66
60	2.16	.72	1.99	.81
80	2.45	.87	2.34	1.00
100	3.07	1.14	2.94	1.28

This theory was subsequently used by Somenkov[41] to explain the ordering of hydrogen atoms in the Group V metal hydrides (including NbH).

We prefer a different approach in order to explain the ordering in the niobium-hydrogen system. A qualitative explanation can be made on the basis of a series of molecular orbital calculations on binary metal hydrides by Switendick[42,43]. On the basis of the one-electron theory of metals, Switendick was able to calculate the various energy states in both the pure metal and the corresponding hydride for the Pd-H and Ni-H systems[42], as well as several rare-earth hydrides[43]. He concluded on the basis of these calculations that the stability of systems with two or more hydrogen atoms per metal atom were strongly dependent on hydrogen-hydrogen interactions (similar to the conclusions reached by Zener and Khachaturyan for interstitial solid solutions). Consequently, Switendick was able to predict a minimum hydrogen-hydrogen distance, below which a particular metal hydride could not be formed. This distance was found to be 2.30 Å for the trihydrides and 2.14 Å for the dihydrides. It seems plausible that these arguments could be extended to explain the ordering found in the β-phase of niobium hydride. Although a minimum hydrogen-hydrogen distance for the monohydrides was not predicted, the above results would lead one to infer a minimum distance of

approximately 2 Å. A statistical distribution of hydrogen in $NbH_{.73}$ would lead to a minimum hydrogen-hydrogen distance of 1.69 Å, well below this value. On this basis therefore, the ordered structure would be preferred. In addition, it should be noted that tantalum deuteride, composition $TaD_{.85}$ (β-phase), was also found to have an ordered structure identical to that found in β-phase niobium hydride (Somenkov-neutron diffraction study[44]). Using the lattice parameters obtained by Brauer and Hermann[26] for $TaH_{.8}$ (the lattice parameters for $TaD_{.85}$ were not reported by Somenkov), one obtains a minimum hydrogen-hydrogen distance of 1.71 Å for a statistical distribution of hydrogen atoms in available sites, as opposed to a distance of 2.36 A for the ordered distribution found experimentally. Again the short hydrogen-hydrogen distance in the statistically disordered model appears to preclude its formation.

Conclusions

The ability, through the use of the profile refinement technique, to obtain accurate structural information from a multiple wavelength neutron beam diffractometer has been demonstrated for both simple and reasonably complex structures. Currently diffraction studies are being carried out on structures of even greater complexity. In conjunction with work carried out by Struss and Corbett[45], neutron powder diffraction data has been collected on the compounds $ZrClD_{.5}$

and ZrClD, both of which appear to crystallize in monoclinic cells. Currently we are attempting to obtain suitable structural models to input into the profile refinement algorithm. A number of additional structural investigations are planned, most involving metal hydrides. From the work done to date one can conclude that the multiple wavelength effect is, at least for the case of neutron powder diffraction, a viable means of increasing the incident neutron beam intensity without extensive or costly equipment modifications to a conventional two-axis diffractometer.

With regards to the profile refinement technique and neutron powder diffraction in general, there are several areas warranting further investigation.

The experiments involving the multiple wavelength neutron beam have been carried out on a fixed experimental configuration; no attempt has been made to optimize the intensity of the multiple wavelength neutron beam. This should be possible either by varying the reflection angle of the monochromator or selecting a more appropriate monochromating crystal. The experimenter now has much greater freedom in selecting a "monochromator", since second (and higher) order contamination is an advantage in this method, as opposed to a monochromatic beam. In addition the multiple wavelength treatment can be extended to single crystal studies. The mode of data collection will depend upon the

number of significant contributions to the multiple wavelength beam; if the experimental configuration is identical to that used in this study (1 Å primary contribution, 2 Å secondary contribution, and no significant 2/3 Å contribution) data collection should be similar to that involving a conventional diffractometer. The chief difficulty occurs in obtaining accurate structure factors from the resulting intensity data. The most likely solution lies in a deconvolution technique similar, though less involved, to that used by Hubbard, Quicksall, and Jacobson[2] in the white radiation experiment.

An additional topic for future research involves the profile refinement method itself. Due to the nature of the technique, an accurate background determination is essential in order to utilize the profile refinement algorithm effectively. The background curve is currently obtained by linear interpolation, using those points in the data due solely to background scattering. While this method is sufficient for most problems, it is inadequate for very complex structures, or data obtained from an instrument with poor resolution. It may be possible to derive an empirical expression which, given the composition of a particular compound under investigation, could provide the background curve using only a few experimental background data points.

The existence of hydrogen ordering in the β-hydrides

of niobium and tantalum indicates the possibility of a minimum hydrogen-hydrogen interaction distance in metal monohydrides, similar to that found by Switendick[42] in metal di- and trihydrides. Neutron diffraction studies could be carried out on other metal hydride systems in order to try to discover further examples of hydrogen ordering. In addition it may be possible to extend Switendick's calculations to obtain a minimum hydrogen-hydrogen distance for metal monohydrides. This information would not only enhance our understanding of the behavior of hydrogen in metals, but also aid in the search for new and better hydrogen storage materials, currently one of the major programs in this laboratory.

SINGLE CRYSTAL X-RAY INVESTIGATIONS OF SUBSTITUTED PROPELLANES AND THEIR SOLVOLYSIS PRODUCTS

Introduction

Lu[46] has recently carried out a series of solvolysis experiments on a variety of propellane systems in order to demonstrate the existence of bridgehead double bond intermediates. He further wished to show that in the case of the [4.3.1] and [3.3.1] propellane systems (1 and 2 respectively) that these intermediates resulted from the collapse of a

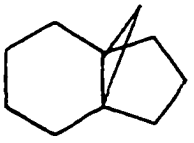

1

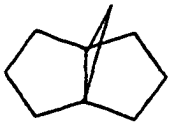

2

"partially-opened" cyclopropyl cation intermediate formed via ring opening[47]. A series of exhaustive synthetic and mechanistic studies were performed; much of the resulting evidence for bridgehead double bond intermediates was based on the products formed in the various solvolysis reactions. In many cases it was essential to know the detailed molecular structure of these products. As non-crystallographic techniques were unable to provide this information, a number of single crystal X-ray investigations were carried out on selected compounds. The results of two of these investigations are reported here. While more than one propellane system was investigated by Lu, we will be

concerned here only with those studies involving the [4.3.1] propellane system, 1.

The first product of interest is obtained from the silver-assisted solvolysis of 10,10-dibromo[4.3.1]propellane 3[48].

(I)

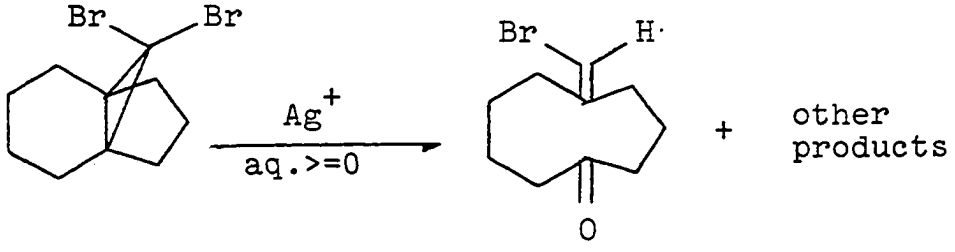

3 4

Proton magnetic resonance studies[49] indicated that the major product of reaction I, 4, had the structure shown above. In addition it was shown by both pmr and cmr studies that only a single stereoisomer of 4 existed. However, before a mechanism for reaction I could be proposed, it was necessary to confirm the proposed structure of 4. In addition, a detailed knowledge of the stereochemistry of 4 is important as one can infer from the structure of 4 (via hydrogenative correlation) the structure of the product 6 of the silver-assisted solvolysis[48] of 10,10-dibromo[4.3.1]propell-3-ene, 5 (reaction II). Consequently a single crystal X-ray

(II)

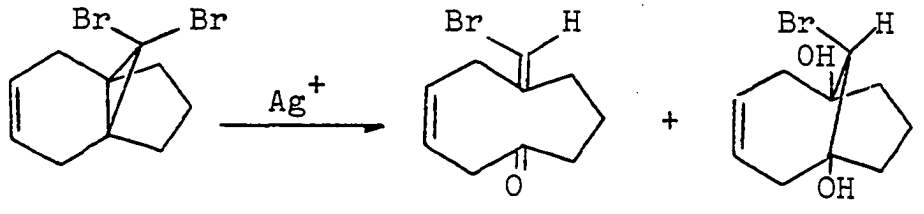

5 6 7

study of the 2,4-dinitrophenylhydrazone derivative of 4, 4a, was carried out, the detailed results of which are reported here.

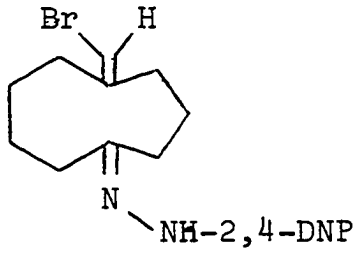

4a

The second structural investigation resulted from studies involving acetolysis of the solvolysis products (4, 6) of 10,10-dibromo[4.3.1]propellane, 3, and its unsaturated analogue, 5[48]. For the case of 4 it was observed that upon treatment of 4 with aluminum trichloride in acetic anhydride, bicyclization occurred (reaction III). This is similar to the transannular acid-catalyzed cyclizations

(III)

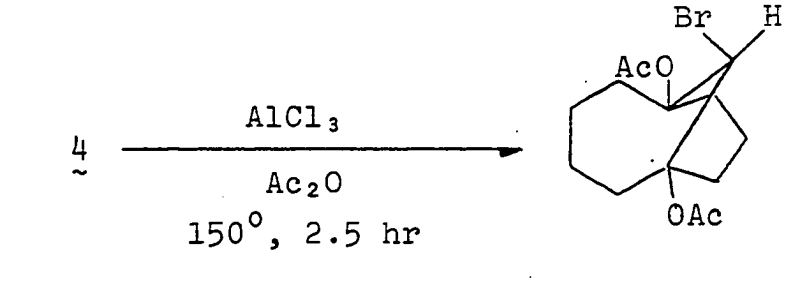

8

undergone by 5-cyclononynone[50] and 5-cyclodecynone[51]. However it is in marked contrast to the case of the ten-membered ketone 9, which when treated in a fashion similar to that of 4, formed no bicyclic material, but instead resulted in a

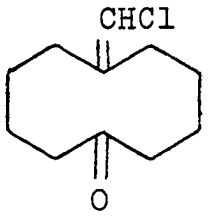

9

mixture of enol acetates. In order to determine if a similar bicyclization occurs with the unsaturated analogue, 6 was acetolyzed in the presence of silver perchlorate (reaction IV). On the basis of spectral data the product was thought

(IV) 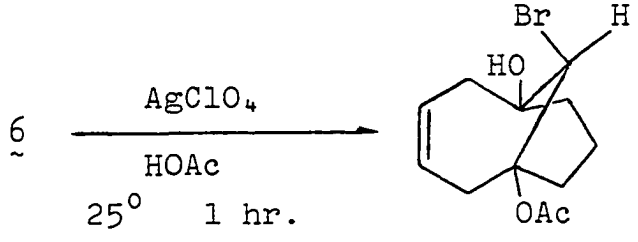

10

to be 10. However, a single crystal X-ray study was necessary to confirm this structure. In addition, it was desirable to determine the relation (if any) between the structure of 10 and that of the corresponding diacetate 11 obtained from the non-assisted acetolysis of 5 (reaction V), the structure of which had been previously determined in an X-ray single crystal diffraction study carried out principally by Myers[52].

(V)

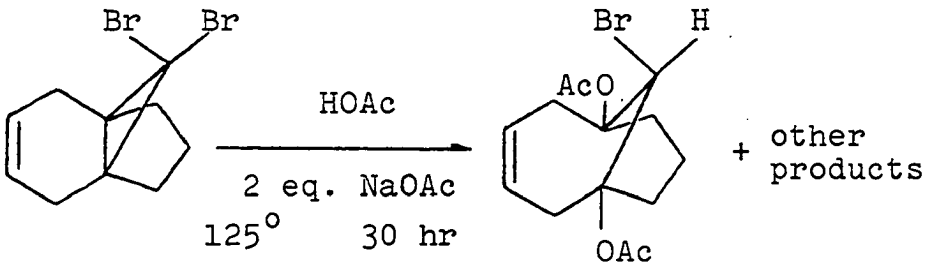

5 11

Samples of both 4a and 10 were kindly supplied by Dr. Lu. The data for both compounds were collected using an automated four-circle diffractometer designed and built in the Ames Laboratory. The upper full circle was purchased from STOE and is equipped with encoders (Baldwin Optical) and drive motors. The design of the base allows the encoders to be directly connected to the main θ and 2θ shafts, using solid and hollow-shaft encoders, respectively. The diffractometer is interfaced to a PDP-15 computer in realtime mode and is equipped with a scintillation counter. Graphite monochromated Mo Kα radiation is used for data collection, with the monochromator mounted between the sample and detector (reflection angle 12.1734°2θ).

The Crystal and Molecular Structure of the 2,4-dinitrophenylhydrazone Derivative of 5-bromomethylidenecyclononanone, 4a

Crystal data

(2,4-DNP)$C_{10}H_{16}N_2Br$, M.W. = 394.9, triclinic $P\bar{1}$, a = 11.048(5), b = 11.997(6), c = 7.514(2) α = 98.42(3), β = 97.09(3), γ = 116.70(4), V = 859.73 Å^3, ρ_{calc} = 1.35, Z = 2, Mo Kα (λ = 0.70954 Å), μ = 25.7 cm^{-1}

Experimental

Bright orange, irregularly shaped crystals were obtained by slow evaporation from $CHCl_3$ solution. The crystals were observed to be air stable, and a single crystal of approximate dimensions .2 x .2 x .3 mm was mounted on a glass fiber with Duco cement and attached to a standard goniometer head. Both preliminary and intensity data were collected using an automated four-circle diffractometer described in the introduction. From six preliminary ω-oscillation photographs taken at various χ and ϕ settings, 13 independent reflections were chosen for input into an automatic indexing algorithm[53]. The resulting reduced cell and reduced cell scalars indicated triclinic symmetry. This was confirmed by inspection of axial ω-oscillation photographs. Observed layer-line spacings were in agreement with the calculated values. The unit cell parameters and their standard deviations were

obtained by a least-squares fit[54] to 14 independent high-angle reflections ($|2\theta| > 19^\circ$) whose centers were determined at $\pm 2\theta$ by half-height techniques on a previously aligned four-circle diffractometer (Mo Kα radiation, $\lambda = 0.70954$ Å). An approximate density measurement utilizing floatation techniques was carried out; the results showed $1.0 < \rho_{exp} < 1.8$ g-cm^{-3}. The only calculated density within this range was $\rho_{calc} = 1.35$ for $Z = 2$.

Four octants of data ($hk\ell$, $hk\bar{\ell}$, $h\bar{k}\ell$, $h\bar{k}\bar{\ell}$) were collected within a 2θ sphere of 50°. Intensities were measured with the stationary crystal, stationary counter method, and background counts were taken at the beginning and end of each measurement by offsetting in ω-2θ. As a check on electronic and crystal stability, the intensities of three standard reflections were remeasured every 75 reflections. The standards did not vary significantly during the course of data collection, indicating that no crystal decomposition occurred. A total of 3368 unique reflections were collected. The intensity data were corrected for Lorentz, polarization, and background effects; however no corrections for absorption or secondary extinction were made. There were 1920 reflections having $|F_o|^2 > 3\sigma_I$ where

$$\sigma_I^2 = C_T + 2C_B + (0.03C_T)^2 + (0.03C_B)^2,$$

C_T and C_B being the total count and the background count, respectively, while the factor 0.03 represents an estimate

of non-statistical errors. The estimated standard deviation in each structure factor was calculated by the finite difference method[55].

Solution and refinement

A Howells, Phillips, and Rogers statistical test[56] indicated a centrosymmetric unit cell. Consequently the space group was assumed to be $P\bar{1}$, with one independent molecule per asymmetric unit. The position of the bromine atom was unambiguously revealed by analysis of a sharpened Patterson map[57]. The remaining non-hydrogen atoms were located by successive structure factor[58] and electron density map[57] calculations. Approximate positions for the aromatic and methylene hydrogens were calculated from the carbon atom positions, using typical C-H distances and angles appropriate for the C-CH-C and C-CH_2-C groups. The remaining hydrogen atom positions were obtained by analysis of electron density difference maps. The positional parameters for all atoms, as well as the anisotropic thermal parameters for all non-hydrogen atoms, were refined by a full-matrix least-squares procedure[58], minimizing the function $\Sigma\omega(|F_o| - |F_c|)^2$, where $\omega = 1/\sigma_F{}^2$. Analysis of the weights was performed via the requirement that $\overline{\omega\Delta^2}$ should be a constant function of $|F_o|$[59]. The analysis indicated that very low and very high values of $|F_o|$ were slightly overweighted, and the weights were subsequently adjusted. Successive iterations of

refinement using the adjusted weights reduced the conventional discrepancy index to 0.078 for the 1920 observed reflections. The weighted R factor was 0.090. The scattering factors used were those of Hanson, et al.[60], except for hydrogen, where the values used were those of Stewart, et al.[61]. The scattering factor of bromine was modified for the real and imaginary parts of anomalous dispersion[62].

Tables 4 and 5 list the positional and thermal parameters along with their estimated standard deviations. Bond distances and angles, along with their standard deviations are calculated from the unit cell parameters and positional parameters using an algorithm developed by Busing, et al.[63]. The standard deviations are computed using the variance-covariance matrix obtained from the final least-squares cycle. The bond distances and angles are given in Tables 6 and 7, respectively. Table 8 lists the observed and calculated structure factors for the observed reflections.

Discussion

A computer-generated drawing[64] of the molecule is shown in Figure 15. The most noteworthy feature is the orientation of the bromine with respect to the carbon ring. On the basis of this structure, as well as other product structures, solvolysis reactions of similar systems, and ^{13}C labeling studies, Lu and Warner have proposed the following mechanism

Table 4. Final atomic positional parameters[a] with their standard deviations[b] for 4a[c]

Atom	x	y	z
Br	5734(1)	6519(1)	-1678(1)
O(1')	3267(6)	5522(6)	4521(8)
O(2')	1420(7)	3713(7)	3592(8)
O(3')	-1064(7)	2114(6)	-2583(9)
O(4')	-0941(6)	3447(6)	-4256(8)
N(1')	4644(6)	8358(6)	1983(9)
N(2')	3968(7)	7165(7)	2423(10)
N(3')	2254(7)	4730(7)	3332(9)
N(4')	-0542(6)	3178(6)	-2877(9)
C(1)	5745(7)	9183(7)	3130(10)
C(2)	6452(9)	10458(8)	2626(14)
C(3)	7844(13)	10880(10)	2133(19)
C(4)	7862(17)	9945(11)	0555(16)
C(5)	8402(10)	9013(10)	0988(14)
C(6)	7495(9)	7972(8)	1347(11)
C(7)	7884(11)	8099(10)	3888(12)
C(8)	7771(13)	9117(14)	5124(14)
C(9)	6367(10)	9064(10)	5007(12)
C(10)	6450(11)	6911(10)	0886(12)

[a]The heavy atom positional parameters are $x10^4$; the hydrogen atom positional parameters are $x10^3$.

[b]In this and all successive tables the estimated standard deviations are given in parentheses for the least significant figure.

[c]Numbering as in Figure 15, with the hydrogen atoms having the same number as the atom to which they are attached.

Table 4 (Continued)

Atom	x	y	z
C(1')	2867(7)	6196(7)	1173(9)
C(2')	2043(7)	4987(7)	1510(9)
C(3')	0944(7)	3998(7)	0208(10)
C(4')	0652(7)	4191(7)	-1530(10)
C(5')	1434(8)	5364(7)	-1962(11)
C(6')	2534(7)	6357(7)	-0634(10)
H(2a)	644(10)	1104(8)	305(12)
H(2b)	563(8)	1052(7)	152(10)
H(3a)	787(8)	1178(8)	148(10)
H(3b)	858(9)	1049(8)	159(12)
H(4a)	792(9)	1026(9)	-038(13)
H(4b)	697(9)	1008(8)	025(11)
H(5a)	921(9)	923(8)	188(11)
H(5b)	849(9)	854(8)	002(11)
H(7a)	888(9)	818(7)	409(10)
H(7b)	665(8)	764(8)	450(10)
H(8a)	704(12)	939(10)	478(15)
H(8b)	814(8)	923(8)	645(11)
H(9a)	622(8)	975(8)	606(11)
H(9b)	582(9)	826(9)	539(11)
H(10)	612(9)	637(9)	145(12)
H(N)	364(10)	734(9)	296(13)
H(3')	321(8)	729(8)	-101(10)
H(5')	118(9)	540(8)	-319(11)
H(6')	036(8)	307(8)	029(11)

Table 5. Final atomic thermal parameters[a] with their standard deviations for 4a [b]

Atom	β_{11}	β_{22}	β_{33}	β_{12}	β_{13}	β_{23}
Br	215(1)	168(1)	309(2)	103(1)	4(1)	-5(1)
O(1')	190(9)	158(7)	252(14)	58(7)	-30(9)	52(8)
O(2')	203(9)	181(9)	322(17)	66(8)	21(10)	113(10)
O(3')	232(10)	100(7)	347(16)	35(7)	-33(10)	14(8)
O(4')	186(9)	168(8)	228(13)	69(7)	-31(8)	16(8)
N(1')	108(8)	101(7)	307(17)	43(6)	11(10)	21(9)
N(2')	131(9)	119(8)	256(17)	53(7)	14(9)	15(9)
N(3')	154(10)	134(9)	238(16)	73(8)	37(11)	56(10)
N(4')	124(8)	97(8)	283(18)	49(7)	15(10)	6(9)
C(1)	113(9)	116(9)	247(17)	55(8)	21(11)	28(10)
C(2)	143(11)	108(10)	388(26)	61(9)	30(14)	34(13)
C(3)	278(20)	162(14)	631(45)	123(14)	161(25)	140(21)
C(4)	454(31)	200(16)	321(30)	192(20)	190(25)	140(18)
C(5)	192(14)	166(13)	344(25)	109(12)	33(16)	48(15)

[a]The β_{ij}'s are $x10^4$. The hydrogen atoms were refined with fixed isotropic thermal parameters $B_H = 4.0$. The form of the anisotropic temperature factor is $\exp(-(\beta_{11}h^2 + \beta_{22}k^2 + \beta_{33}\ell^2 + \beta_{12}hk + \beta_{13}h\ell + \beta_{23}k\ell))$.

[b]Numbering as in Figure 15, with the hydrogen atoms having the same number as the atom to which they are attached.

Table 5 (Continued)

Atom	β_{11}	β_{22}	β_{33}	β_{12}	β_{13}	β_{23}
C(6)	179(12)	124(10)	277(20)	95(10)	42(13)	62(12)
C(7)	243(16)	237(15)	255(22)	161(14)	6(15)	31(14)
C(8)	270(20)	351(24)	253(25)	201(20)	-52(17)	-6(18)
C(9)	140(11)	157(12)	213(19)	51(10)	16(13)	29(13)
C(10)	219(16)	117(12)	291(23)	100(13)	77(16)	76(13)
C(1')	118(8)	102(8)	211(16)	62(7)	31(10)	39(9)
C(2')	130(9)	116(9)	182(15)	70(8)	44(9)	53(9)
C(3')	134(10)	96(8)	243(18)	65(8)	43(11)	44(10)
C(4')	125(10)	109(8)	216(17)	66(8)	20(10)	5(10)
C(5')	134(10)	111(9)	219(17)	51(8)	35(11)	45(11)
C(6')	131(10)	109(9)	247(18)	58(8)	23(11)	48(10)

Table 6. Selected bond distances (Å) for 4a

C(10)-Br	1.893(9)	C(5')-C(6')	1.393(10)
C(1)-C(2)	1.504(12)	C(6')-C(1')	1.426(10)
C(2)-C(3)	1.502(15)	C(1)-N(1')	1.269(9)
C(3)-C(4)	1.517(16)	N(1')-N(2')	1.399(9)
C(4)-C(5)	1.540(16)	C(1')-N(2')	1.356(10)
C(5)-C(6)	1.501(13)	C(4')-N(4')	1.450(8)
C(6)-C(7)	1.506(12)	N(4')-O(3')	1.210(8)
C(7)-C(8)	1.484(15)	N(4')-O(4')	1.221(8)
C(8)-C(9)	1.514(15)	C(2')-N(3')	1.460(9)
C(9)-C(1)	1.546(12)	N(3')-O(1')	1.225(8)
C(10)-C(6)	1.295(12)	N(3')-O(2')	1.216(8)
C(1')-C(2')	1.406(10)	N(2')-O(1')	2.610(10)
C(2')-C(3')	1.382(10)	C(1)-C(6)	3.059(10)
C(3')-C(4')	1.384(10)	C(1)-C(10)	3.431(11)
C(4')-C(5')	1.395(11)		

Table 7. Selected bond angles for 4a

Angle	Degrees	Angle	Degrees
C(1)-C(2)-C(3)	119.1(10)	N(2')-C(1')-C(2')	123.9(7)
C(2)-C(3)-C(4)	114.0(9)	C(1')-C(2')-C(3')	123.3(7)
C(3)-C(4)-C(5)	119.1(11)	C(2')-C(3')-C(4')	118.8(7)
C(4)-C(5)-C(6)	115.6(11)	C(3')-C(4')-C(5')	120.9(6)
C(5)-C(6)-C(7)	119.1(7)	C(4')-C(5')-C(6')	119.8(8)
C(6)-C(7)-C(8)	116.8(11)	C(5')-C(6')-C(1')	121.0(7)
C(7)-C(8)-C(9)	118.8(8)	C(6')-C(1')-C(2')	116.3(5)
C(8)-C(9)-C(1)	114.5(8)	C(1')-C(2')-N(3')	121.0(5)
C(9)-C(1)-C(2)	117.2(6)	C(3')-C(2')-N(3')	115.6(6)
C(5)-C(6)-C(10)	122.7(8)	C(2')-N(3')-O(2')	117.9(5)
C(7)-C(6)-C(10)	117.9(8)	C(2')-N(3')-O(1')	119.5(7)
C(6)-C(10)-Br	126.3(8)	O(2')-N(3')-O(1')	122.6(7)
C(2)-C(1)-N(1')	114.4(8)	C(5')-C(4')-N(4')	119.9(7)
C(9)-C(1)-N(1')	128.1(7)	C(3')-C(4')-N(4')	119.0(6)
C(1)-N(1')-N(2')	115.5(7)	C(4')-N(4')-O(3')	118.4(7)
N(1')-N(2')-C(1')	118.7(7)	C(4')-N(4')-O(4')	117.9(6)
N(2')-C(1')-C(6')	119.8(8)	O(3')-N(4')-O(4')	123.7(5)

Table 8. Observed and calculated structure factors for 4a

H = 0																											
K	L	FO	FC	-4	-2	32	27	0	-2	46	45	4	-4	15	16	10	-2	3	3	-4	1	2	1	0	1	38	38
				-4	-1	39	41	0	-1	38	36	4	-3	17	18	10	3	3	5	-4	2	18	16	0	1	38	38
-11	0	3	3	-4	0	50	49	0	-1	38	36	4	-2	16	18	11	-2	5	5	-4	3	47	44	0	2	46	47
-11	1	2	4	-4	1	15	15	0	1	38	36	4	-1	15	15	11	0	3	3	-4	4	4	4	0	2	47	47
-11	2	5	5	-4	2	18	18	0	1	38	36	4	0	51	49					-4	6	18	15	0	3	51	49
-10	-3	2	5	-4	3	18	18	0	2	46	45	4	1	39	41	H = 1				-4	7	2	4	0	3	51	49
-10	2	4	3	-4	4	16	16	0	2	47	45	4	2	33	27	K	L	FO	FC	-4	8	3	4	0	4	23	21
-9	-2	7	7	-4	5	13	12	0	3	62	56	4	3	21	23	-12	2	7	6	-3	-2	51	56	0	4	23	21
-9	-1	19	17	-4	6	6	6	0	3	61	56	4	4	37	34	-12	3	3	3	-3	-1	21	21	0	6	4	4
-9	0	6	6	-4	7	3	2	0	4	10	10	4	5	2	4	-11	-3	2	2	-3	0	26	26	0	6	2	4
-9	1	18	16	-3	-6	2	3	0	4	11	10	4	6	9	8	-11	-1	8	6	-3	1	69	75	1	-8	6	7
-9	2	6	5	-3	-4	7	8	0	5	6	7	4	7	3	5	-11	0	7	7	-3	2	4	3	1	-7	2	4
-9	3	3	6	-3	-3	4	5	0	5	7	7	5	-7	3	5	-11	2	11	10	-3	3	47	44	1	-5	12	13
-9	5	3	5	-3	-2	3	5	0	6	17	15	5	-5	18	18	-11	3	6	6	-3	4	55	46	1	-4	32	30
-8	-5	3	6	-3	-1	6	6	0	6	14	15	5	-4	7	7	-10	-3	12	12	-3	5	2	5	1	-3	27	27
-8	-4	12	11	-3	0	55	56	0	8	2	3	5	-2	10	12	-10	-2	5	5	-3	6	4	4	1	-2	30	32
-8	-2	20	19	-3	1	89	88	1	-8	4	5	5	-1	4	5	-10	-1	19	17	-2	-8	3	5	1	-1	71	75
-8	-1	21	19	-3	3	31	31	1	-5	34	32	5	0	5	5	-10	0	12	12	-2	-7	9	10	1	0	40	38
-8	1	7	7	-3	4	15	12	1	-4	19	17	5	1	27	28	-10	1	8	6	-2	-5	8	9	1	1	114	113
-8	2	10	9	-3	6	11	10	1	-3	25	24	5	2	28	27	-9	-3	2	4	-2	-4	26	24	1	2	9	10
-8	3	5	5	-3	7	4	4	1	-2	46	43	5	3	4	5	-9	-2	7	6	-2	-2	16	16	1	4	18	16
-8	5	9	9	-2	-7	6	7	1	-1	45	46	5	4	14	14	-9	1	9	9	-2	-1	48	52	1	5	17	16
-8	7	3	3	-2	-6	15	15	1	0	56	52	5	7	4	5	-9	2	16	12	-2	0	33	33	1	6	15	16
-7	-6	2	3	-2	-5	29	26	1	1	4	6	6	-5	10	10	-9	3	6	6	-2	1	71	71	1	7	7	7
-7	-4	6	8	-2	-4	11	10	1	2	18	18	6	-4	13	13	-9	4	8	8	-2	2	88	81	1	8	5	5
-7	-3	13	13	-2	-2	60	62	1	3	17	15	6	-3	5	6	-8	-4	7	8	-2	3	64	59	2	-7	9	9
-7	-1	8	8	-2	-1	41	43	1	4	35	34	6	-2	5	4	-8	-3	10	9	-2	4	33	29	2	-6	8	7
-7	0	34	32	-2	0	3	4	1	5	6	8	6	-1	23	24	-8	-1	12	11	-2	5	11	12	2	-4	47	44
-7	2	27	24	-2	1	61	60	1	6	13	13	6	0	23	25	-8	0	11	9	-2	8	5	5	2	-3	5	4
-7	3	7	7	-2	2	5	6	1	7	16	15	6	2	21	21	-8	2	21	19	-1	-6	12	11	2	-2	32	31
-7	4	7	8	-2	3	12	10	2	-7	10	10	6	3	15	14	-8	3	8	6	-1	-4	41	39	2	-1	86	87
-7	5	11	11	-2	4	7	8	2	-6	7	7	6	4	4	6	-8	5	11	11	-1	-3	51	49	2	0	9	9
-7	6	10	10	-2	5	16	14	2	-5	15	14	6	5	7	8	-7	-6	7	7	-1	-2	32	31	2	1	29	30
-6	-6	2	3	-2	6	8	7	2	-4	7	8	6	6	2	3	-7	-5	4	6	-1	-1	7	7	2	2	56	56
-6	-5	8	8	-2	7	10	10	2	-3	12	10	7	-6	9	10	-7	-4	6	8	-1	0	18	15	2	3	33	33
-6	-4	6	6	-1	-7	16	15	2	-2	6	6	7	-5	10	11	-7	-3	17	16	-1	1	55	52	2	4	9	10
-6	-3	16	14	-1	-6	16	13	2	-1	60	60	7	-4	7	8	-7	-2	17	16	-1	2	7	8	2	5	38	32
-6	-2	22	21	-1	-5	7	8	2	0	3	4	7	-3	8	7	-7	0	9	9	-1	3	25	23	2	6	14	14
-6	0	25	26	-1	-4	34	34	2	1	40	43	7	-2	25	24	-7	1	23	20	-1	4	6	7	2	7	6	6
-6	1	23	24	-1	-3	16	15	2	2	59	62	7	0	32	32	-7	3	3	4	-1	5	13	10	3	-6	10	10
-6	2	5	4	-1	-2	18	18	2	4	11	10	7	1	8	8	-7	4	17	16	-1	6	14	13	3	-5	7	6
-6	3	6	6	-1	-1	5	6	2	5	30	26	7	3	13	13	-7	5	6	7	-1	8	4	4	3	-4	2	3
-6	4	13	13	-1	0	52	52	2	6	15	15	7	4	7	8	-7	6	8	7	0	-8	2	3	3	-3	14	15
-6	5	10	10	-1	1	46	46	2	7	8	7	7	6	2	3	-6	0	13	12	0	-7	3	4	3	-1	11	11
-5	-5	2	2	-1	2	47	43	3	-7	2	4	8	-5	8	9	-6	1	85	80	0	-7	2	4	3	0	35	42
-5	-4	14	14	-1	3	27	24	3	-6	10	10	8	-3	3	5	-6	2	12	14	0	-6	19	19	3	1	38	38
-5	-3	4	5	-1	4	20	17	3	-5	1	1	8	-2	9	9	-6	3	29	27	0	-6	20	19	3	2	42	40
-5	-2	27	27	-1	5	37	32	3	-4	12	12	8	-1	7	7	-6	4	32	29	0	-5	14	13	3	3	26	25
-5	-1	27	28	-1	8	4	5	3	-3	30	31	8	1	18	19	-6	5	12	12	0	-5	15	13	3	4	13	12
-5	0	5	5	0	-8	3	3	3	-1	92	88	8	2	18	19	-6	7	2	3	0	-4	13	12	3	6	13	14
-5	1	4	5	0	-6	14	15	3	0	52	56	8	4	13	11	-5	0	1	4	0	-4	10	12	4	-7	3	4
-5	2	11	12	0	-6	14	15	3	1	6	6	8	5	4	6	-5	1	29	29	0	-3	46	48	4	-5	14	14
-5	4	7	7	0	-5	8	7	3	2	4	5	9	-5	4	5	-5	2	25	25	0	-3	48	48	4	-4	18	19
-5	5	21	18	0	-5	6	7	3	3	5	5	9	-3	2	6	-5	3	23	23	0	-2	2	3	4	-3	19	17
-5	7	3	5	0	-4	10	10	3	4	8	7	9	-2	5	5	-5	4	23	20	0	-2	2	3	4	-2	43	47
-4	-6	9	8	0	-4	9	10	3	6	1	3	9	-1	17	16	-5	5	15	15	0	-1	1	1	4	-1	10	11
-4	-5	1	4	0	-3	58	56	4	-7	2	2	9	0	5	6	-5	7	8	7	0	-1	1	1	4	0	10	10
-4	-4	36	34	0	-3	59	56	4	-6	5	6	9	1	17	17	-5	8	6	6	0	0	29	31	4	1	34	38
-4	-3	21	23	0	-2	45	45	4	-5	12	12	9	2	7	7	-4	0	29	32	0	0	29	31	4	2	2	5

Table 8 (Continued)

4	3	1	2	-11	1	9	8	-5	2	24	23	-1	7	6	7	3	0	20	21	-11	6	2	4	-5	5	9	8
4	4	26	25	-11	4	4	5	-5	3	19	16	0	-6	1	3	3	1	7	7	-10	-5	7	7	-5	6	11	11
4	6	5	5	-11	5	5	5	-5	4	5	6	0	-5	26	23	3	3	30	31	-10	-4	3	4	-4	-8	3	5
4	7	5	5	-10	-3	8	6	-5	5	14	11	0	-5	27	23	3	4	13	12	-10	-3	9	8	-4	-7	9	9
5	-5	3	4	-10	-2	13	11	-5	7	2	6	0	-4	45	42	3	6	11	10	-10	-2	10	10	-4	-6	3	6
5	-4	6	6	-10	0	14	13	-4	-7	4	6	0	-4	46	42	3	7	5	5	-10	-1	6	6	-4	-5	20	18
5	-3	4	5	-10	1	10	10	-4	-6	22	20	0	-3	13	13	4	-5	26	23	-10	1	10	10	-4	-4	5	5
5	-1	20	22	-10	3	6	7	-4	-5	13	13	0	-3	13	13	4	-4	17	17	-10	2	5	4	-4	-3	28	26
5	0	27	28	-10	4	12	10	-4	-4	13	12	0	-2	102	105	4	-3	6	6	-10	4	7	7	-4	-2	36	39
5	1	13	15	-9	-4	6	6	-4	-3	27	26	0	-2	103	105	4	-2	72	70	-9	-4	8	7	-4	-1	10	11
5	2	21	21	-9	-3	4	5	-4	-2	16	17	0	-1	15	16	4	-1	10	10	-9	-3	4	6	-4	0	45	48
5	3	12	11	-9	-2	14	13	-4	-1	7	7	0	-1	15	16	4	0	3	5	-9	-2	2	4	-4	1	36	36
5	4	10	11	-9	-1	14	13	-4	0	77	80	0	0	23	24	4	1	21	22	-9	-1	17	15	-4	2	17	18
5	5	8	8	-9	1	3	4	-4	1	27	28	0	0	23	24	4	2	21	21	-9	0	9	8	-4	3	1	3
5	6	2	4	-9	2	9	8	-4	2	16	17	0	1	37	36	4	4	8	8	-9	1	15	14	-4	4	30	28
6	-6	12	12	-9	3	7	7	-4	3	34	33	0	1	37	36	4	5	10	10	-9	2	8	8	-4	6	7	7
6	-5	33	30	-9	4	11	10	-4	4	28	27	0	2	22	22	5	-7	5	5	-9	3	12	11	-4	7	2	5
6	-4	6	7	-9	5	15	14	-4	5	15	11	0	2	22	22	5	-6	7	8	-9	5	12	11	-3	-8	2	5
6	-3	24	24	-8	-6	4	5	-4	6	10	11	0	3	13	13	5	-5	13	13	-8	-6	3	4	-3	-7	11	12
6	-2	6	7	-8	-4	9	10	-4	7	7	7	0	3	14	13	5	-4	3	4	-8	-4	8	7	-3	-5	13	12
6	-1	17	17	-8	-3	13	13	-4	8	2	3	0	4	36	32	5	-3	5	6	-8	-3	21	20	-3	-4	23	22
6	0	17	17	-8	-1	7	6	-3	-6	8	8	0	4	35	32	5	-2	8	8	-8	-2	13	12	-3	-3	3	4
6	1	11	11	-8	0	28	27	-3	-5	18	16	0	5	2	3	5	-1	12	14	-8	-1	18	18	-3	-2	20	22
6	2	11	12	-8	1	2	2	-3	-4	4	3	0	6	8	7	5	0	23	23	-8	0	23	22	-3	-1	94	100
6	3	20	18	-8	2	24	22	-3	-3	2	3	0	6	8	7	5	2	14	14	-8	1	1	1	-3	0	90	91
6	5	5	6	-8	3	20	18	-3	-2	55	61	0	7	11	10	5	3	13	13	-8	2	6	7	-3	1	22	22
6	6	5	5	-8	4	27	26	-3	-1	5	5	0	7	11	10	5	5	11	12	-8	3	4	5	-3	2	53	51
7	-8	2	3	-8	5	20	18	-3	0	62	64	1	-7	9	8	6	-4	4	3	-7	-5	8	9	-3	3	26	23
7	-6	8	9	-7	-5	10	10	-3	1	5	5	1	-5	23	21	6	-3	19	18	-7	-4	8	9	-3	4	26	24
7	-5	8	8	-7	-4	5	4	-3	2	44	41	1	-4	43	41	6	-2	10	11	-7	-3	15	14	-3	5	16	13
7	-3	12	10	-7	-3	9	8	-3	3	24	20	1	-3	20	20	6	-1	2	3	-7	-2	19	17	-3	7	8	8
7	-1	8	8	-7	-2	20	19	-3	4	30	26	1	-2	21	22	6	0	15	15	-7	-1	18	18	-2	-6	11	10
7	0	9	8	-7	-1	14	15	-3	5	7	7	1	-1	18	19	6	1	1	3	-7	0	3	2	-2	-4	36	34
7	1	16	16	-7	0	17	17	-3	6	3	3	1	0	14	13	6	2	6	6	-7	1	21	20	-2	-3	43	42
7	3	6	7	-7	1	11	12	-3	7	9	9	1	1	30	32	6	3	17	15	-7	2	11	10	-2	-1	180	200
7	4	3	3	-7	2	19	17	-3	8	2	3	1	2	53	52	7	-4	10	11	-7	3	12	13	-2	0	82	79
8	-5	9	10	-7	3	4	5	-2	-7	6	7	1	3	6	5	7	-2	12	11	-7	4	25	24	-2	1	42	40
8	-4	11	12	-7	4	4	5	-2	-5	3	4	1	4	23	20	7	0	8	10	-7	5	5	5	-2	2	27	27
8	-2	9	10	-6	-7	5	6	-2	-4	40	39	1	5	12	11	7	1	9	11	-7	6	5	5	-2	3	32	27
8	-1	18	17	-6	-5	14	13	-2	-3	44	45	1	6	4	4	7	2	11	11	-6	-5	18	15	-2	5	19	16
8	0	4	4	-6	-4	15	14	-2	-2	19	19	1	7	2	3	8	-3	5	7	-6	-4	17	16	-2	6	16	15
8	1	17	16	-6	-3	2	3	-2	-1	53	60	2	-8	4	6	8	-1	13	12	-6	-3	12	11	-1	-6	16	17
8	2	9	11	-6	-2	22	22	-2	0	23	23	2	-7	5	5	8	0	21	22	-6	-2	17	17	-1	-4	13	14
8	4	3	5	-6	-1	28	31	-2	1	2	3	2	-5	7	7	8	2	17	15	-6	-1	39	40	-1	-3	16	16
9	-6	5	6	-6	1	25	27	-2	2	50	47	2	-4	26	24	9	-4	2	4	-6	0	8	8	-1	-2	2	3
9	-4	2	2	-6	2	17	17	-2	3	6	6	2	-3	33	30	9	-3	9	11	-6	1	6	7	-1	-1	40	41
9	2	4	5	-6	3	15	16	-2	5	30	28	2	-1	39	42	9	-1	5	5	-6	2	26	27	-1	0	15	16
9	3	2	4	-6	4	14	12	-2	7	2	2	2	0	56	61	10	-3	3	5	-6	4	7	7	-1	1	40	34
10	-1	8	8	-6	5	14	14	-1	-6	12	12	2	1	6	6	10	1	5	5	-6	5	11	11	-1	2	7	8
10	0	6	6	-6	6	8	6	-1	-4	1	4	2	2	42	40	11	-1	3	4	-6	7	4	4	-1	3	20	19
10	1	5	7	-6	7	2	2	-1	-3	12	13	2	3	34	32					-5	-7	2	4	-1	4	28	24
				-5	-7	3	5	-1	-2	5	6	2	5	7	7		H =	3		-5	-3	22	22	-1	5	6	8
	H =	2		-5	-6	9	9	-1	-1	3	5	2	6	7	8	K	L	FO	FC	-5	-2	6	7	-1	6	21	19
K	L	FO	FC	-5	-4	14	14	-1	0	56	56	3	-6	10	11	-11	-3	4	5	-5	-1	13	13	0	-8	5	6
-12	-1	2	5	-5	-3	41	43	-1	1	42	41	3	-5	26	23	-11	-2	17	15	-5	0	50	52	0	-8	4	6
-12	1	5	5	-5	-2	10	9	-1	2	19	18	3	-4	2	2	-11	0	16	13	-5	1	30	31	0	-7	5	6
-12	5	3	4	-5	-1	30	30	-1	3	77	72	3	-3	9	10	-11	1	10	10	-5	2	26	25	0	-7	6	6
-11	-2	4	6	-5	0	35	37	-1	5	15	14	3	-2	54	53	-11	2	3	5	-5	3	1	2	0	-5	9	9
-11	0	1	2	-5	1	21	22	-1	6	4	4	3	-1	32	31	-11	4	4	4	-5	4	6	7	0	-5	9	9

Table 8 (Continued)

0	-4	10	11	4	0	12	11	-9	2	3	5	-4	2	21	20	0	2	42	43	6	0	10	10	-7	6	9	10
0	-4	11	11	4	1	9	9	-9	3	25	22	-4	3	35	29	0	4	24	21	6	1	18	15	-6	-7	8	8
0	-3	3	5	4	2	22	22	-9	4	8	8	-4	4	6	8	0	4	23	21	7	-3	3	6	-6	-6	8	8
0	-3	3	5	4	3	10	10	-9	5	7	7	-4	5	9	9	0	5	21	19	7	2	3	3	-6	-4	12	12
0	-2	46	46	4	4	3	3	-8	-6	3	4	-4	7	6	6	0	5	19	19	8	-2	3	7	-6	-3	20	20
0	-2	45	46	4	5	6	6	-8	-5	4	5	-3	-7	5	5	1	-6	3	3	8	0	7	7	-6	-2	12	13
0	-1	46	45	5	-6	6	9	-8	-3	7	7	-3	-6	4	6	1	-5	6	7					-6	-1	43	43
0	-1	44	45	5	-3	11	11	-8	-2	9	9	-3	-5	7	9	1	-4	4	4	H =	5			-6	0	26	26
0	0	25	26	5	-2	11	11	-8	-1	6	7	-3	-4	34	33	1	-3	14	14	K	L	FO	FC	-6	1	18	16
0	0	25	26	5	-1	23	23	-8	0	40	40	-3	-2	6	6	1	-2	5	6	-13	-2	2	3	-6	2	10	10
0	1	68	71	5	0	16	16	-8	1	22	21	-3	-1	5	5	1	-1	19	20	-13	0	6	5	-6	3	22	20
0	1	68	71	5	1	10	11	-8	2	5	6	-3	0	58	56	1	0	47	47	-12	-3	6	5	-6	5	11	11
0	2	6	7	5	2	8	8	-8	3	20	18	-3	1	26	26	1	1	18	20	-12	-2	5	5	-6	6	7	7
0	2	5	7	5	3	15	12	-8	4	13	14	-3	2	33	34	1	2	22	21	-12	0	9	9	-5	-6	6	8
0	3	3*	4	5	4	11	11	-8	5	7	9	-3	3	21	20	1	3	17	16	-12	3	8	7	-5	-5	7	7
0	3	3	4	6	-6	2	7	-8	7	2	5	-3	4	4	4	1	4	10	11	-11	-4	3	4	-5	-4	9	9
0	4	36	33	6	-3	4	4	-7	-7	2	3	-3	5	11	11	1	5	12	12	-11	-3	2	4	-5	-3	15	15
0	4	34	33	6	-2	8	8	-7	-5	8	9	-3	7	2	4	1	6	4	6	-11	-2	8	7	-5	-2	21	22
0	5	10	10	6	-1	13	14	-7	-4	20	16	-2	-6	9	9	2	-6	3	5	-11	1	4	4	-5	-1	13	15
0	5	9	10	6	0	16	18	-7	-3	4	4	-2	-5	13	14	2	-5	13	13	-11	2	12	11	-5	0	19	18
0	6	12	11	6	1	24	23	-7	-2	22	21	-2	-4	16	18	2	-3	31	29	-11	4	17	16	-5	1	22	20
0	6	14	11	6	3	7	9	-7	-1	18	19	-2	-3	24	23	2	-2	22	25	-11	5	2	6	-5	2	4	2
1	-7	3	5	6	4	7	8	-7	0	12	13	-2	-2	11	11	2	-1	7	7	-10	-4	7	7	-5	3	31	28
1	-5	3	5	7	-5	2	1	-7	1	19	19	-2	-1	6	6	2	0	24	25	-10	-3	3	5	-5	4	13	14
1	-4	21	20	7	-4	2	5	-7	2	25	23	-2	0	48	54	2	1	10	11	-10	-1	17	16	-5	6	8	7
1	-3	20	19	7	-2	11	11	-7	3	6	7	-2	1	8	9	2	3	24	22	-10	1	10	10	-4	-5	11	11
1	-2	26	28	7	-1	8	9	-7	4	13	12	-2	2	32	31	2	4	12	11	-10	2	10	9	-4	-4	24	21
1	-1	62	67	7	0	14	14	-7	5	3	4	-2	3	35	32	2	6	5	5	-10	3	11	12	-4	-2	26	26
1	0	17	19	7	1	6	6	-7	7	6	8	-1	-8	4	4	3	-6	8	7	-10	4	12	11	-4	-1	5	6
1	1	18	18	7	2	4	4	-6	-7	3	6	-1	-5	20	17	3	-5	3	5	-9	-6	3	3	-4	0	8	8
1	2	14	11	8	-3	2	5	-6	-6	2	3	-1	-2	41	45	3	-4	12	12	-9	-5	2	1	-4	1	17	19
1	3	24	24	8	-1	4	5	-6	-4	22	19	-1	-1	38	40	3	-3	8	9	-9	-3	11	10	-4	2	26	25
1	4	6	9	8	2	5	4	-6	-3	25	24	-1	0	40	38	3	-2	2	4	-9	-1	8	8	-4	3	12	14
1	6	6	8	8	3	5	5	-6	-2	8	8	-1	1	28	27	3	-1	21	21	-9	0	14	13	-4	4	28	24
2	-6	9	10	9	-2	2	6	-6	-1	18	18	-1	2	16	14	3	1	17	17	-9	1	17	16	-4	5	2	4
2	-5	14	15	9	1	2	5	-6	0	15	15	-1	3	7	7	3	2	22	19	-9	3	4	6	-4	7	2	4
2	-3	12	12					-6	2	41	40	-1	4	24	19	3	3	2	4	-9	4	2	4	-3	-7	4	4
2	-1	7	7		H =	4		-6	3	12	13	-1	5	39	33	3	4	6	7	-9	6	2	2	-3	-6	4	4
2	0	43	42	K	L	FO	FC	-6	5	11	12	-1	6	5	7	3	5	9	8	-8	-5	10	9	-3	-3	27	25
2	1	40	37	-14	1	2	5	-6	7	3	4	-1	7	8	8	4	-7	4	5	-8	-4	7	8	-3	-2	15	16
2	2	5	5	-13	-1	8	6	-5	-6	5	8	0	-8	2	3	4	-6	17	17	-8	-3	5	5	-3	-1	18	20
2	3	41	39	-12	-2	6	7	-5	-5	14	14	0	-8	3	3	4	-4	23	19	-8	-2	19	18	-3	0	25	25
2	4	14	12	-12	-1	6	6	-5	-4	12	11	0	-7	5	6	4	-2	6	8	-8	-1	14	13	-3	1	5	7
2	5	5	7	-11	0	6	6	-5	-3	24	24	0	-7	5	6	4	-1	15	13	-8	0	11	12	-3	2	39	38
2	6	4	7	-11	1	8	8	-5	-2	8	9	0	-5	18	19	4	0	20	19	-8	1	18	19	-3	3	19	16
3	-5	7	6	-11	3	4	6	-5	-1	16	16	0	-5	19	19	4	2	14	16	-8	3	3	5	-3	4	7	8
3	-3	7	7	-10	-4	7	6	-5	0	47	49	0	-4	14	16	4	3	7	6	-8	4	22	20	-3	5	7	6
3	-2	11	12	-10	-3	5	5	-5	1	44	46	0	-4	15	16	4	5	3	5	-7	-7	7	7	-3	6	10	9
3	-1	19	19	-10	-2	6	6	-5	2	18	19	0	-3	11	12	5	-6	4	5	-7	-6	2	4	-2	-6	11	10
3	0	23	21	-10	-1	10	11	-5	3	52	47	0	-3	11	12	5	-5	10	10	-7	-5	5	6	-2	-5	27	25
3	1	25	25	-10	0	1	3	-5	4	20	18	0	-2	31	32	5	-3	5	5	-7	-4	17	16	-2	-4	5	5
3	2	15	13	-10	1	14	13	-4	-8	3	4	0	-2	31	32	5	-2	9	9	-7	-3	6	5	-2	-3	47	45
3	3	2	3	-10	2	8	9	-4	-5	12	12	0	-1	15	16	5	0	9	9	-7	-2	8	8	-2	-2	9	10
3	4	2	5	-10	4	9	10	-4	-4	17	15	0	-1	15	16	5	1	9	9	-7	-1	22	23	-2	-1	2	2
4	-6	13	12	-9	-4	9	9	-4	-3	7	8	0	0	35	34	5	3	2	5	-7	1	8	9	-2	0	12	14
4	-5	8	8	-9	-3	14	12	-4	-2	35	39	0	0	35	34	5	4	3	5	-7	2	13	14	-2	1	36	33
4	-4	15	13	-9	-1	4	4	-4	-1	14	14	0	1	35	34	6	-5	6	6	-7	3	7	8	-2	3	29	28
4	-3	12	12	-9	0	22	20	-4	0	21	22	0	1	35	34	6	-2	12	13	-7	4	9	9	-2	4	11	11
4	-1	31	32	-9	1	17	17	-4	1	34	33	0	2	43	43	6	-1	7	9	-7	5	2	4	-2	6	3	6

Table 8 (Continued)

-1	-5	18	18	3	-2	9	9	-7	-3	11	11	-2	-2	28	27	4	-1	13	12	-5	-5	9	9	0	-1	10	10
-1	-4	23	21	3	-1	22	21	-7	-2	3	4	-2	-1	15	16	4	0	17	18	-5	-4	8	7	0	0	5	5
-1	-3	2	3	3	1	7	7	-7	-1	19	19	-2	0	33	31	4	3	5	6	-5	-3	7	8	0	0	5	5
-1	-2	16	17	3	2	14	13	-7	0	35	31	-2	3	21	20	5	-2	4	5	-5	-1	31	26	0	1	11	11
-1	-1	40	39	3	3	3	6	-7	1	4	6	-2	4	3	4	5	2	7	7	-5	0	5	4	0	1	11	11
-1	0	14	16	3	4	11	10	-7	2	6	6	-2	5	6	5	6	2	2	4	-5	1	24	25	0	2	11	10
-1	1	24	26	4	-5	2	3	-7	3	5	5	-2	6	2	2	7	-3	2	4	-5	2	15	17	0	2	11	10
-1	2	30	27	4	-3	10	9	-7	5	13	13	-1	-5	6	6					-5	3	5	5	0	3	8	8
-1	3	11	12	4	-1	7	6	-6	-6	6	7	-1	-4	11	12		H =	7		-5	4	9	9	0	3	7	8
-1	4	14	14	4	2	10	11	-6	-5	8	7	-1	-3	7	8	K	L	FO	FC	-4	-6	5	5	0	4	5	5
-1	5	4	7	4	3	4	2	-6	-4	6	5	-1	-2	31	29	-13	1	2	5	-4	-4	11	11	0	4	6	5
-1	7	6	6	5	-5	2	4	-6	-3	11	11	-1	-1	10	10	-12	-2	4	5	-4	-3	6	6	1	-7	2	5
0	-6	5	5	5	-3	5	6	-6	-2	16	13	-1	0	18	18	-12	-1	2	3	-4	-2	3	3	1	-6	5	6
0	-6	2	5	5	-1	11	12	-6	0	24	24	-1	1	13	12	-12	3	8	8	-4	-1	17	19	1	-5	7	7
0	-5	5	5	5	0	18	18	-6	2	8	8	-1	2	17	17	-11	-1	11	12	-4	0	13	14	1	-4	9	9
0	-5	4	5	5	1	11	10	-6	3	22	22	-1	3	21	22	-11	0	11	11	-4	2	25	23	1	-3	6	5
0	-4	14	13	5	2	8	9	-6	4	4	5	-1	5	6	7	-11	2	13	14	-4	4	11	12	1	-2	7	6
0	-4	13	13	5	4	6	6	-6	6	5	6	0	-6	9	9	-11	3	6	6	-3	-6	3	5	1	-1	11	11
0	-3	20	19	6	-4	10	9	-5	-6	2	4	0	-6	8	9	-10	-3	7	6	-3	-5	8	8	1	0	6	5
0	-3	18	19	6	-2	10	10	-5	-5	10	10	0	-5	4	5	-10	-1	15	14	-3	-3	17	17	1	1	11	12
0	-1	33	33	6	-1	16	16	-5	-4	7	7	0	-5	2	5	-10	0	14	16	-3	-2	21	20	1	3	3	5
0	-1	33	33	6	1	9	9	-5	-3	6	6	0	-4	9	9	-10	2	5	6	-3	-1	6	6	1	4	3	5
0	0	19	18	7	-4	5	5	-5	-2	43	42	0	-4	10	9	-10	3	10	10	-3	0	14	15	2	-7	4	5
0	0	19	18	7	0	2	5	-5	-1	64	63	0	-2	3	4	-10	4	4	6	-3	1	17	16	2	-6	3	4
0	1	16	16	8	1	2	4	-5	0	1	2	0	-2	4	4	-9	-5	6	7	-3	3	13	12	2	-5	5	6
0	1	17	16					-5	1	31	30	0	-1	25	24	-9	-4	5	6	-3	4	36	32	2	-4	2	3
0	2	36	35		H =	6		-5	2	17	20	0	-1	24	24	-9	-3	5	5	-3	6	7	8	2	-2	7	5
0	2	36	35	K	L	FO	FC	-5	3	5	6	0	0	34	32	-9	-2	13	12	-2	-6	4	5	2	-1	15	15
0	3	4	4	-13	0	5	5	-5	4	7	8	0	0	34	32	-9	0	7	8	-2	-5	7	6	2	1	10	10
0	3	5	4	-12	-2	2	5	-5	5	9	10	0	1	2	2	-9	1	16	15	-2	-4	12	10	2	2	7	6
0	5	2	5	-12	0	2	6	-5	6	8	7	0	2	21	20	-9	2	5	5	-2	-3	8	9	2	4	2	2
0	5	6	5	-12	1	4	5	-4	-7	4	5	0	2	20	20	-9	3	6	6	-2	-2	14	13	3	-3	2	4
0	6	6	7	-11	-4	4	5	-4	-6	5	5	0	3	12	13	-9	4	7	6	-2	-1	28	26	3	0	12	10
0	6	5	7	-11	-2	5	5	-4	-5	16	15	0	3	12	13	-8	-5	3	4	-2	0	13	12	3	2	2	4
1	-6	15	14	-11	-1	8	9	-4	-4	25	23	0	5	2	5	-8	-4	12	11	-2	1	29	29	3	3	2	4
1	-5	7	8	-11	1	9	9	-4	-3	9	9	0	5	4	5	-8	-3	5	5	-2	2	6	5	4	-4	2	3
1	-3	30	28	-11	2	9	9	-4	-2	69	64	0	6	3	3	-8	-2	6	6	-2	3	9	10	4	-3	4	6
1	-2	31	29	-11	4	10	9	-4	-1	46	45	1	-2	23	23	-8	-1	6	7	-2	4	10	11	4	-2	4	4
1	-1	7	6	-11	5	3	5	-4	1	22	22	1	-1	4	5	-8	0	10	9	-1	-6	2	3	4	-1	6	4
1	0	1	2	-10	-4	8	9	-4	2	14	14	1	0	13	13	-8	1	10	10	-1	-4	4	5	4	0	9	9
1	1	16	18	-10	-3	11	10	-4	3	15	15	1	1	17	17	-8	2	19	18	-1	-3	8	9	5	-2	5	5
1	2	16	17	-10	-1	10	10	-4	4	12	12	1	6	3	4	-7	-4	10	9	-1	-2	1	1	5	-1	7	6
1	3	10	11	-10	3	2	3	-4	5	14	17	2	-7	6	6	-7	-3	8	9	-1	-1	16	16				
1	4	13	12	-9	-5	6	7	-3	-4	4	3	2	-5	7	7	-7	-1	25	25	-1	0	10	10		H =	8	
1	5	8	9	-9	-3	9	8	-3	-3	5	6	2	-4	5	5	-7	0	27	26	-1	1	10	10	K	L	FO	FC
1	6	2	4	-9	-2	11	10	-3	-2	6	6	2	-3	4	5	-7	2	32	28	-1	2	10	11	-13	1	6	7
2	-6	14	14	-9	-1	8	9	-3	-1	17	20	2	-2	10	10	-7	3	14	14	-1	3	15	16	-13	3	9	10
2	-5	9	10	-9	0	8	9	-3	0	28	29	2	-1	19	18	-7	4	4	6	-1	4	6	7	-12	-2	5	6
2	-4	5	5	-9	1	12	13	-3	1	15	15	2	1	11	12	-6	-6	3	4	-1	5	5	5	-11	-1	4	4
2	-3	35	31	-9	3	13	14	-3	2	9	10	2	2	14	11	-6	-5	10	9	-1	6	3	5	-11	0	11	10
2	-2	15	14	-9	4	5	6	-3	3	18	17	2	5	3	5	-6	-4	5	5	0	-7	2	1	-10	-5	3	4
2	-1	5	6	-9	6	3	3	-3	4	5	6	3	-3	7	7	-6	-3	23	20	0	-5	2	3	-10	-2	5	6
2	0	12	12	-8	-5	5	6	-3	5	22	19	3	-2	10	9	-6	-2	4	5	0	-4	8	9	-10	0	8	9
2	1	18	17	-8	-2	23	22	-3	6	2	3	3	-1	9	9	-6	0	12	13	0	-4	10	9	-10	3	12	11
2	3	2	4	-8	-1	9	9	-2	-7	2	4	3	0	17	16	-6	2	7	8	0	-3	9	9	-9	-4	2	4
2	4	10	11	-8	1	18	18	-2	-6	1	2	3	2	2	6	-6	3	10	9	0	-3	9	9	-9	-2	12	12
3	-6	7	7	-8	4	9	9	-2	-5	6	6	3	3	16	15	-6	5	3	3	0	-2	5	6	-9	-1	6	5
3	-4	8	8	-7	-6	2	3	-2	-4	7	7	4	-3	3	6	-6	6	5	5	0	-2	5	6	-9	1	6	7
3	-3	7	7	-7	-4	13	13	-2	-3	11	10	4	-2	19	16	-5	-7	2	2	0	-1	11	10	-9	2	3	3

Table 8 (Continued)

-9 5	6	7	-2 -1	6	4	-8 -4	3	3	0 0	4	5	-3 2	6	7	-8 -2	3	4							
-8 -4	11	10	-2 1	20	19	-8 -3	4	5	0 0	6	5	-2 0	5	5	-7 -1	2	3							
-8 -3	8	8	-2 5	4	6	-8 -2	6	6	0 1	4	4	-2 2	5	5	-6 -3	3	4							
-8 -2	7	8	-1 -7	5	5	-8 -1	7	6	0 1	5	4	-2 3	3	4	-5 -2	4	5							
-8 -1	19	20	-1 -6	8	7	-8 0	3	4	0 2	8	7	-1 -5	4	4	-5 -1	5	5							
-8 0	10	9	-1 -4	10	10	-8 1	5	5	0 2	7	7	-1 -2	7	6	-5 1	7	7							
-8 2	12	12	-1 -3	20	17	-8 2	6	7	1 -2	3	3	-1 0	2	4	-4 -2	3	4							
-8 3	6	6	-1 -1	5	5	-8 3	2	2	1 -1	12	12	-1 1	4	5	-4 -1	2	4							
-8 5	7	7	-1 0	13	12	-7 -5	4	5	1 0	2	2	0 -2	4	4	-2 -2	5	4							
-7 -6	3	3	-1 2	8	7	-7 -4	5	6	1 1	2	3	0 -2	2	4	-1 -2	5	5							
-7 -3	7	8	-1 3	9	11	-7 -3	16	16	1 2	9	10	1 -1	5	5										
-7 -1	5	6	0 -7	6	7	-7 -2	30	26	2 -3	7	7	1 0	5	5	H = 13									
-7 0	6	10	0 -7	6	7	-7 -1	9	9	2 -2	2	4	2 -4	3	3	K L	FO	FC							
-7 1	7	7	0 -6	3	4	-7 0	17	16	2 -1	10	9	2 -1	4	3	-7 -1	3	3							
-7 2	2	5	0 -4	3	4	-7 1	9	9																
-7 3	15	14	0 -4	4	4	-7 3	2	3	H = 10				H = 11											
-7 6	2	4	0 -3	6	5	-7 4	9	9	K L	FO	FC	K L	FO	FC										
-6 -5	5	6	0 -3	6	5	-6 -5	10	8	-13 1	2	6	-11 -2	3	4										
-6 -3	6	6	0 -2	9	9	-6 -3	9	9	-12 0	3	4	-10 -2	3	5										
-6 -1	4	4	0 -2	10	9	-6 -2	18	17	-11 3	3	4	-10 -1	4	4										
-6 1	14	15	0 0	8	8	-6 -1	6	6	-10 -4	3	3	-10 2	3	5										
-6 2	11	12	0 0	8	8	-6 1	9	9	-10 -2	2	4	-9 -1	2	3										
-6 3	6	7	0 1	2	6	-6 2	8	8	-10 -1	5	6	-9 2	3	4										
-6 4	5	7	0 1	4	6	-6 4	13	13	-10 1	11	10	-8 -2	2	3										
-5 -4	11	11	0 3	7	7	-5 -2	3	4	-9 -4	3	4	-8 0	5	5										
-5 -3	17	17	0 3	7	7	-5 -1	11	11	-9 -2	4	6	-8 1	5	5										
-5 -2	12	11	0 4	2	4	-5 0	8	8	-9 -1	13	12	-8 3	2	4										
-5 -1	13	12	1 -7	2	2	-5 2	10	9	-9 0	2	3	-7 -4	4	6										
-5 0	10	9	1 -4	4	5	-5 3	5	5	-9 1	8	8	-7 -1	2	3										
-5 1	9	10	1 -2	8	6	-5 4	6	7	-9 2	11	10	-7 1	4	4										
-5 2	10	11	1 1	5	4	-5 5	4	5	-9 3	2	4	-7 2	5	5										
-5 4	6	6	1 2	11	9	-4 -5	5	5	-7 -4	2	4	-6 -1	6	6										
-5 5	4	5	1 3	2	5	-4 -3	12	12	-7 -2	9	9	-6 0	3	4										
-4 -6	8	8	2 -4	2	3	-4 -2	11	11	-7 -1	2	3	-5 -3	4	4										
-4 -5	10	9	2 -3	1	4	-4 -1	6	6	-7 0	2	5	-5 -2	3	4										
-4 -4	12	10	2 -2	3	3	-4 0	4	3	-7 1	8	8	-5 0	9	8										
-4 -3	4	3	2 -1	6	7	-3 -5	2	3	-6 -4	2	3	-5 1	3	6										
-4 -2	10	10	3 -2	12	10	-3 -3	7	8	-6 -3	4	5	-5 2	5	4										
-4 -1	7	6	3 -1	12	12	-3 -2	5	5	-6 -2	5	4	-4 -4	4	5										
-4 0	18	18	3 1	10	10	-3 -1	14	14	-6 -1	9	8	-4 0	4	4										
-4 1	10	10	4 -2	8	7	-3 0	9	9	-6 0	7	5	-4 2	3	3										
-4 2	16	16				-3 1	10	9	-6 1	8	8	-3 -4	3	4										
-4 3	11	9	H = 9			-3 2	16	17	-6 3	7	8	-3 -3	3	3										
-3 -6	6	6	K L	FO	FC	-3 4	3	4	-6 4	5	6	-3 -1	5	5										
-3 -5	7	7	-11 -3	4	6	-2 -3	3	4	-5 -3	6	5	-3 2	6	6										
-3 -4	3	4	-11 -2	5	6	-2 -2	5	4	-5 -2	4	5	-2 -3	2	4										
-3 -3	3	3	-11 0	10	10	-2 -1	17	15	-5 -1	1	3	-1 0	2	1										
-3 -2	15	15	-11 2	2	5	-2 0	9	7	-5 0	10	10	0 -2	2	4										
-3 -1	3	5	-11 3	2	4	-2 2	5	5	-5 1	6	5	0 -1	2	3										
-3 0	6	7	-10 -3	3	5	-1 -3	6	5	-5 2	8	6	0 -1	2	3										
-3 1	18	17	-10 -2	4	5	-1 -1	2	3	-5 3	19	18	1 -3	4	5										
-3 2	6	7	-10 -1	3	3	-1 0	7	6	-4 -3	6	5	1 -2	6	6										
-3 3	13	13	-9 -5	2	3	-1 1	4	5	-4 -2	7	7	1 0	2	5										
-3 4	2	3	-9 -4	5	4	0 -3	1	2	-4 0	8	9													
-3 6	4	5	-9 -3	2	4	0 -3	2	2	-4 1	2	3	H = 12												
-2 -5	3	4	-9 -1	12	12	0 -2	9	9	-3 -4	6	5	K L	FO	FC										
-2 -4	9	9	-9 2	2	4	0 -2	10	9	-3 -2	4	4	-9 -3	8	9										
-2 -3	7	5	-9 3	3	4	0 -1	9	8	-3 -1	6	6	-9 -2	4	4										
-2 -2	14	13	-9 4	2	4	0 -1	9	8	-3 1	6	6	-9 0	2	3										

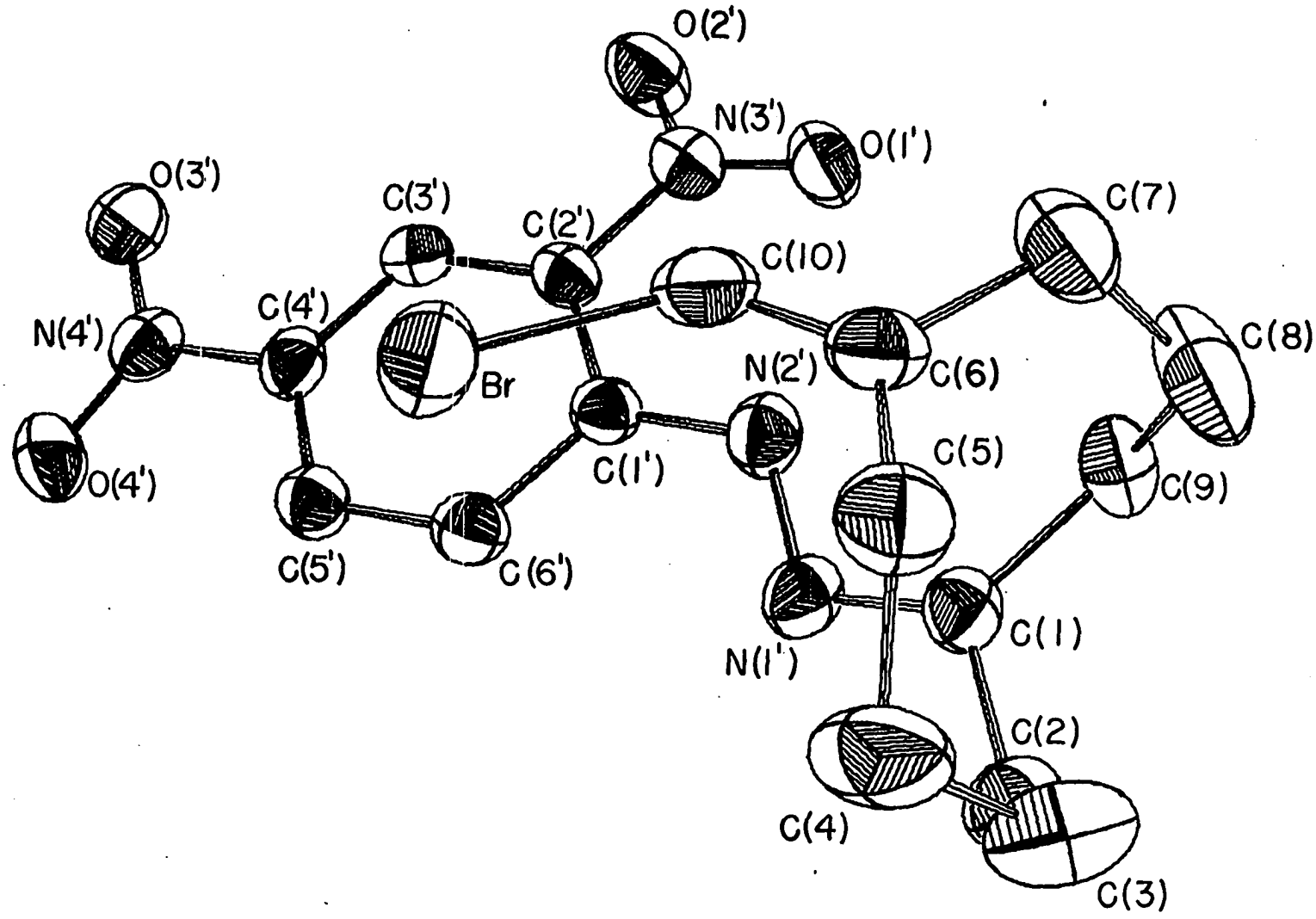

Figure 15. Computer-generated drawing of 2,4-DNP derivative of 5-bromomethylidene-cyclononanone, 4a. 30% probability ellipsoids depicted.

for the silver-assisted solvolysis of 10,10-dibromo[4.3.1]-propellane[48] (reaction I).

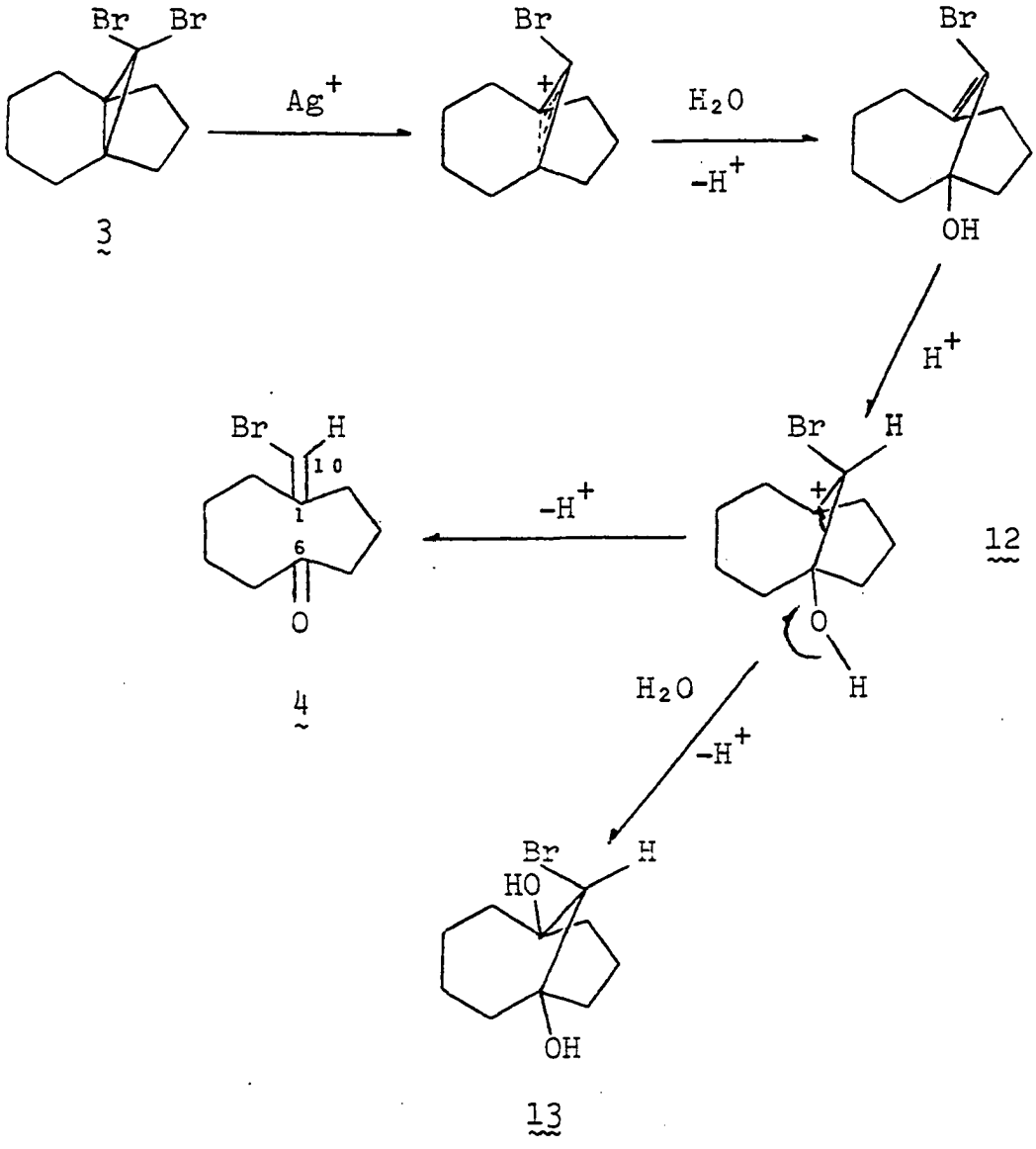

The conformation of 13 (and consequently of 12) had been previously determined by Warner, et al.[65]. The stereochemistry of 4, as evidenced in Figure 15, implies retention

at C(10) of the orientation of the bromine with respect to the carbon ring in the fragmentation of 12 to 4 (it should be recalled that only one stereoisomer of 4 was detected).

Another interesting conformational feature is the position of the exocyclic carbon C(10) with respect to the nine-membered ring, indicating the possibility of transannular interaction across the ring. The C(1)-C(6) distance is 3.06(1) Å as opposed to 2.58(2) Å for a similar bridged system[65]. The C(1)-C(10) distance is 3.43(1) Å. This transannular interaction is indeed observed in the bicyclization of the parent compound 4 to the diacetate 7 (reaction III). The conformation of 7 has been unambiguously determined (via hydrogenative correlation) from a single crystal X-ray study of its unsaturated analogue[52]. As with the silver-assisted solvolysis of 10,10-dibromo[4.3.1]propellane described above, the stereochemistry of 4 implies retention at C(10) in the bicyclization reaction.

The conformation of the nine-membered ring most closely resembles the "twisted chair boat" (TCB) conformation (see Figure 16) found in cyclononanone[66]. A comparison of torsional angles in the two rings is given in Figure 17. This conformation is also found in the structure of cyclononylamine hydrobromide[67]. It is interesting to note that while the same conformation is found in the three different nine-membered ring systems, this conformation is

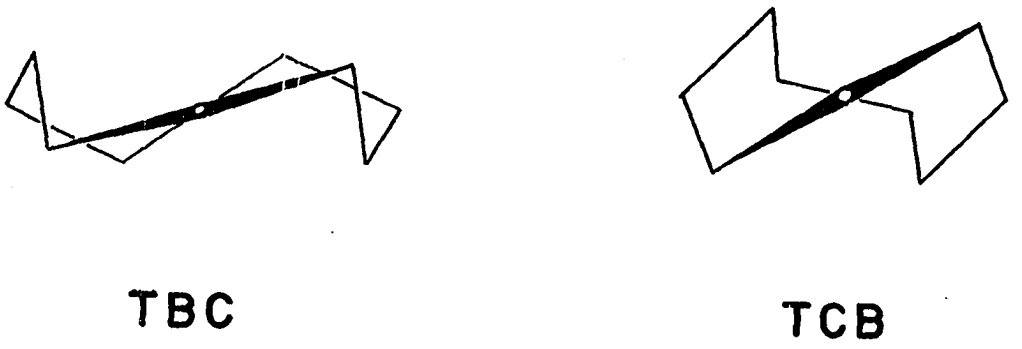

Figure 16. Perspective illustration of the "twisted boat chair"(TBC) and "twisted chair boat"(TCB) conformations in cyclononane.

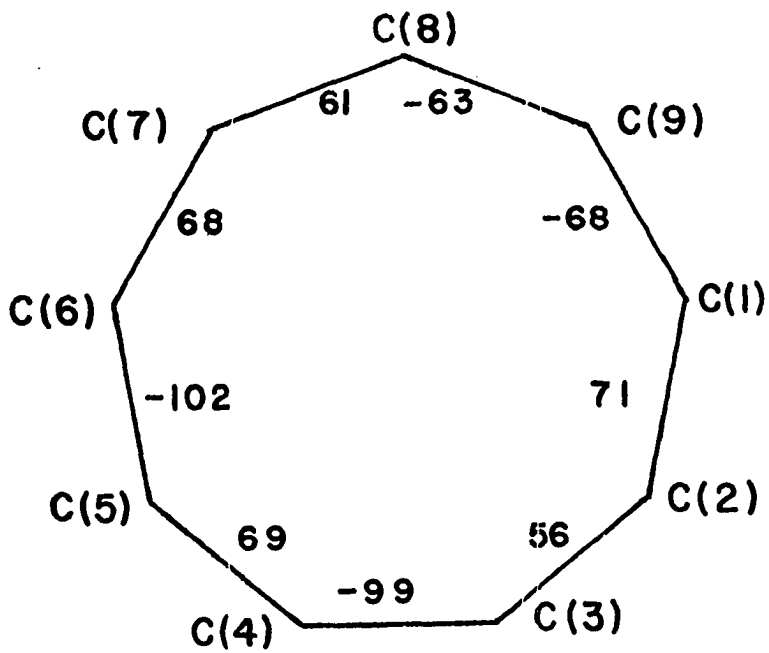

4a

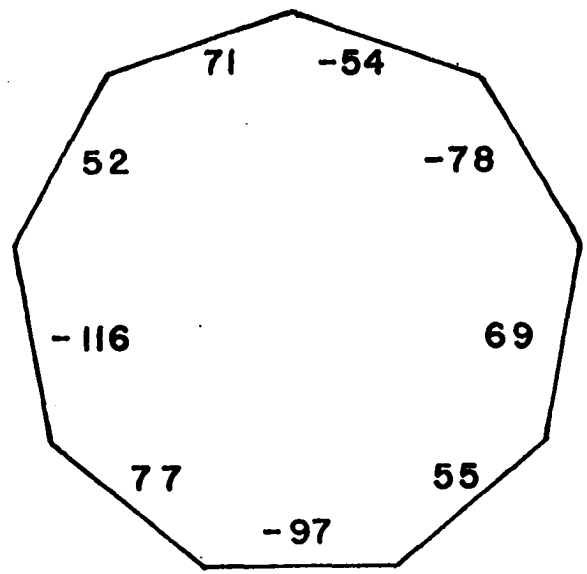

CYCLONONANONE

Figure 17. A comparison of the torsional angles in the nine-membered ring in the 2,4-DNP derivative of 5-bromomethylidenecyclononanone, 4a, and cyclononanone(atom designations as in Figure 15).

not considered to be energetically the most stable. Strain energy minimization calculations[68,69] for cyclononane predict the "twisted boat chair" (TBC) conformation depicted in Figure 16 as the energetically favored conformation by approximately 2.2 kcal/mole over the TCB conformation. ^{1}H and ^{13}C temperature dependent nmr studies on cyclononane[70] support this contention. The TBC conformation has also been proposed as the stable conformation in 1,1,4,4-tetramethylcyclononanone and related derivatives on the basis of low temperature nmr measurements and steric strain considerations[71]. The only crystallographic evidence for the TBC conformation results from an X-ray crystal structure determination of trimeric acetone peroxide[72], where the ring skeleton consists of six oxygen and three carbon atoms. Bixon and Lifson[68] suggest that the occurrence of the TCB conformation in cyclononylamine hydrobromide results from intermolecular packing forces. It is also possible that the substituents attached to the carbon rings in the structures found to have the TCB conformation distort these rings from an energetically more favorable conformation. Effects of this type have been extensively studied, especially with respect to six-membered carbon ring systems (see, for example, Kellie and Riddell[73]). 4a with its bulky dinitrophenylhydrazone group, appears to be the most likely candidate for substituent effects. However, it seems likely

that any substituent effect would be due to an unsymmetrical substitution on the carbon ring, as the structure of symmetrically substituted 1,1,4,4-tetramethylcyclononanone was found to have the TBC conformation[71]. For cyclononanone and 4a there is the additional possibility that the presence of unsaturated carbon atoms in the ring could lead to further ring distortion. Still, it is interesting that essentially the same conformation should be found in three nine-membered carbon ring systems with varying substituents and varying degrees of unsaturation.

A comparison of the bond distances and angles in 4a with those of cyclononanone and cyclononylamine hydrobromide shows that, on the average, there is a fair degree of agreement in the bond angles. The C-C-C angles range from 114° to 119° in 4a with a mean value of 117.1°, while in cyclononylamine hydrobromide they range from 114° to 120° with a mean value of 116.7° (average for the two stereoisomers found in the asymmetric unit), and in cylononanone the range is from 109° to 122.5° with a mean value of 116.4° (average of two stereoisomers found within the asymmetric unit). The bond distances are, on the average, shorter in 4a (mean value 1.513 Å) than those found for both cyclononylamine hydrobromide (mean value 1.532 Å) and cyclononanone (mean value 1.533 Å). The shorter average bond distance may be due to the presence of two unsaturated carbons in the ring, as

opposed to cyclononanone, in which there is only one unsaturated carbon, and cyclononylamine hydrobromide, which contains a saturated nine-membered ring.

One of the more interesting aspects of the structure of 4a lies in the dinitrophenylhydrazone moiety. There is an unusually high degree of planarity in the dinitrophenylhydrazone group, as shown by the atomic displacements of the atoms in the group from the least-squares plane of the benzene ring (Table 9). In addition, the C(1')-N(2') distance (1.36(1) Å) is midway between that of a conjugated system, such as cyanuric chloride[74] (average C-N distance 1.33 Å) and a benzylic carbon-nitrogen single bond, such as that found in 4-bromo-2,3-dimethyl-1-phenyl-5-pyrazolone[75] (1.39 Å). Also the N(1')-N(2')-C(1') angle of 118.7(7)° is more representative of sp^2 hybridization than sp^3. These three observations imply an increased π-character in N(2'). This increased π-character can be explained by placing the lone pair in an orbital with predominantly p-character, thus enhancing the possibility of π-bonding with the dinitrophenyl ring and subsequent withdrawal of electron density from the hydrogen H(N). The electron deficient character of this hydrogen would be expected to enhance its chances for hydrogen bond formation to the oxygen atom on the adjacent nitro group. This appears to be the case, as evidenced by the N(2')-O(1') distance of 2.61(1) Å, as well as the high degree of

Table 9. Atomic displacements from the least squares plane[a] defined by the benzene ring of the 2,4-DNP group in 4a

Plane defined by atoms (C(1'), C(2'), C(3'), C(4'), C(5'), C(6'))

$-.91704\ X + .26185\ Y + .30076\ Z = 2.54242$

Atom	Deviation from plane (Å)
C(1')	.008
C(2')	-.007
C(3')	.003
C(4')	-.001
C(5')	.003
C(6')	-.007
O(1')	-.052
N(1')	.093
N(2')	.033
N(3')	.052
N(4')	.069
C(1)	-.086
C(2)	.055

[a]Plane is defined by $C_1X + C_2Y + C_3Z - d = 0$ where X, Y, and Z are coordinates along the cartesian a, b, and c axes.

planarity in the O(1')-N(3')-O(2') group with respect to the benzene ring (the angle between the plane defined by O(1')-N(3')-O(2') group and that of the benzene ring is 6.2° as opposed to 23.2° between the benzene ring plane and the plane defined by O(3')-N(4')-O(4')).

There appears to be a large degree of distortion in the C-C-C angles of the dinitrophenyl group from the ideal value of 120°. However, both bond distances and angles generally agree well with those found in 2,6-dinitrophenol[76].

A stereoscopic view of the unit cell is given in Figure 18. No abnormally short intermolecular distances were found, indicating that crystal packing is governed primarily by van der Waals forces.

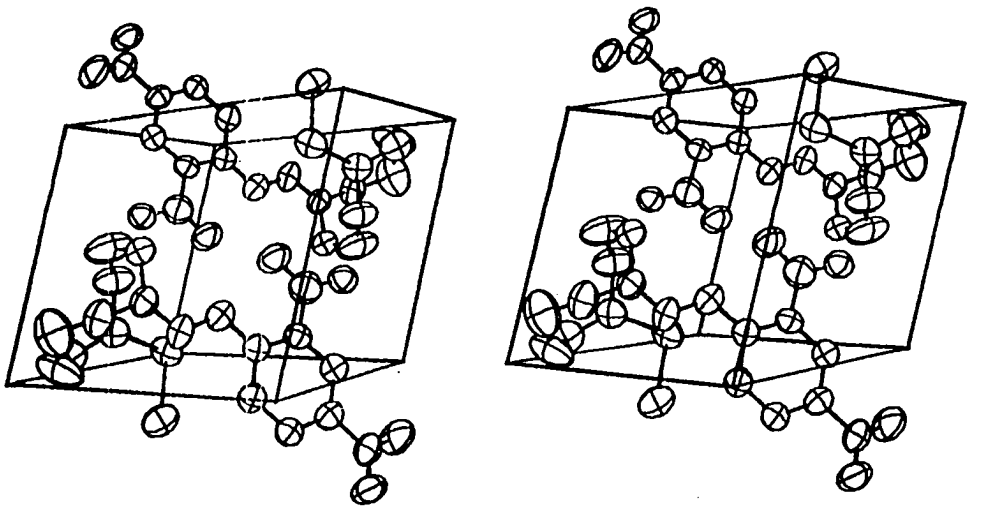

Figure 18. Unit cell stereograph of the 2,4-dinitrophenylhydrazone derivative of 5-bromomethylidenecyclononanone.

The Crystal and Molecular Structure of 1-hydroxy-6-acetoxy-10α-bromo-bicyclo[4.3.1]deca-3-ene, 10

Crystal data

$C_{12}H_{17}O_3Br$, M.W. = 289.1, monoclinic $P2_1/n$,
a = 10.45(2), b = 14.38(4), c = 8.06(2), β = 93.81(2),
V = 1208.6 Å^3, ρ_{calc} = 1.59, Z = 4, Mo Kα (λ = 0.70954 Å),
μ = 35.4 cm^{-1}

Experimental

White, irregularly shaped crystals were obtained by recrystallization from a CH_2Cl_2-hexane solution. The crystals were observed to be reasonably air stable (decomposing slowly if left standing at room temperature for an extended period of time), and a single crystal of approximate dimensions .2 x .2 x .1 mm was mounted on a glass fiber with Duco cement and attached to a standard goniometer head. Both preliminary data and intensity data were collected using an automated four-circle diffractometer described in the introduction. From four preliminary ω-oscillation photographs taken at various χ and ϕ settings, 10 independent reflections were chosen for input into an automatic indexing algorithm[53]. The resulting reduced cell and reduced cell scalars indicated monoclinic symmetry. The unit cell parameters and their standard deviations were obtained by a least-squares fit[54] to 20 independent high angle reflections ($|2\theta| > 23^\circ$), whose

centers were determined at ± 2θ by half-height techniques on a previously aligned four-circle diffractometer (Mo Kα radiation, λ = 0.70954 Å).

Two octants of data (hkℓ, hk$\bar{\ell}$) were collected within a 2θ sphere of 50°. Intensities were measured by the stationary crystal, stationary counter method, and background counts were taken at the beginning and end of each measurement by offsetting in ω-2θ. As a check on electronic and crystal stability, the intensities of three standard reflections were remeasured every 50 reflections. The standards did not vary significantly during the course of data collection, indicating that no crystal decomposition occurred. A total of 1933 unique non-zero reflections were collected. Examination of the data revealed systematic absences of hOℓ reflections for h + ℓ = 2n + 1 and 0k0 reflections for k = 2n + 1, thus uniquely defining the space group as $P_{2_1/n}$, with one molecule per asymmetric unit. The intensity data were corrected for Lorentz, polarization and background effects; however no corrections for absorption or secondary extinction were made. There were 1044 reflections having $|F_o|^2 > 3\sigma_I$, where

$$\sigma_I^2 = C_T + 2C_B + (0.03C_T)^2 + (0.03C_B)^2,$$

C_T and C_B being the total count and background count, respectively, while the factor 0.03 represents an estimate of the non-statistical errors. The estimated standard deviation

in each structure factor was calculated by the finite difference method[55].

Solution and refinement

The position of the bromine atom was determined by analysis of an unsharpened Patterson map[57]. The remaining non-hydrogen atoms were located by successive structure factor[58] and electron density map[57] calculations. Approximate positions for the methylene hydrogens were calculated from the carbon atom positions using typical C-H distances and H-C-H angles appropriate for the $C-CH_2-C$ group. The remaining hydrogen atom positions were obtained by analysis of electron density difference maps. The positional parameters for all atoms, as well as the anisotropic thermal parameters for all non-hydrogen atoms, were refined by a full-matrix least-squares procedure[58], minimizing the function $\Sigma\omega(|F_o| - |F_c|)^2$, where $\omega = 1/\sigma_F{}^2$. Analysis of the weights was performed via the requirement that $\overline{\omega\Delta^2}$ should be a constant function of $|F_o|$[59]. The analysis showed the reflections at large $|F_o|$ to be overweighted, and the weights were subsequently adjusted. Successive iterations of refinement reduced the conventional discrepancy index to 0.084 for 1044 observed reflections. The weighted R factor was 0.104. The scattering factors used were those of Hanson, et al.[60], except for hydrogen, where the values used were those of Stewart, et al.[61]. The scattering factors of

bromine were modified for the real and imaginary parts of anomalous dispersion[62].

Tables 10 and 11 list the positional and thermal parameters and their estimated standard deviations. Bond distances (Table 12) and angles (Table 13), along with their estimated standard deviations were calculated from the unit cell parameters and positional parameters using a procedure developed by Busing, et al.[63]. The standard deviations were computed using the variance-covariance matrix obtained from the final least-squares cycle. Table 4 lists the observed and calculated structure factors for the observed reflections.

Discussion

A computer generated[64] drawing of 1-hydroxy-6-acetoxy-10α-bromo-bicyclo[4.3.1]deca-3-ene, 10 is given in Figure 19. The six-membered ring is in the chair conformation. Comparison of the torsional angles for this ring (see Figure 23) with the most probable value (56°) for cyclohexane[77] (as determined by electron diffraction and strain energy minimization calculations) shows the ring to be slightly flattened with respect to that of cyclohexane. The seven-membered ring also lies in the chair conformation with six of the seven carbons in a near-planar conformation (Table 15). With one exception, the bond distances and angles generally agree with accepted values. The exception is the C(2)-C(1)-O(1) angle of 99°(1) which is significantly smaller than

Table 10. Final atomic positional parameters[a] with their standard deviations for 10[b]

Atom	x	y	z
Br	1580(1)	3761(1)	-0417(1)
O(1)	-0070(8)	4178(6)	2668(1)
O(2)	-0280(10)	2627(6)	3121(13)
O(3)	3958(9)	2732(8)	1475(13)
C(1)	3488(12)	3526(8)	2307(16)
C(2)	4193(15)	4358(11)	1647(22)
C(3)	3900(19)	5328(14)	2208(27)
C(4)	2810(17)	5674(10)	2598(19)
C(5)	1514(14)	5279(11)	2641(22)
C(6)	1339(12)	4248(8)	3006(16)
C(7)	1694(20)	4032(11)	4855(29)
C(8)	3107(16)	4007(13)	5259(19)
C(9)	3769(17)	3341(15)	4166(23)
C(10)	2047(13)	3574(9)	1978(15)
C(11)	-0696(14)	3389(10)	2793(15)
C(12)	-2099(15)	3558(14)	2402(26)
H(2a)	257(16)	382(10)	-003(19)
H(2b)	510(18)	445(12)	178(23)
H(3)	447(24)	549(18)	227(31)

[a]The heavy atom positional parameters are $x10^4$; the hydrogen atom positional parameters are $x10^3$.

[b]Numbering as in Figure 19, with the hydrogen atoms having the same number as the atom to which they are attached.

Table 10 (Continued)

Atom	x	y	z
H(4)	250(20)	633(12)	239(23)
H(5a)	088(19)	550(14)	315(23)
H(5b)	100(17)	542(12)	188(21)
H(7a)	148(18)	442(12)	564(21)
H(7b)	107(27)	361(14)	502(33)
H(8a)	322(16)	469(12)	512(19)
H(8b)	333(19)	380(13)	612(24)
H(9a)	444(17)	347(14)	443(23)
H(9b)	342(16)	283(12)	404(21)
H(10)	176(16)	294(13)	205(20)
H(12a)	-267(18)	340(13)	322(22)
H(12b)	-237(19)	398(13)	220(26)
H(12c)	-189(16)	390(10)	074(21)
H(O)	459(18)	278(13)	208(23)

Table 11. Final atomic thermal parameters[a] with their standard deviations for 10 [b].

Atom	β_{11}	β_{22}	β_{33}	β_{12}	β_{13}	β_{23}
Br	117(2)	93(1)	121(2)	-19(2)	-0(2)	-3(2)
O(1)	69(10)	31(5)	192(19)	-0(6)	34(11)	5(7)
O(2)	130(12)	30(5)	231(21)	-6(7)	70(13)	-6(9)
O(3)	85(10)	55(6)	194(20)	19(8)	24(12)	-13(9)
C(1)	65(13)	28(8)	147(22)	12(8)	19(14)	9(9)
C(2)	62(16)	50(10)	261(36)	-9(10)	20(19)	9(15)
C(3)	120(28)	50(12)	205(31)	-12(13)	14(23)	1(15)
C(4)	140(20)	19(8)	206(30)	-3(12)	38(19)	13(12)
C(5)	74(16)	33(8)	229(35)	2(10)	26(19)	-3(13)
C(6)	58(13)	30(7)	162(23)	-5(8)	12(14)	-3(11)
C(7)	78(14)	49(11)	234(40)	-3(12)	38(19)	-20(16)
C(8)	91(19)	61(12)	167(28)	16(11)	-23(20)	-6(15)

[a]The β_{ij}'s are $x10^4$. The hydrogen atoms were refined with fixed isotropic thermal parameters $B_H = 4.0$. The form of the anisotropic temperature factor is $\exp(-(\beta_{11}h^2 + \beta_{22}k^2 + \beta_{33}\ell^2 + 2\beta_{12}hk + 2\beta_{13}h\ell + 2\beta_{23}k\ell))$.

[b]Numbering as in Figure 19 with the hydrogen atoms having the same number as the heavy atom to which they are attached.

Table 11 (Continued)

Atom	β_{11}	β_{22}	β_{33}	β_{12}	β_{13}	β_{23}
C(9)	104(20)	67(11)	195(33)	22(13)	6(21)	9(16)
C(10)	91(4)	29(7)	107(20)	-2(8)	3(13)	-3(10)
C(11)	121(18)	28(7)	109(21)	-6(10)	54(16)	-19(10)
C(12)	70(16)	64(14)	287(46)	-11(11)	23(20)	-5(18)

Table 12. Selected bond distances (Å) for 10

C(1)-C(2)	1.54(2)	C(10)-C(6)	1.50(2)
C(2)-C(3)	1.50(3)	C(10)-Br	1.99(1)
C(3)-C(4)	1.31(2)	C(1)-O(3)	1.43(2)
C(4)-C(5)	1.47(2)	C(6)-O(1)	1.49(2)
C(5)-C(6)	1.53(2)	C(11)-O(1)	1.32(2)
C(6)-C(7)	1.56(2)	C(11)-O(2)	1.21(2)
C(7)-C(8)	1.51(2)	C(11)-C(12)	1.51(2)
C(8)-C(9)	1.49(3)	C(1)-C(6)	2.58(2)
C(9)-C(1)	1.55(2)	O(2)-O(3)[a]	2.94(2)
C(10)-C(1)	1.52(2)		

[a]Position equivalent to reference molecule; related by symmetry operation $x-\frac{1}{2}$; $\frac{1}{2}-y$; $\frac{1}{2}+z$

Table 13. Selected bond angles for 10

Angle	Degrees	Angle	Degrees
C(1)-C(2)-C(3)	121.5(14)	C(1)-C(10)-Br	111.0(8)
C(2)-C(3)-C(4)	128.3(15)	C(1)-C(10)-C(6)	117.1(11)
C(3)-C(4)-C(5)	132.9(14)	C(2)-C(1)-O(3)	106.7(11)
C(4)-C(5)-C(6)	120.1(12)	C(10)-C(1)-O(3)	108.9(11)
C(5)-C(6)-C(7)	111.1(12)	C(9)-C(1)-O(3)	106.0(11)
C(6)-C(7)-C(8)	112.2(13)	C(10)-C(6)-O(1)	111.8(11)
C(7)-C(8)-C(9)	112.0(14)	C(7)-C(6)-O(1)	109.5(11)
C(8)-C(9)-C(1)	113.8(14)	C(5)-C(6)-O(1)	99.1(10)
C(9)-C(1)-C(2)	114.4(13)	C(6)-O(1)-C(11)	122.3(11)
C(9)-C(1)-C(10)	107.8(12)	C(12)-C(11)-O(2)	121.5(12)
C(2)-C(1)-C(10)	112.9(11)	C(12)-C(11)-O(1)	109.1(12)
C(5)-C(6)-C(10)	116.5(12)	O(2)-C(11)-O(1)	129.4(14)
C(7)-C(6)-C(10)	108.5(10)		
C(6)-C(10)-Br	110.9(9)		

Table 14. Observed and calculated structure factors for 10.

H = 0

K	L	FO	FC
0	-8	16	14
0	-4	118	106
0	-2	87	81
0	2	88	81
0	4	109	106
0	8	16	14
1	-9	18	14
1	-8	18	11
1	-6	40	44
1	-4	60	64
1	-3	22	20
1	-2	43	37
1	-1	54	50
1	1	47	50
1	2	32	37
1	3	18	20
1	4	83	84
1	6	42	44
1	8	16	13
1	9	17	14
2	-9	18	21
2	-7	38	41
2	-5	56	55
2	-4	39	35
2	-3	119	102
2	-2	16	14
2	-1	101	87
2	0	89	85
2	1	91	87
2	2	13	14
2	3	99	102
2	4	33	35
2	5	55	55
2	7	41	41
2	8	9	3
2	9	21	21
3	-8	17	16
3	-6	29	30
3	-5	16	16
3	-4	44	44
3	-3	34	32
3	-2	32	29
3	-1	57	57
3	1	59	57
3	2	28	29
3	3	28	32
3	4	41	44
3	5	13	16
3	6	32	32
3	8	13	16
4	-5	12	14
4	-4	54	57
4	-2	84	84
4	-1	62	65
4	0	193	155
4	1	69	52
4	2	81	84
4	4	60	67
4	5	14	14
5	-8	17	18
5	-6	14	13
5	-4	62	55
5	-3	35	29
5	-2	35	31
5	-1	51	40
5	1	40	40
5	2	32	31
5	3	25	29
5	4	52	55
5	6	13	13
5	8	18	18
5	9	12	10
6	-7	36	36
6	-6	14	14
6	-5	21	21
6	-3	84	78
6	0	65	52
6	3	74	78
6	5	21	21
7	-8	14	12
7	-7	16	15
7	-6	23	23
7	-5	26	26
7	-4	24	21
7	-3	22	21
7	-2	17	14
7	-1	50	44
7	1	47	44
7	2	16	14
7	3	19	21
7	4	21	21
7	5	18	26
7	6	22	23
7	7	11	15
7	8	14	12
8	-4	18	17
8	-3	10	8
8	-2	52	49
8	-1	19	18
8	0	59	51
8	1	22	18
8	2	52	49
8	4	12	17
9	-8	12	10
9	-4	26	25
9	-2	12	10
9	-1	34	29
9	1	33	29
9	2	10	10
9	3	12	11
9	4	24	25
10	-7	13	11
10	-5	33	30
10	-3	16	12
10	-2	40	36
10	-1	22	19
10	0	32	26
10	1	22	19
10	2	34	36
10	3	13	12
10	5	28	30
10	7	12	11
11	-5	12	12
11	-4	14	14
11	-1	35	30
11	1	35	30
11	4	15	14
12	-2	29	25
12	-1	35	31
12	1	31	31
12	2	26	25
13	-4	17	15
13	-1	12	12
13	1	14	12
13	4	16	15
14	-2	17	16
14	-1	19	20
14	1	18	20
14	2	17	16
15	-1	14	11
15	1	14	11

H = 1

K	L	FO	FC
0	-9	27	30
0	-7	31	34
0	-5	80	80
0	-3	22	20
0	-1	106	103
0	1	51	40
0	3	209	189
0	5	31	28
0	7	33	37
1	-8	19	20
1	-6	29	33
1	-5	32	31
1	-4	11	12
1	-3	74	69
1	-1	33	36
1	0	63	65
1	1	67	68
1	2	35	37
1	3	68	61
1	4	80	83
1	6	23	23
1	7	22	21
1	8	12	9
1	9	17	16
2	-6	49	51
2	-5	12	11
2	-4	48	44
2	-3	57	52
2	-2	186	177
2	-1	40	39
2	0	158	157
2	1	32	34
2	2	70	73
2	3	24	25
2	4	17	15
2	6	27	25
2	8	31	29
3	-8	19	23
3	-7	10	8
3	-6	16	17
3	-5	12	12
3	-4	32	29
3	-3	69	65
3	-1	12	11
3	0	48	47
3	1	35	38
3	2	29	36
3	4	74	80
3	6	26	22
3	7	27	27
3	9	13	12
4	-9	28	27
4	-7	27	29
4	-6	12	12
4	-5	35	37
4	-3	44	39
4	-2	46	43
4	-1	37	35
4	0	13	14
4	1	104	103
4	2	19	25
4	3	49	54
4	5	50	55
4	7	22	24
5	-8	17	14
5	-6	28	28
5	-5	46	48
5	-3	38	35
5	-1	67	63
5	0	62	60
5	1	21	23
5	2	49	49
5	3	10	15
5	4	31	36
5	6	20	23
5	7	20	22
6	-6	19	20
6	-4	76	75
6	-3	15	12
6	-2	44	43
6	-1	18	15
6	0	102	90
6	1	37	34
6	2	38	37
6	3	32	33
6	6	24	25
6	8	16	15
7	-8	16	17
7	-4	38	35
7	-3	28	28
7	-2	13	9
7	-1	21	21
7	0	20	16
7	1	40	37
7	2	44	43
7	4	28	29
7	5	12	11
7	6	12	10
8	-7	22	20
8	-5	22	23
8	-3	10	6
8	-2	25	25
8	0	30	28
8	1	49	48
8	2	19	19
8	3	37	37
8	4	16	18
8	5	34	37
9	-6	16	15
9	-5	30	31
9	-3	14	11
9	-1	44	44
9	0	21	19
9	1	22	21
9	2	21	21
9	4	16	20
9	6	13	14
10	-4	26	27
10	-2	38	32
10	-1	14	10
10	0	29	24
10	1	15	17
10	2	13	14
10	3	11	11
10	4	12	9
11	-4	20	18
11	-2	15	19
11	-1	27	28
11	2	14	12
11	3	20	18
11	4	17	16
12	-4	19	16
12	-3	15	15
12	1	18	15
12	2	19	23
12	3	14	13
12	5	19	19
13	-4	11	8
13	-1	22	25
13	2	22	23
14	-4	17	14

H = 2

K	L	FO	FC
0	-8	25	25
0	-6	49	48
0	-4	74	76
0	-2	150	146
0	0	65	64
0	2	13	14
0	4	11	7
0	6	58	53
0	8	37	33
1	-8	24	25
1	-5	43	48
1	-3	42	41
1	-2	94	88
1	-1	56	60
1	1	29	28
1	2	67	70
1	3	29	29
1	4	71	68
1	5	37	33
1	7	26	27
1	9	17	14
2	-9	22	23
2	-7	26	26
2	-6	18	19
2	-5	24	22
2	-3	41	45
2	-2	17	14
2	-1	56	64
2	0	24	30
2	1	108	127
2	2	11	15
2	3	75	81
2	4	9	7
2	5	39	39
2	6	9	9
3	-8	23	22
3	-5	57	61
3	-3	27	26
3	-2	28	29
3	-1	85	89
3	0	103	103
3	1	19	23
3	2	51	55
3	3	30	35
3	4	32	34
3	5	27	27
3	6	14	14
3	7	24	26
4	-8	18	14
4	-6	50	51
4	-5	17	17
4	-4	74	77
4	-3	29	29
4	-2	43	44
4	-1	53	53
4	0	92	95
4	1	19	20
4	4	34	39
4	5	11	11
4	6	32	33
4	8	30	29
5	-8	15	15
5	-5	30	31
5	-4	16	14
5	-3	26	29
5	-2	59	53
5	0	41	41
5	1	13	16
5	2	52	55
5	3	10	14
5	4	12	13
5	5	28	31
5	6	22	21
5	7	29	18
6	-7	12	11
6	-2	66	64
6	-1	97	91
6	0	23	22
6	1	43	42
6	2	12	10
6	3	49	57
6	5	20	23
7	-8	12	8
7	-6	15	11
7	-5	40	42
7	-3	15	16
7	-2	30	31
7	-1	34	33
7	0	49	46
7	1	10	11
7	2	33	35
7	4	28	33
7	5	23	26
8	-8	11	8
8	-6	22	20
8	-5	10	11
8	-4	45	47
8	-3	24	25
8	-2	34	34
8	-1	44	45
8	0	30	27
8	1	14	14
8	4	24	25
8	6	19	20
9	-5	11	6
9	-4	15	15
9	-3	24	22
9	-2	40	38
9	2	28	28
9	3	15	15
9	4	13	14
9	7	12	13
10	-7	17	15
10	-2	18	17
10	-1	37	36
10	1	18	18
10	3	32	31
11	-6	14	10
11	-5	18	17
11	-3	14	7
11	-1	24	28
11	0	24	24

11	2	20	20	3	5	37	36	10	-6	12	8	3	-1	18	23	9	1	22	21	4	-7	21	19
12	-6	12	7	3	7	16	14	10	-4	27	29	3	0	38	40	9	2	15	14	4	-5	37	39
12	-4	20	18	3	8	12	13	10	2	20	21	3	1	31	38	9	3	13	14	4	-3	43	44
12	-2	11	4	4	-5	12	12	10	4	22	22	3	3	34	37	9	4	15	14	4	-1	28	27
12	0	15	19	4	-3	41	43	11	-5	17	14	3	5	29	33	9	5	13	11	4	0	10	7
13	-3	17	17	4	-2	30	31	11	2	14	15	3	6	19	20	10	-5	20	21	4	2	15	17
13	1	10	8	4	-1	90	96	11	3	12	13	3	8	16	16	10	-3	16	14	4	3	27	29
13	2	11	8	4	1	53	63	12	-3	24	22	4	-8	24	23	10	-1	37	35	4	5	21	20
14	-1	15	16	4	3	37	42	12	0	15	13	4	-6	24	25	11	-2	24	27	4	6	12	11
14	2	13	11	4	7	16	13	12	1	22	21	4	-4	24	26	11	-1	19	19	4	7	32	29
14	3	15	13	5	-7	21	22	13	-3	11	10	4	-2	23	26	11	1	14	15	5	-8	15	11
				5	-6	13	15	13	-1	14	12	4	-1	22	22	11	2	15	16	5	-6	15	15
	H =	3		5	-5	28	27	13	0	19	21	4	0	30	34	11	5	14	13	5	-5	15	16
K	L	FO	FC	5	-3	16	17	13	3	14	13	4	1	9	8	12	-1	13	11	5	-4	34	36
0	-9	17	14	5	-2	68	68	14	-2	11	11	4	2	69	85	12	0	14	17	5	-2	21	22
0	-7	13	11	5	0	53	57	15	0	12	9	4	4	46	52	12	4	18	20	5	-1	24	27
0	-5	36	37	5	2	37	42	16	-1	12	8	4	6	27	28	13	3	14	11	5	1	44	50
0	-3	32	35	5	3	43	52					5	-7	16	15	15	1	12	9	5	3	17	17
0	-1	76	78	5	4	11	13		H =	4		5	-5	20	21					5	6	24	21
0	1	160	149	5	5	33	38	K	L	FO	FC	5	-4	27	29		H =	5		5	8	16	12
0	3	59	53	5	8	16	13	0	-8	20	21	5	-3	14	13	K	L	FO	FC	6	-4	12	12
0	7	19	16	6	-8	17	16	0	-6	39	41	5	-2	62	68	0	-7	27	26	6	-2	18	21
0	9	18	15	6	-6	41	40	0	-4	36	38	5	0	13	15	0	-5	44	42	6	-1	17	17
1	-7	16	19	6	-5	13	13	0	-2	44	34	5	1	35	40	0	-3	59	56	6	0	55	61
1	-6	13	12	6	-4	26	27	0	0	109	96	5	3	31	36	0	1	72	62	6	2	37	39
1	-5	26	26	6	-2	31	29	0	2	99	88	5	5	17	19	0	3	76	72	6	3	11	9
1	-4	41	38	6	2	31	33	0	4	66	59	5	6	14	14	0	5	20	16	6	4	30	37
1	-3	52	50	6	4	42	51	0	6	46	41	5	8	16	16	0	7	38	32	6	5	12	12
1	-2	58	58	6	6	27	28	1	-9	16	13	6	-7	11	9	1	-6	27	28	7	-4	30	32
1	-1	20	19	6	8	18	15	1	-6	30	29	6	-5	20	24	1	-4	33	33	7	-1	35	37
1	0	72	67	7	-7	16	14	1	-5	17	17	6	-4	24	22	1	-3	28	27	7	3	26	27
1	1	62	65	7	-5	15	16	1	-4	54	57	6	-3	54	56	1	-2	23	26	7	4	16	18
1	2	66	66	7	-4	16	18	1	-3	11	12	6	-2	19	18	1	-1	76	73	7	6	16	12
1	3	25	23	7	-3	15	17	1	-2	22	23	6	-1	39	40	1	0	44	43	8	-7	13	13
1	5	50	45	7	-2	35	33	1	-1	45	46	6	0	23	21	1	1	14	11	8	-5	19	20
1	7	22	21	7	0	51	53	1	0	89	83	6	1	26	29	1	2	38	41	8	-3	30	33
1	8	17	17	7	1	26	30	1	1	15	16	6	2	15	16	1	3	44	42	8	0	10	12
2	-8	30	29	7	3	15	15	1	2	9	7	6	6	17	15	1	4	19	17	8	3	14	16
2	-6	47	47	7	4	11	16	1	3	44	43	6	7	19	22	1	6	33	29	8	5	17	19
2	-5	15	13	7	5	15	18	1	4	24	26	7	-7	17	14	1	8	18	14	8	7	15	16
2	-4	68	71	7	7	16	14	1	5	33	32	7	-6	13	11	2	-8	14	13	9	-4	14	17
2	-3	33	33	8	-3	29	28	1	6	16	16	7	-4	33	33	2	-4	19	19	9	-3	12	12
2	-2	27	33	8	-2	27	29	1	8	19	16	7	-2	14	14	2	-2	36	38	9	-1	20	22
2	-1	27	28	8	-1	50	48	2	-7	21	19	7	0	35	37	2	-1	15	14	9	0	16	14
2	0	42	40	8	1	36	39	2	-5	37	39	7	1	25	29	2	0	121	118	9	1	23	25
2	1	10	9	8	2	11	11	2	-3	51	49	7	2	18	15	2	2	43	47	9	4	10	10
2	2	40	44	8	3	14	13	2	-2	11	11	7	3	32	39	2	4	63	66	9	5	11	14
2	4	61	62	8	5	11	12	2	-1	77	78	7	5	13	14	2	6	10	5	10	-2	26	26
2	6	43	42	8	7	16	12	2	1	42	44	8	-6	21	20	3	-6	22	23	10	0	12	11
2	8	28	25	9	-5	13	11	2	2	15	14	8	0	23	23	3	-4	30	31	10	2	20	24
3	-9	12	13	9	-4	18	16	2	3	12	14	8	1	11	12	3	-2	26	28	10	3	14	13
3	-6	12	10	9	-3	13	13	2	4	15	18	8	2	34	37	3	-1	33	37	11	-6	12	9
3	-5	48	49	9	-2	18	19	2	5	27	27	8	4	31	32	3	0	25	28	11	0	11	10
3	-4	39	36	9	0	25	27	2	7	24	21	8	6	11	10	3	1	22	25	11	1	23	27
3	-2	63	66	9	1	16	19	3	-9	12	14	9	-5	14	10	3	2	17	21	11	5	12	10
3	0	41	45	9	2	28	27	3	-6	22	21	9	-4	15	13	3	3	37	40	12	-1	13	16
3	2	38	43	9	3	17	16	3	-5	18	17	9	-3	10	9	3	4	29	30	12	2	17	22
3	3	45	50	9	4	13	14	3	-4	23	26	9	-2	21	20	3	6	22	22	13	-4	13	13
3	4	9	7	9	5	15	16	3	-2	70	75	9	-1	19	18	3	8	15	14	13	-1	15	16

14	-2	10	10				
	H =	6					
K	L	FO	FC				
0	-6	19	19				
0	-4	24	24				
0	-2	81	76				
0	0	86	79				
0	2	26	24				
0	4	56	53				
0	6	20	20				
1	-8	18	18				
1	-4	8	5				
1	-3	50	51				
1	-2	20	25				
1	-1	10	11				
1	0	18	15				
1	1	34	32				
1	2	36	34				
1	4	34	34				
1	6	22	16				
1	7	15	12				
2	-7	23	23				
2	-5	33	33				
2	-3	26	25				
2	0	11	11				
2	1	13	16				
2	2	9	9				
2	3	57	63				
2	5	19	18				
2	7	24	24				
3	-6	20	20				
3	-5	17	21				
3	-4	21	22				
3	-3	27	27				
3	-1	43	43				
3	0	17	19				
3	1	21	23				
3	2	25	27				
3	4	21	25				
3	6	22	22				
3	7	17	15				
4	-6	13	13				
4	-4	29	32				
4	-3	18	20				
4	-2	39	40				
4	0	58	63				
4	1	18	16				
4	2	38	42				
4	4	12	14				
5	-4	24	25				
5	-3	20	18				
5	-2	18	16				
5	-1	14	16				
5	1	24	29				
5	2	14	12				
5	4	30	32				
6	-7	14	12				
6	-5	25	28				

Table 14 (Continued)

6	-3	17	17	3	1	12	10	1	3	29	27	1	0	22	20	5	3	12	10
6	-1	10	9	3	2	43	45	1	5	13	12	1	1	19	16	6	-5	12	10
6	0	13	16	3	3	10	10	2	-4	11	12	1	5	22	16	7	0	13	13
6	1	14	15	3	4	12	12	2	-3	11	13	1	6	14	8	7	1	13	10
6	3	27	29	3	5	16	15	2	-2	21	21	2	-6	20	22	9	-1	10	6
6	4	13	15	3	7	18	11	2	-1	29	28	2	-4	11	10				
6	5	22	23	4	-5	23	22	2	1	38	36	2	0	16	11		H = 11		
6	7	17	16	4	-2	13	11	2	3	26	23	2	2	23	19	K	L	FO	FC
7	-6	20	20	4	-1	31	31	3	-6	12	9	2	4	24	22	0	-3	16	15
7	-5	19	22	4	0	12	14	3	-2	37	37	3	-5	14	18	1	-4	12	10
7	-1	46	49	4	1	18	21	3	-1	15	16	3	-3	16	17	1	-3	12	10
7	0	12	14	4	3	34	39	3	0	25	25	3	-2	32	29	1	1	12	10
7	1	12	15	4	3	23	19	3	1	15	14	3	-1	14	16	2	0	18	19
7	2	20	22	4	7	9	7	3	2	18	19	3	0	13	12	5	-4	16	12
7	4	13	14	5	-7	15	11	3	3	13	8	3	1	28	27	5	-1	16	14
7	6	16	15	5	-3	12	10	3	4	13	16	3	2	13	14	6	0	13	12
8	-4	13	14	5	-1	47	48	3	5	18	19	3	3	13	14				
8	-2	30	29	5	0	32	34	4	-6	27	26	4	-4	11	9		H = 12		
8	0	32	35	5	1	17	12	4	-4	17	15	4	-3	28	25	K	L	FO	FC
8	1	15	18	5	2	19	18	4	-2	27	29	4	-1	12	9	0	-2	13	13
8	2	13	12	5	4	26	26	4	0	12	13	4	1	18	17				
9	-1	14	15	5	5	15	16	4	2	23	19	5	-6	13	8				
9	2	11	11	6	-6	20	21	4	6	14	16	5	-2	27	28				
9	4	17	16	6	-4	16	18	5	-6	13	10	5	1	12	10				
10	-5	14	12	6	-2	34	33	5	-5	14	17	5	2	18	16				
10	1	16	14	6	-1	22	24	5	-4	25	24	5	3	13	14				
10	3	11	12	6	0	28	33	5	-2	14	10	6	-3	15	13				
10	5	17	17	6	6	11	11	5	0	27	23	6	-2	12	12				
11	-1	15	17	7	-3	18	22	5	3	16	17	6	0	14	14				
11	4	11	9	7	-2	36	40	6	-3	17	20	6	4	14	12				
12	-2	13	11	7	0	16	18	6	-2	13	16	7	-4	12	9				
				7	2	33	35	6	-1	15	16	8	-4	12	10				
	H =	7		8	-2	17	19	6	1	13	17	8	-1	13	14				
K	L	FO	FC	8	-1	13	11	6	2	27	25	9	0	13	12				
0	-5	25	24	8	1	17	15	6	3	18	22	9	1	13	9				
0	1	68	62	8	2	14	16	7	-3	17	13								
0	3	50	47	8	3	22	25	7	0	21	22		H = 10						
0	7	18	15	9	-5	19	21	7	2	18	16	K	L	FO	FC				
1	-5	32	33	9	-1	33	36	7	4	16	12	0	0	12	11				
1	-3	14	15	9	0	15	14	8	-4	17	19	0	2	34	25				
1	-1	33	31	9	1	11	13	8	-1	11	12	0	4	22	18				
1	0	51	47	9	2	14	16	8	1	14	16	1	-6	14	8				
1	2	24	22	9	4	13	13	8	4	12	7	1	-2	18	20				
1	4	30	27	10	-4	15	15	9	-5	12	10	1	1	13	12				
1	5	19	17	11	2	14	16	9	-4	11	4	1	3	18	16				
1	6	13	10					9	-2	15	12	2	-5	15	14				
1	7	17	16		H =	8		9	2	14	15	2	-3	15	12				
2	-6	28	28	K	L	FO	FC	10	-1	17	19	2	-1	16	15				
2	-4	35	36	0	-6	32	32	10	2	12	9	3	-3	11	9				
2	-2	49	50	0	-4	31	33					3	-2	20	19				
2	0	35	34	0	-2	28	26		H =	9		3	1	13	11				
2	1	10	7	0	4	28	22	K	L	FO	FC	4	-2	11	10				
2	2	12	11	0	6	24	19	0	-3	26	21	4	0	17	13				
2	6	18	21	1	-7	12	8	0	-1	27	24	4	2	18	18				
3	-5	15	16	1	-5	16	14	0	1	20	21	4	3	10	4				
3	-4	16	17	1	-3	15	13	1	-6	11	8	4	4	13	11				
3	-3	16	15	1	-2	37	34	1	-5	14	13	5	-4	12	8				
3	-2	41	42	1	0	29	26	1	-3	13	9	5	-1	11	8				
3	-1	19	18	1	2	26	25	1	-2	33	32	5	1	12	14				

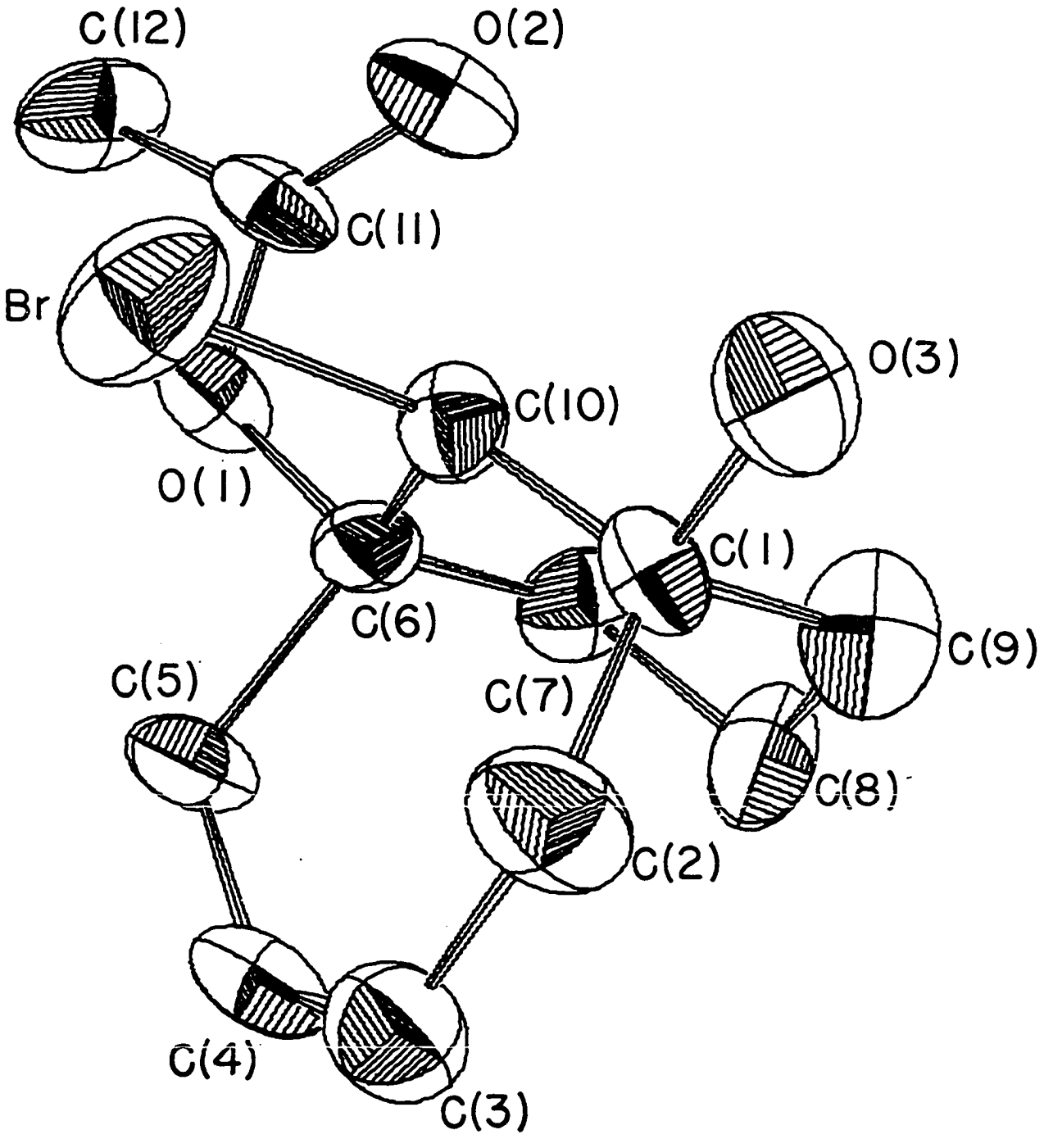

Figure 19. Computer-generated drawing of 1-hydroxy-6-acetoxy-10α-bromo-bicyclo[4.3.1]deca-3-ene, 10. 50% probability ellipsoids depicted.

Table 15. Atomic displacements from the least-squares plane[a] formed by six of the seven carbons in the cycloheptane ring found in 10

Plane defined by atoms (C(1), C(2), C(3), C(4), C(5), C(6))

.25453 X - .01093 Y + .96700 Z = 2.54242

Atom	Deviation from plane (Å)
C(1)	.110
C(2)	-.223
C(3)	.115
C(4)	.120
C(5)	-.187
C(6)	.064

[a]Plane is defined by $C_1X + C_2Y + C_3Z - d = 0$, where X, Y, and Z are coordinates along the cartesian a, b, and c axes.

expected. As predicted, the bromine atom is directed towards the seven-membered ring, indicating that reaction III proceeds with retention of configuration.

A computer-generated drawing[64] of the corresponding diacetate, 11[52], which results from the non-assisted solvolysis of 10,10-dibromo[4.3.1]propell-3-ene (reaction V) is given in Figure 20. Comparisons of the bond distances and angles for 10 and 11 are given in Figures 21 and 22, respectively, while comparisons of the torsional angles for the six and seven-membered rings are given in Figures 23 and 24, respectively. Inspection of these figures shows 10 and 11 to be essentially isostructural with respect to their carbon ring conformations. The dihedral angle between the six and seven-membered rings is approximately 67° for 10, as opposed to a value of 64° for 11. The C(1)-C(6) distance across the bridge is 2.55(1) Å for 10 and 2.58(2) Å for 11. The ring conformation found in both 10 and 11 is also closely related to that of the corresponding diol, 7[65], which results from the silver-assisted solvolysis of 10,10-dibromo[4.3.1]propell-3-ene (reaction II). It should also be noted that each of the acetoxy substituents in 11 contains one abnormally short angle with the corresponding bridgehead carbon (C(2)-C(1)-O(1), 99.3°, and C(10)-C(6)-O(3), 100.7°), as was the case for the acetoxy group in 4a. This short angle most likely can be explained in terms of steric effects.

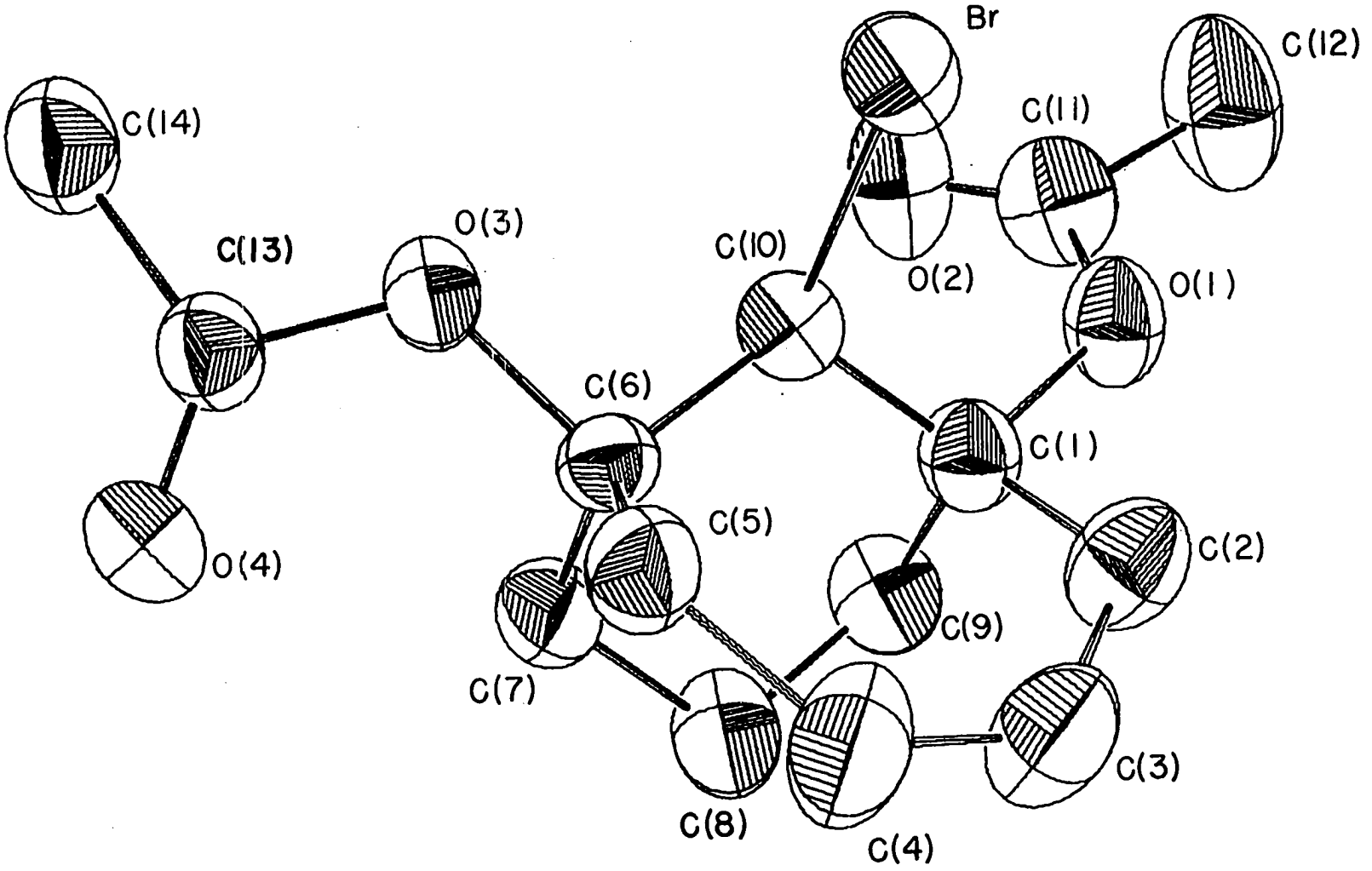

Figure 20. Computer-generated drawing of 1,6-acetoxy-10α-bromo-bicyclo[4.3.1]deca-3-ene, 11. 50% probability ellipsoids depicted.

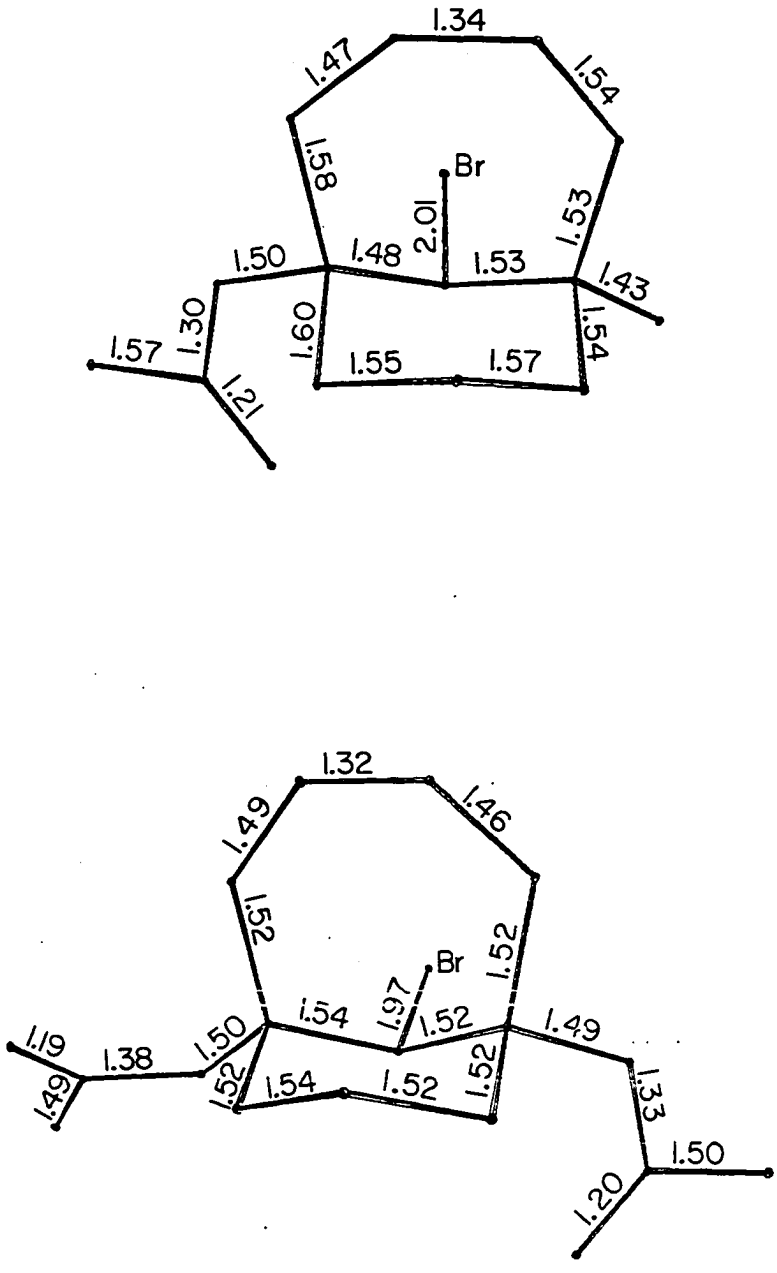

Figure 21. A comparison of bond distances in 1-hydroxy-6-acetoxy-10α-bromo-bicyclo[4.3.1]deca-3-ene (top), and 1,6-acetoxy-10α-bromo-bicyclo[4.3.1]deca-3-ene(bottom).

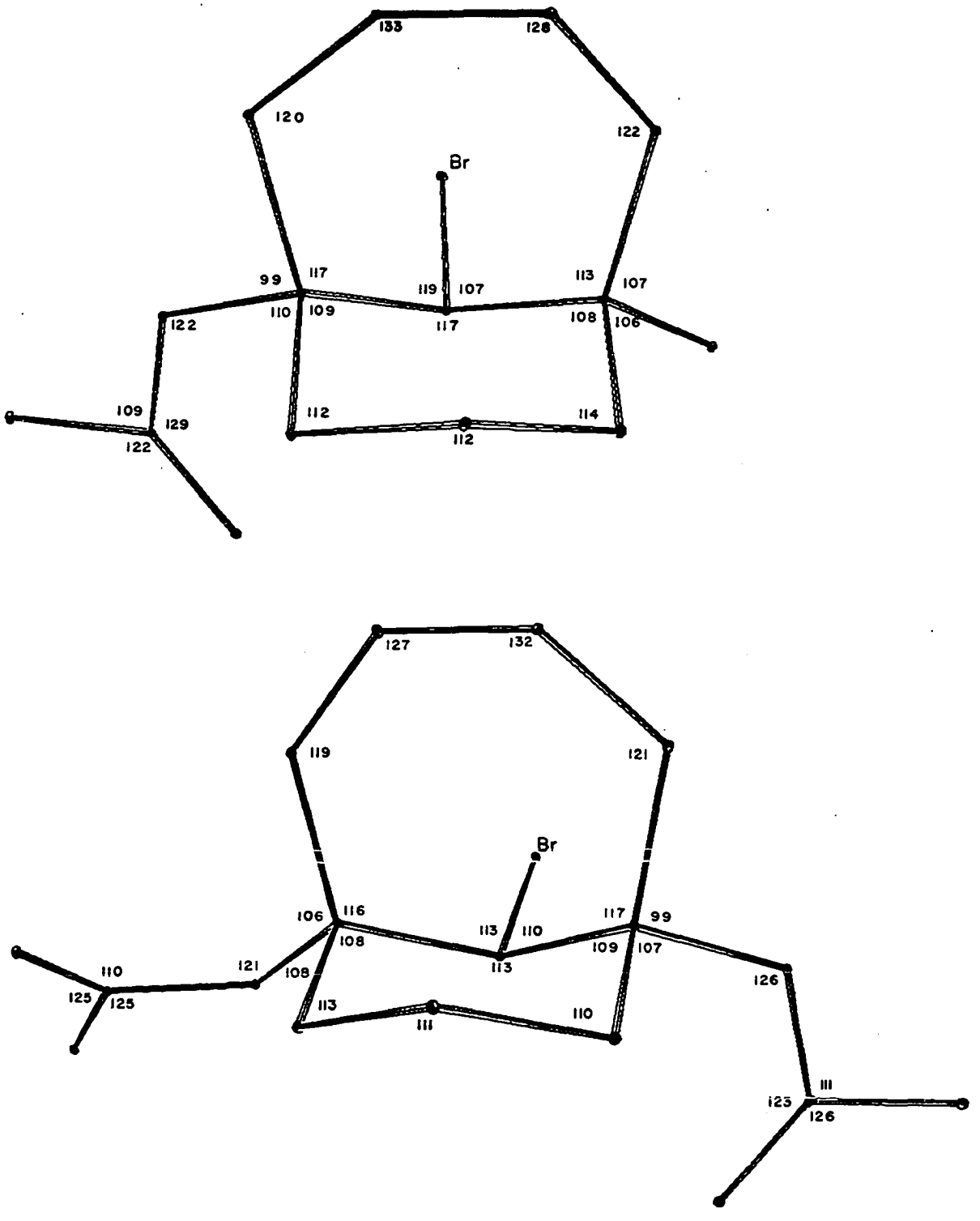

Figure 22. A comparison of bond angles in 1-hydroxy-6-acetoxy-10α-bromo-bicyclo[4.3.1]deca-3-ene (top), and 1,6-acetoxy-10α-bromo-bicyclo[4.3.1]deca-3-ene(bottom).

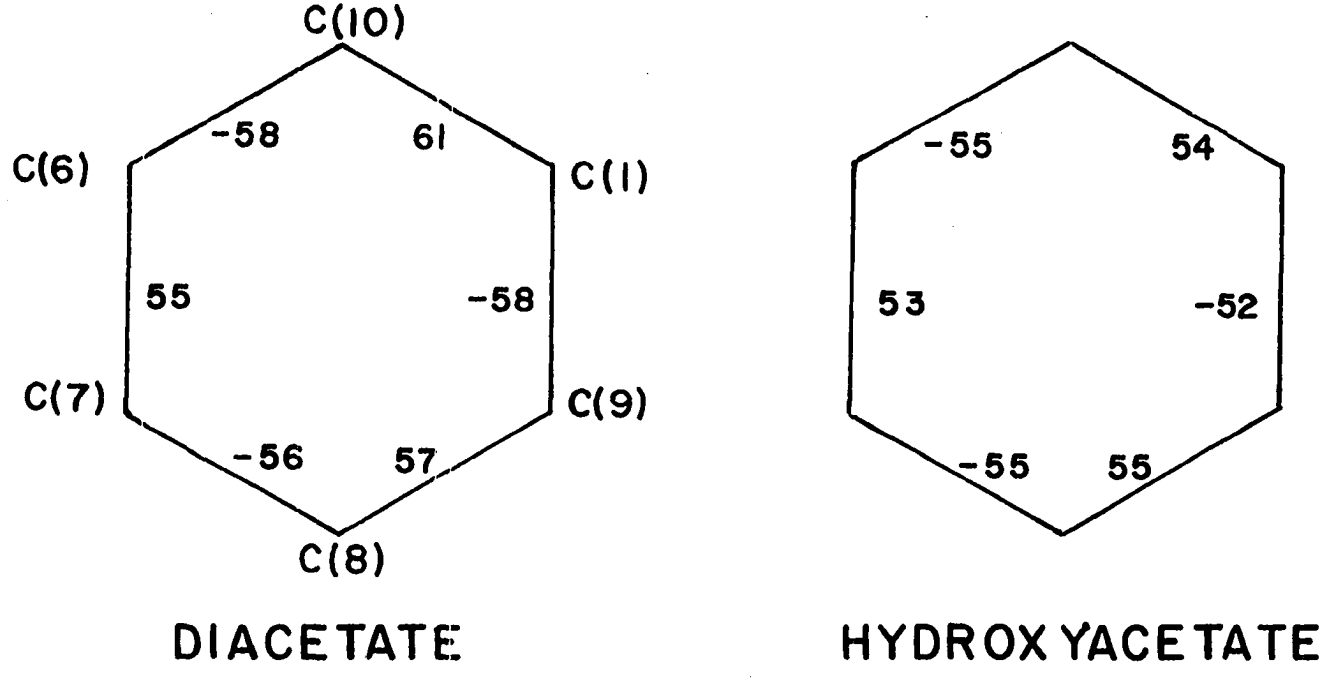

Figure 23. A comparison of the torsional angles in the six-membered rings of 1-hydroxy-6-acetoxy-10α-bromo-bicyclo[4.3.1]deca-3-ene, 10, and 1,6-acetoxy-10α-bromo-bicyclo[4.3.1]deca-3-ene, 11 (atom designations as in Figure 20).

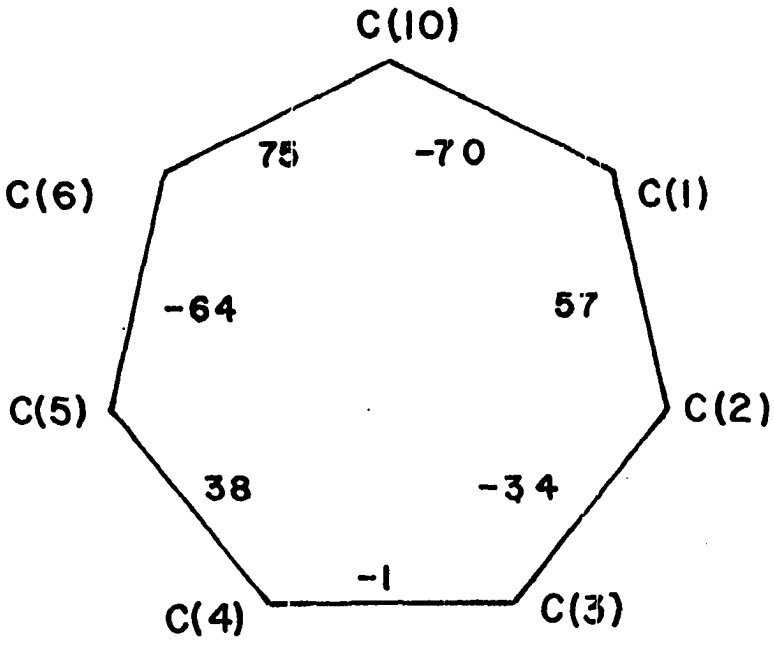

DIACETATE

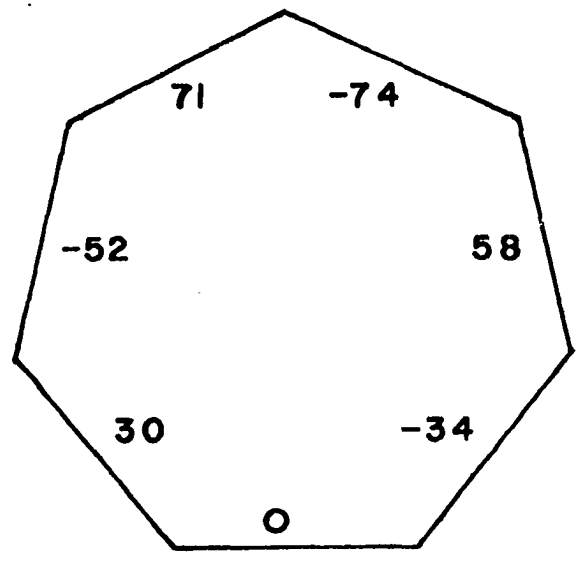

HYDROXYACETATE

Figure 24. A comparison of the torsional angles in the seven-membered rings of 1-hydroxy-6-acetoxy-10α-bromo-bicyclo 4.3.1 deca-3-ene, 10, and 1,6-acetoxy-10α-bromo-bicyclo[4.3.1]deca-3-ene, 11(atom designations as in Figure 20).

A stereoscopic view of the unit cell is given in Figure 25. The packing suggests the presence of infinite molecular chains, possibly joined by hydrogen bonds between the hydroxy group of one molecule and the acetoxy group of an adjacent molecule. The O(2)-O(3) distance of 2.94(2) Å seems to support this hypothesis, though the distance is relatively long for a hydrogen bond. Hydrogen bonding may explain the higher melting point of 10 (88-89.5°C) compared to that of 11 (84-85.5°C). No other abnormally short intermolecular distances were found, indicating that crystal packing is primarily a result of van der Waals forces.

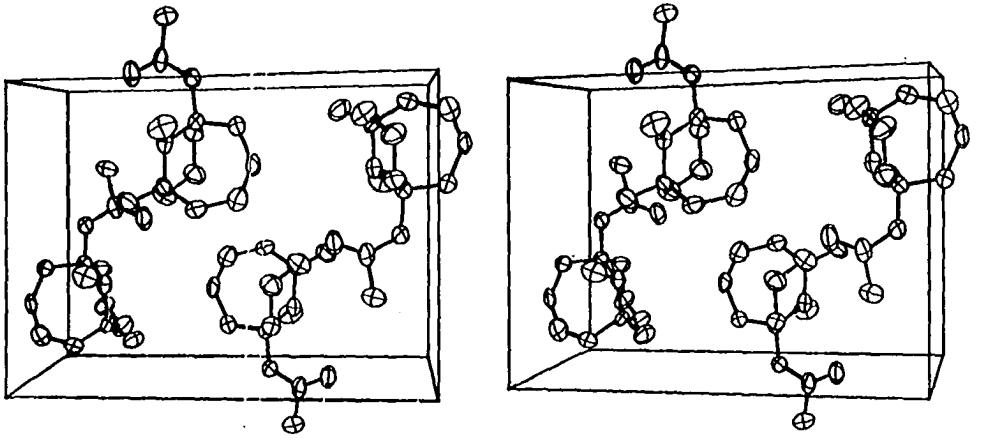

Figure 25. Unit cell stereograph of 1-hydroxy-6-acetoxy-10α-bromo-bicyclo[4.3.1]deca-3-ene, 10.

BIBLIOGRAPHY

1. R. D. Lowde, Acta Cryst., 9, 151 (1956).

2. C. R. Hubbard, C. O. Quicksall, and R. A. Jacobson, Acta Cryst., A28, 236 (1972).

3. K. C. Turberfield in "Thermal Neutron Diffraction," T. M. Willis, Ed., Oxford University Press, London, England, 1970, p 34.

4. H. M. Rietveld, Acta Cryst., 22, 151 (1967).

5. H. M. Rietveld, Acta Cryst., 2, 65 (1969).

6. A. W. Hewat, UKAEA Research Group Report (unpublished), 1973.

7. G. Caglioti in "Thermal Neutron Diffraction," T. M. Willis, Ed., Oxford University Press, London, England, 1970, pp 14-21.

8. H. P. Klug and L. E. Alexander, "X-ray Diffraction Procedures," Wiley, New York, N.Y., 1954, pp 235-258.

9. M. J. Cooper and J. P. Sayer, J. Appl. Cryst., 8, 615 (1975).

10. R. Weinstock, Phys. Rev., 65, 1 (1944).

11. W. N. Lipscomb and R. A. Jacobson in "Physical Methods of Chemistry," Part IIID, A. Weissberger and B. W. Rossiter, Ed., Wiley, New York, N.Y., 1972, pp 62-63.

12. N. Nilsson, Ark. Fys., 12, 247 (1957).

13. M. J. Cooper in "Thermal Neutron Diffraction," T. M. Willis, Ed., Oxford University Press, London, England, 1970, p 51.

14. D. J. Dahm and R. A. Jacobson, USAEC Report IS-1740, Ames, Iowa, 1967.

15. T. Riste and K. Otnes, Nucl. Instrum. Meth., 75, 197 (1969).

16. D. G. Scranton and E. F. Manchester, USAEC Report IS-2305, Ames, Iowa, 1971.

17. M. Atoji, USAEC Report ANL-6920, Argonne, Illinois, 1964.

18. "International Tables of X-ray Crystallography," Vol. III, Table 4.3, Kynoch Press, Birmingham, England, 1962, p 282.

19. "International Tables of X-ray Crystallography," Vol. III, Table 3.3.5.1A, Kynoch Press, Birmingham, England, 1962, pp 234-235.

20. G. E. Bacon, "Neutron Diffraction," 3rd ed, Clarendon Press, London, England, 1975, pp 39-41.

21. T. E. Scott, USERDA Report IS-3634, Ames, Iowa, 1975.

22. B. Siegel and G. G. Libowitz in "Metal Hydrides," W. M. Mueller, J. P. Blackledge, and G. G. Libowitz, Eds., Academic Press, New York, N.Y., 1968, p 592.

23. M. A. Pick, Report No. JÜL-951-FF, Jülich, Germany, 1973.

24. R. J. Walter and W. T. Chandler, Trans. Met. Soc. AIME, 233, 762 (1965).

25. H. D. Carstanjen and R. Sizmann, Ber. Bunsen Ges. physik. Chem., 76, 1223 (1972).

26. G. Brauer and R. Hermann, Z. Anorg. Allgen. Chem., 274, 11 (1953).

27. I. Amato and A. Negro, J. Less-Common Metals, 16, 468 (1968).

28. M. S. Rashid and T. E. Scott, J. Less-Common Metals, 30, 399 (1972).

29. V. A. Somenkov, A. V. Gurskaya, M. G. Zemlyanov, M. E. Kost, N. A. Chernophekov, and A. A. Chertkov, Sov. Phys. Solid State, 10, 1076 (1968).

30. T. Schober, M. A. Pick, and H. Wenzel, Phys. Stat. Sol. (a), 18, 175 (1973).

31. V. A. Somenkov, V. F. Petrunin, S. Sh. Shil'shtein, and A. A. Chertkov, Sov. Phys. Cryst., 14, 522 (1970).

32. S. S. Pan, M. L. Yeater, and W. E. Moore, "Proc. Symp. Molecular Dynamics and Structure of Solids," National Bureau of Standards Circular 301, Washington, D.C., 1969, p 315.

33. N. A. Chernoplekov, M. G. Zemlyanov, V. A. Somenkov, and A. A. Chertkov, Sov. Phys. Solid State, 11, 2343 (1970).

34. F. Takusagawa, Ames Laboratory, USERDA, Iowa State University, personal communication, 1976.

35. F. Takusagawa, Ames Laboratory, USERDA, Iowa State University, personal communication, 1975.

36. R. G. Barnes, K. P. Roenker, H. R. Brooker, Ber. Bunsen Ges. physik Chem., in press.

37. F. A. Kuijpers and B. O. Loopstra, J. Phys. Chem. Solids, 35, 301 (1974).

38. S. Komjathy, J. Less-Common Metals, 2, 466 (1960).

39. C. Zener, Phys. Rev., 74, 639 (1948).

40. A. G. Khachaturyan, Sov. Phys. Solid State, 9, 2249 (1968).

41. V. A. Somenkov, Ber. Bunsen Ges. physik Chem., 76, 733 (1972).

42. A. C. Switendick, Ber. Bunsen Ges. physik. Chem., 76, 535 (1972).

43. A. C. Switendick, Int. J. of Quantum Chem., 5, 459 (1971).

44. V. A. Somenkov, A. V. Gurskaya, M. G. Zemlyanov, M. E. Kost, N. A. Chernoplekov, and A. A. Chertkov, Sov. Phys. Solid State, 10, 2123 (1969).

45. A. W. Struss and J. D. Corbett, accepted for publication in Inorg. Chem.

46. S. Lu, Ph.D. Thesis, Iowa State University, Ames, Iowa, 1976.

47. V. Schöllkopf, Ang. Chem. Int. Ed. Engl., 7, 588 (1968).

48. P. Warner and S. Lu, submitted for publication in J. Amer. Chem. Soc.

49. C. B. Reese and M. R. D. Steebles, Chem. Comm., 1231 (1972).

50. G. L. Lange and T. Hall, J. Org. Chem., 39, 3819 (1974).

51. C. E. Harding and M. Hanack, Tetrahedron Lett., 1253 (1971).

52. E. Myers, P. DeHaven, and R. A. Jacobson, to be published.

53. R. A. Jacobson, J. Appl. Cryst., 9, 115 (1976).

54. D. E. Williams, USAEC Report IS-1052, Ames, Iowa, 1964.

55. S. L. Lawton and R. A. Jacobson, Inorg. Chem., 7, 2124 (1968).

56. E. R. Howells, D. C. Phillips, and D. Rogers, Acta Cryst., 3, 210 (1950).

57. C. A. Hubbard, C. O. Quicksall, and R. A. Jacobson, USAEC Report IS-2625, Ames, Iowa, 1971.

58. W. R. Busing, K. O. Martin, and H. A. Levy, USAEC Report ORNL-TM-305, Oak Ridge, Tenn., 1965.

59. D. W. Cruickshank and D. E. Pilling in "Computing Methods and the Phase Problem in X-ray Crystal Analysis," R. Pepinsky, J. M. Roberts, and J. C. Speakmann, Eds., Pergamon Press, Inc., New York, N.Y., 1961, pp 45-46.

60. H. P. Hanson, F. Herman, J. D. Lea, and S. Skillman, Acta Cryst., 17, 1040 (1964).

61. R. F. Stewart, E. R. Davidson, and W. T. Simpson, J. Chem. Phys., 42, 3175 (1965).

62. D. H. Templeton in "International Tables for X-ray Crystallography," Vol. III, Table 3.3.2c, The Kynoch Press, Birmingham, England, 1962, pp 215-6.

63. W. R. Busing, K. O. Martin, and H. A. Levy, USAEC Report ORNL-TM-306, Oak Ridge, Tenn., 1964.

64. C. A. Johnson, USAEC Report ORNL-3794 (Second Revision With Supplemental Instructions), Oak Ridge, Tenn., 1971.

65. P. Warner, J. Fayos, and J. Clardy, Tetrahedron Lett., 45, 4473 (1973).

66. S. Dahl and P. Groth, Acta Chem. Scand., 25, 1114 (1971).

67. R. F. Bryan and J. D. Dunhitz, Helv. Chim. Acta, 43, 3 (1960).

68. M. Bixon and S. Lifson, Tetrahedron, 23, 769 (1967).

69. J. B. Hendrickson, J. Am. Chem. Soc., 89, 7043 (1967).

70. F. A. L. Anet and J. J. Wagner, J. Am. Chem. Soc., 93, 5266 (1971).

71. G. Borgen and J. Dale, Chem. Comm., 1105 (1970).

72. P. Groth, Acta Chem. Scand., 23, 1311 (1969).

73. G. M. Kellie and F. G. Riddell in "Topics in Stereochemistry," Volume 8, E. L. Eliel and N. L. Allinger, Interscience, New York, N.Y., 1974 p 225.

74. F. J. Adrian, J. Chem. Phys., 29, 1381 (1958).

75. P. Romain, Bull. Soc. franc. Min. Cryst., 81, 35 (1958).

76. F. Iwasaki, M. Sato, and A. Aihara, Acta Cryst., B32, 102 (1976).

77. R. Bucourt in "Topics in Stereochemistry," Volume 8, E. L. Eliel and N. L. Allinger, Interscience, New York, N.Y., 1974.

78. W. R. Busing and H. A. Levy, Acta Cryst., 22, 457 (1967).

79. D. Shoemaker and G. Bassi, Acta Cryst., A26, 97 (1970).

80. W. N. Lipscomb and R. A. Jacobson in "Physical Methods of Chemistry," Part IIID, A. Weissberger and B. W. Rossiter, Ed., Wiley, New York, N.Y., 1972, p 111.

81. J. Waser, Acta Cryst., 16, 1091 (1963).

82. J. H. Campbell, G. F. Covert, and B. J. Helland, USERDA Report IS-3339, Ames, Iowa, 1976.

83. P. W. DeHaven and R. A. Jacobson, to be published.

84. P. W. DeHaven and R. A. Jacobson, Crystal Struct. Comm., 5, 31 (1976).

85. V. Katovic, J. L. Templeton, R. J. Hoxmeier, and R. E. McCarley, J. Am. Chem. Soc., 97, 5300 (1975).

86. F. Takusagawa and R. A. Jacobson, J. Solid State Chem., 18, 163 (1976).

ACKNOWLEDGEMENTS

The author is deeply indebted to Dr. R. A. Jacobson for his incomparable guidance and assistance over the past five years, to James Benson and Barb Helland, whose herculean efforts managed to keep the instruments running in spite of power failures and inept graduate students, and to Brenda Smith for her patience and effort in typing this thesis.

In addition, the author would like to thank Dr. John C. Taylor, who generously supplied his version of the Rietveld profile refinement program, and to all the members of X-ray group I, especially Wayne Rohrbaugh, Michael Babich, and Walt Riley, for their advice and friendship over the years.

Finally the author would like to thank his parents, without whom none of this would have been possible.

APPENDIX: REFINEMENT OF THE CRYSTAL ORIENTATION MATRIX BY CONSTRAINED LEAST-SQUARES

Introduction

One of the major efforts of this group in recent years has been toward the development of a highly efficient and accurate routine for the collection of X-ray single crystal diffraction data. In order to collect data of highest accuracy it is necessary to employ the most accurate crystal orientation matrix possible. There are two major ways to obtain such an orientation matrix.

(A.) Use of more than three standard reflections to refine the elements of the orientation matrix by a least-squares procedure.

(B.) Inclusion of crystal symmetry in the orientation matrix determination.

Method (A) is relatively straightforward and can be easily accomplished. However, there is no generally accepted method of including the crystal symmetry in the determination of the orientation matrix elements. Busing and Levy[78] attack the problem by simultaneous refinement of the direct cell constants and primary and secondary orienting reflections. Crystal symmetry is included by fixing the appropriate cell parameters in the least-squares procedure. This method has the disadvantage in that the orientation matrix is not refined

directly, but is calculated from the refined cell parameters and orienting reflections. Shoemaker and Bassi[79] have proposed a method in which the orientation matrix is included in the refinement. The entity refined is the matrix

$$\tilde{D} = \tilde{B}_o^{-1} \tilde{B}$$

where $\tilde{B}$ is the orientation matrix and $\tilde{B}_o$ is an initial approximation of the orientation matrix (constant). Here crystal symmetry is included through a series of constraint equations which involve the elements of $\tilde{D}$. These are combined by means of Lagrangian undetermined multipliers with the normal equations which would result from an unconstrained least-squares determination. A comparison of the relative merits of these two methods has been given previously[79]. We present here a method similar to that of Shoemaker and Bassi, but which is more straightforward in that the elements of the orientation matrix are treated directly, and in which the constraint equations are treated as an additional set of observational equations.

Mathematical Background

The relationship between the reciprocal lattice vectors and the laboratory axis system which defines the orientation of the crystal has been previously described in detail (Busing and Levy[78], Lipscomb and Jacobson[80]). In the following description the notation of Lipscomb and Jacobson will be

used.

For the case where the unit cell parameters are unknown, the orientation matrix can be calculated from the indices (h_{1i}, h_{2i}, h_{3i}) and diffractometer angles (θ_i, ω_i, χ_i, ϕ_i) of three observed reflections by means of the equation:

$$(A1)\quad \underset{\tilde{B}}{\begin{pmatrix} b_{1x} & b_{2x} & b_{3x} \\ b_{1y} & b_{2y} & b_{3y} \\ b_{1z} & b_{2z} & b_{3z} \end{pmatrix}} \underset{\tilde{H}}{\begin{pmatrix} h_{11} & h_{12} & h_{13} \\ h_{21} & h_{22} & h_{23} \\ h_{31} & h_{32} & h_{33} \end{pmatrix}} = \underset{\tilde{\tilde{X}}\tilde{\tilde{X}}}{\begin{pmatrix} X_1 & X_2 & X_3 \\ Y_1 & Y_2 & Y_3 \\ Z_1 & Z_2 & Z_3 \end{pmatrix}}$$

where

$$X_i = |\vec{h}_i| \cos\chi_i \cos\phi_i$$

$$Y_i = |\vec{h}_i| \cos\chi_i \sin\phi_i \qquad \text{for } \omega_i = \theta_i$$

$$Z_i = |\vec{h}_i| \sin\chi_i$$

or

$$X_i = |\vec{h}_i| (\cos\chi_i \cos\phi_i \cos\Delta_i - \sin\phi_i \sin\Delta_i)$$

$$Y_i = -|\vec{h}_i| (\cos\chi_i \sin\phi_i \cos\Delta_i + \cos\phi_i \sin\Delta_i) \quad \text{for } \omega_i \neq \theta_i$$

$$Z_i = |\vec{h}_i| \sin\chi_i \cos\Delta_i$$

$$\Delta_i = \theta_i - \omega_i \qquad |\vec{h}_i| = 2\sin\theta_i/\lambda$$

b_{1x}, b_{2x}, etc. are the components of the three reciprocal lattice vectors along the instrument cartesian axis system as defined by Lipscomb and Jacobson.

The indices and angles of more than three reflections can

be used to obtain a more accurate orientation matrix. Given the indices and angles for n reflections we can, by application of the method of least-squares, obtain the following set of nine normal equations.

$$\sum_{i=1}^{n} w_i h_{1i}(h_{1i}b_{1x} + h_{2i}b_{2x} + h_{3i}b_{3x} - X_i) = 0$$

$$\sum_{i=1}^{n} w_i h_{1i}(h_{1i}b_{1y} + h_{2i}b_{2y} + h_{3i}b_{3y} - Y_i) = 0 \quad \text{(A2)}$$

$$\vdots$$

$$\sum_{i=1}^{n} w_i h_{3i}(h_{1i}b_{1z} + h_{2i}b_{2z} + h_{3i}b_{3z} - Z_i) = 0$$

which can be solved for b_{1x}, b_{2x}, etc. by standard methods.

For each crystal class (except triclinic) crystal symmetry imposes one or more constraints upon the reciprocal lattice vectors. These constraints may be expressed in terms of relations between the lattice vectors. These are listed in Table A1. One can expand these relations in terms of their components along the cartesian (lab) axis system.

$$\vec{b}_1 \cdot \vec{b}_2 = 0$$

$$b_{1x}b_{2x} + b_{1y}b_{2y} + b_{1z}b_{2z} = 0 \quad \text{(A3a)}$$

$$\vec{b}_1 \cdot \vec{b}_3 = 0$$

$$b_{1x}b_{3x} + b_{1y}b_{3y} + b_{1z}b_{3z} = 0 \quad \text{(A3b)}$$

$$\vec{b}_2 \cdot \vec{b}_3 = 0$$

(A3c)
$$b_{2x}b_{3x} + b_{2y}b_{3y} + b_{2z}b_{3z} = 0$$

$$|\vec{b}_1| = |\vec{b}_2|$$

(A3d)
$$(b_{1x}^2 + b_{1y}^2 + b_{1z}^2)^{\frac{1}{2}} = (b_{2x}^2 + b_{2y}^2 + b_{2z}^2)^{\frac{1}{2}}$$

$$|\vec{b}_2| = |\vec{b}_3|$$

(A3e)
$$(b_{2x}^2 + b_{2y}^2 + b_{2z}^2)^{\frac{1}{2}} = (b_{3x}^2 + b_{3y}^2 + b_{3z}^2)^{\frac{1}{2}}$$

(A3f)
$$\frac{\vec{b}_1 \cdot \vec{b}_2}{|\vec{b}_1|^2} = \cos 60^\circ = \frac{1}{2}$$

$$\frac{b_{1x}b_{2x} + b_{1y}b_{2y} + b_{1z}b_{2z}}{(b_{1x}^2 + b_{1y}^2 + b_{1z}^2)} = \frac{1}{2}$$

$$\vec{b}_1 \cdot \vec{b}_2 = \vec{b}_2 \cdot \vec{b}_3$$

(A3g)
$$b_{2x}(b_{1x} - b_{3x}) + b_{2y}(b_{1y} - b_{3y}) + b_{2z}(b_{1z} - b_{3z}) = 0$$

$$\vec{b}_1 \cdot \vec{b}_3 = \vec{b}_2 \cdot \vec{b}_3$$

(A3h)
$$b_{3x}(b_{1x} - b_{2x}) + b_{3y}(b_{1y} - b_{2y}) + b_{3z}(b_{1z} - b_{2z}) = 0$$

Using a technique developed by Waser[81], the constraint equations can be included in the least-squares determination without increasing the number of normal equations. Waser's method is based on the approximation that the constraints

Table A1. Constraints imposed by crystal symmetry

Crystal Class	Constraints
Monoclinic (b-unique)	$\vec{b}_1 \cdot \vec{b}_2 = 0$
	$\vec{b}_2 \cdot \vec{b}_3 = 0$
Orthorhombic	$\vec{b}_1 \cdot \vec{b}_2 = 0$
	$\vec{b}_1 \cdot \vec{b}_3 = 0$
	$\vec{b}_2 \cdot \vec{b}_3 = 0$
Tetragonal (c-unique)	$\vec{b}_1 \cdot \vec{b}_2 = 0$
	$\vec{b}_1 \cdot \vec{b}_3 = 0$
	$\vec{b}_2 \cdot \vec{b}_3 = 0$
	$\lvert\vec{b}_1\rvert = \lvert\vec{b}_2\rvert$
Cubic	$\vec{b}_1 \cdot \vec{b}_2 = 0$
	$\vec{b}_1 \cdot \vec{b}_3 = 0$
	$\vec{b}_2 \cdot \vec{b}_3 = 0$
	$\lvert\vec{b}_1\rvert = \lvert\vec{b}_2\rvert$
	$\lvert\vec{b}_2\rvert = \lvert\vec{b}_3\rvert$
Hexagonal (c-unique)	$\lvert\vec{b}_1\rvert = \lvert\vec{b}_2\rvert$
	$\vec{b}_1 \cdot \vec{b}_3 = 0$
	$\vec{b}_2 \cdot \vec{b}_3 = 0$
	$\vec{b}_1 \cdot \vec{b}_2 = \lvert\vec{b}_1\rvert^2 \cos 60^\circ$

Table A1 (Continued)

Trigonal	$\lvert\vec{b}_1\rvert = \lvert\vec{b}_2\rvert$ $\lvert\vec{b}_2\rvert = \lvert\vec{b}_3\rvert$ $\vec{b}_1 \cdot \vec{b}_2 = \vec{b}_2 \cdot \vec{b}_3$ $\vec{b}_1 \cdot \vec{b}_3 = \vec{b}_2 \cdot \vec{b}_3$

applied are not exact. As such they may be considered an additional set of observational equations in the least-squares treatment. In application of this technique to the refinement of the orientation matrix, the constraints are non-linear functions of the parameters. Consequently the constraint equations must be linearized by means of a Taylor series expansion with terms higher than first order dropped.

$$(A4)\quad f(b_i) = f(b_i^{\,o}) + \sum_{i=1}^{9} (b_i - b_i^{\,o}) \left.\frac{\delta f}{\delta b_i}\right|_{b_i^{\,o}}$$

The b_i represent the elements of the orientation matrix b_{1x}, b_{1y}, etc. With the above approximation we can now write our normal equations (A2) as

$$(A5)\quad \sum_{i=1}^{n} w_i h_{1i}(h_{1i}b_{1x} + h_{2i}b_{2x} + h_{3i}b_{3x} - X_i) + \sum_{j=1}^{\ell} w_j (\delta f_j/\delta b_{1x})_{b_{1x}^{\,o}} \left[f_j^{\,o} - f_j + \sum_{k=1}^{9} (b_k - b_k^{\,o})(\delta f_j/\delta b_k)_{b_k^{\,o}} \right] = 0$$

$$\vdots$$

ℓ = total # of constraints.

Equation (A5) is solved in the same manner as equation (A2).

Several difficulties arise in the use of such a constrained least squares procedure.

(a) Introduction of the Taylor series expansion results in the necessity of a reasonably good set of initial values for the elements of the orientation matrix.

(b) The approximation that the applied constraints are not exact, coupled with the neglect of the higher order terms in the Taylor series expansion, results in the need for more than one least-squares cycle.

(c) An appropriate weighting scheme must be developed for the constraints.

In general a good initial orientation matrix may be obtained by an unconstrained least-squares fit to the standard reflections (equations (A1) and (A2)).

The number of least-squares cycles required is more or less arbitrary and depends mainly on the weighting scheme used and the desired accuracy of the resulting orientation matrix (as measured by the calculated cell constants). We have found that the best means of determining the number of cycles is by monitoring the average variation in the elements of the orientation matrix. We define this variation by the following relation:

$$\text{(A6)} \qquad \text{var} = \frac{\sum_{i=1}^{9} | b_i(\text{new}) - b_i(\text{old}) |}{\sum_{i=1}^{9} | b_i(\text{old}) |}$$

Refinement is considered to be complete when the variance drops below a preassigned value (for our case var < 0.01).

Choice of an appropriate weighting scheme is probably the most critical aspect of the constrained least-squares method. Derivation of a weighting scheme for the observations follows standard techniques and is relatively straightforward. In order to obtain accurate values for the standard deviations, the weights of the observations X_i, Y_i, Z_i must be proportional to the reciprocals of the variances $\sigma^2(X_i)$, $\sigma^2(Y_i)$, $\sigma^2(Z_i)$. As the values of X_i, Y_i, Z_i are functions of the diffractometer angles θ_i, ω_i, χ_i (ϕ_i being kept fixed throughout the tuning procedure), the variances of X_i, Y_i, Z_i are expressed in terms of the variances θ_i, ω_i, χ_i by the following equation:

$$\sigma^2(X_i) = \left| \frac{\delta X_i}{\delta \theta_i} \right|^2_{\omega_i, \chi_i} \sigma^2(\theta_i) + \left| \frac{\delta X_i}{\delta \omega_i} \right|^2_{\theta_i, \chi_i} \sigma^2(\omega_i) + \left| \frac{\delta X_i}{\delta \chi_i} \right|^2_{\theta_i, \omega_i} \sigma^2(\chi_i) \quad \text{(A7)}$$

Here the assumption has been made that the errors in θ_i, ω_i, χ_i are uncorrelated. Equation (A7) can be simplified by application of a pair of relations relating the variances of θ_i and χ_i to the variance of ω_i. It has been shown

experimentally[†] that

$$\text{(A7a)} \quad \sigma^2(\theta_i) = K\sigma^2(\omega_i)$$

and

$$\text{(A7b)} \quad \sigma^2(\chi_i) = \frac{K}{\sin^2\theta_i}\,\sigma^2(\omega_i)$$

where K is a constant, approximately equal to 1.57. Using these relations, equation (A7) becomes

$$\text{(A7c)} \quad \sigma^2(X_i) = \sigma^2(\omega_i)\left[1.5725\left|\frac{\delta X_i}{\delta\theta_i}\right|^2_{\omega_i,\chi_i} + \left|\frac{\delta X_i}{\delta\omega_i}\right|^2_{\theta_i,\chi_i} + \frac{1.5725}{\sin^2\theta_i}\left|\frac{\delta X_i}{\delta\chi_i}\right|^2_{\theta_i,\omega_i}\right]$$

Similar equations can be derived for $\sigma^2(Y_i)$ and $\sigma^2(Z_i)$. The weight of each observation is given by

$$\text{(A8)} \quad W_i = \frac{A}{\sigma^2(X_i)}$$

where for our case $A = \left(4/\lambda^2\right)\sigma^2(\omega_i)$. The choice of the

---

[†]A series of investigations into the relation between the variance of ω and that of χ and θ were carried out on an automated four-circle diffractometer designed and built at Ames Laboratory. Although the value of the constant K may differ slightly from instrument to instrument, the general relations should hold for any standard four-circle diffractometer.

normalization constant A is arbitrary; the value of $\left(4/\lambda^2\right)\sigma^2\ (\omega_i)$ was chosen as this value is common to the expressions for $\sigma^2(X_i)$, $\sigma^2(Y_i)$, and $\sigma^2(Z_i)$.

Development of a weighting scheme for the constraints is more difficult. As the constraint equations are in reality exact, and as the weight is proportional to the reciprocal of the variance, in principle W_i (constraint) should equal to infinity ($\sigma_i^2 = 0$). In practice one simply assigns to the constraint equations a weight much larger than the weights of the observational equations. Care must be taken that these weights are not too large, or the resulting normal matrix will be singular. Another consideration in the assignment of constraint weights is that of speed. In general the larger the weight assigned to the constraints, the slower the convergence of the least-squares parameters in the refinement. On the other hand, if a weight below the optimum weight is used, there will be a decrease in the accuracy of the resulting orientation matrix. The actual choice of weights is based on trial and error, in which the best balance between speed of computation (number of refinement cycles) and accuracy is strived for.

Calculation of the standard deviations for the orientation matrix elements is based on the relation

$$\text{(A9)} \qquad \sigma^2(b_i) = N_{ii}^{-1} \left[\frac{\sum_{j=1}^{n} (\ell_j^{obs} - \ell_j^{calc})\, W_j}{n-m} \right]$$

where the sum is over both the observations and the constraints (n = # observations + # constraints). N_{ii}^{-1} is the ith diagonal element of the inverted normal matrix, m the number of least-squares parameters (nine), and W_j the weight of the particular observation (or constraint). The values of ℓ_j^{obs} are, in the case of the observations, the actual experimental values X_i, Y_i, Z_i, while in the case of the constraints they are the idealized values f_j of the constraints. The values ℓ_j^{calc} are the best estimates of the ℓ_j^{obs}.

Program Description

Refinement of the orientation matrix by the constrained least-squares method has been programmed as an integral part of the crystal indexing and data collection algorithm developed in this Laboratory. The programming language used is a subset of PL/1, ALECS[82], which was developed at this laboratory. Program details, including block diagrams, program descriptions, and program listings are given elsewhere[83]. Input consists of the crystallographic indices and tuned θ, ω, χ, ϕ values for the standard reflections, as well as the crystal class designation. The crystal class is input by the user prior to refinement; if one wishes to bypass the constrained least-squares refinement, he simply inputs the designator for a triclinic cell. An initial orientation matrix is calculated by the unconstrained least-

squares method. This matrix, along with the input data, is passed to the constrained least-squares program CLSQ. Here the normal matrix from the unconstrained least-squares treatment is expanded to include the constraints appropriate for the particular crystal class. A new orientation matrix is then obtained from equation (A5).

As was mentioned in the previous section, the weighting scheme for the constraints must be one which affords a good balance between speed of computation and accuracy of the final matrix. In order to achieve this the constraints are initially assigned a weight which is a fraction (1/8 to 1/16) of the optimum weight (i.e. that weight which will give the most accurate results). CLSQ will cycle through a predetermined number of times (15) using this weight. The weight is then doubled and another set of cycles run. This process continues until the optimum weight has been reached. CLSQ then cycles until VAR drops below .01 (equation (A6)). Optimum weights range from $4.5*10^3$ to $8.*10^4$ times the weights of the standards depending on the crystal class.

Output from CLSQ consists of the orientation matrix obtained from the unconstrained refinement, the corresponding reciprocal cell scalars, and direct cell constants. These are followed by the number of cycles required by CLSQ, the final orientation matrix, reciprocal cell scalars,

and direct cell parameters. Sample input and output listings are given in Figure A1.

Application

The constrained least-squares algorithm was tested for each of the seven crystal classes (except triclinic). The results are shown on the following pages (Table A2). In each case $\omega = \theta$. Angles for the standards (θ, χ, ϕ) are given in degrees. For the orientation matrix obtained from the constrained least-squares, the values in parenthesis refer to the standard deviation for the least significant figures.

Evaluation

The constrained least-squares method has several advantages over previous methods. The primary advantage is due to the fact that the orientation matrix elements are refined directly. In Busing and Levy's procedure the elements of the orientation matrix are not involved in the least-squares refinement, while in the method of Shoemaker and Bassi the parameters refined are linear combinations of the orientation matrix elements. Besides being a more straightforward determination, direct refinement of the orientation matrix allows us to calculate directly the standard deviations for the matrix elements. The standard

```
REFINE,Y OR N?Y
XTAL SYS:1-7,TR,M,O,TE,C,H,RH?6

APPROX       588 RFLNS/HEMSIPHERE

ORIENTATION MTRX - NO CONSTRAINTS
-0.2549389E-00  -0.3300491E-00  -0.4011042E-02
-0.2116290E-00   0.1054565E-00  -0.2021462E-01
 0.1023108E-00  -0.1573353E-01  -0.5191803E-01
    CELL VOLUME=  171.94

***CELL SCALARS***
   11.09   11.09  320.49
    -.05     .05   -5.55

      A=   3.331       B=   3.330       C=  17.902
  ALPHA=   90.05   BETA=   89.94  GAMMA=  120.04

     63  CYCLES REQ


STD DEV
 0.1077538E-03   0.1343891E-03   0.1918272E-04
 0.1533158E-03   0.1286285E-03   0.2456501E-04
 0.1090164E-03   0.1138625E-03   0.3177750E-04


FINAL MTRX
-0.2549060E-00  -0.3298581E-00  -0.4017557E-02
-0.2116354E-00   0.1056897E-00  -0.2024005E-01
 0.1022548E-00  -0.1568401E-01  -0.5190828E-01
    CELL VOLUME=  171.94

***CELL SCALARS***
   11.09   11.09  320.48
    -.00     .00   -5.54

      A=   3.330       B=   3.330       C=  17.902
  ALPHA=   90.00   BETA=   89.99  GAMMA=  120.00
```

Figure A1. Sample I/O listing for CLSQ.

Table A2. Sample runs for the constrained least-squares algorithm

---

A.) Monoclinic

Compound: Pyridinium Tetrabromoantimonate
$(C_5H_5NH)\ Sb^{III}\ Br_4$ [84]

Input Data:

h	k	ℓ	θ	χ	φ
0	6	0	9.39	3.99	345.79
8	0	0	13.98	279.90	52.50
4	0	4	13.16	333.30	73.75

Orientation Matrix ($\times 10^{-2}$) - No Constraints:

$b_{1x} = 0.889$ $b_{2x} = 7.400$ $b_{3x} = 3.115$
$b_{1y} = -1.159$ $b_{2y} = 1.874$ $b_{3y} = -12.579$
$b_{1z} = -8.372$ $b_{2z} = 0.532$ $b_{3z} = 1.175$

Direct Cell Constants

$a = 11.794$ Å $b = 13.067$ Å $c = 7.703$ Å
$\alpha = 90.06^\circ$ $\beta = 93.89^\circ$ $\gamma = 89.95^\circ$

Orientation Matrix ($\times 10^{-2}$) - With Constraints

$b_{1x} = 0.895(2)$ $b_{2x} = 7.400(1)$ $b_{3z} = 3.105(7)$
$b_{1y} = -1.159(1)$ $b_{2y} = 1.876(4)$ $b_{3y} = -12.579(2)$
$b_{1z} = -8.372(1)$ $b_{2z} = 0.532(1)$ $b_{3z} = 1.175(2)$

Direct Cell Constants

$a = 11.793$ Å $b = 13.067$ Å $c = 7.704$ Å
$\alpha = 90.00^\circ$ $\beta = 93.90^\circ$ $\gamma = 89.99^\circ$

# of cycles required: 33

Table A2 (Continued)

B.) Orthorhombic

Compound: $MoW(O_2CCMe_3)_4I \cdot CH_3CN$ [85]

Input Data:

h	k	ℓ	θ	χ	φ
24	0	0	13.91	0.43	177.04
0	24	0	13.67	359.98	267.02
0	0	8	16.55	270.38	168.61

Orientation Matrix ($\times 10^{-3}$) - No Constraints

$b_{1x} = -28.150$ $b_{2x} = -1.445$ $b_{3x} = -0.634$
$b_{1y} = -1.456$ $b_{2y} = 27.674$ $b_{3y} = -0.128$
$b_{1z} = 0.207$ $b_{2z} = -0.010$ $b_{3z} = -100.201$

Direct Cell Constants

$a = 35.475$ Å $b = 36.086$ Å $c = 9.979$ Å
$\alpha = 89.96^\circ$ $\beta = 89.94^\circ$ $\gamma = 90.03^\circ$

Orientation Matrix ($\times 10^{-3}$) - With Constraints

$b_{1x} = -28.150(4)$ $b_{2x} = -1.439(13)$ $b_{3x} = -0.744(22)$
$b_{1y} = -1.462(13)$ $b_{2y} = 27.674(4)$ $b_{3y} = -0.085(18)$
$b_{1z} = 0.207(4)$ $b_{2z} = -0.012(4)$ $b_{3z} = -100.201(13)$

Direct Cell Constants

$a = 35.475$ Å $b = 36.086$ Å $c = 9.979$ Å
$\alpha = 90.00$ $\beta = 90.00^\circ$ $\gamma = 90.00^\circ$

# of cycles required: 48

Table A2 (Continued)

C.) Tetragonal

Compound: Tetragonal Sodium Tungsten Bronze [86]
$Na_{0.48}WO_3$

Input Data:

h	k	ℓ	θ	χ	φ
8	0	0	13.51	55.18	63.98
0	0	4	22.13	31.07	214.18
0	8	0	13.53	14.04	312.91

Orientation Matrix (x 10^{-2}) - No Constraints:

b_{1x} = 2.059 b_{2x} = 5.435 b_{3x} = -18.780
b_{1y} = -4.215 b_{2y} = 5.845 b_{3y} = 12.753
b_{1z} = 6.744 b_{2z} = 1.994 b_{3z} = 13.618

Direct Cell Constants

a = 12.173 Å b = 12.155 Å c = 3.773 Å
α = 89.93° β = 89.95° γ = 89.99°

Orientation Matrix (x 10^{-2}) - With Constraints

b_{1x} = 2.055(6) b_{2x} = 5.427(4) b_{3x} = -18.762(18)
b_{1y} = -4.216(4) b_{2y} = 5.841(5) b_{3y} = 12.756(11)
b_{1z} = 6.749(4) b_{2z} = 1.996(4) b_{3z} = 13.681(9)

Direct Cell Constants

a = 12.167 Å b = 12.167 Å c = 3.772 Å
α = 89.99° β = 90.00° γ = 89.99°

# of cycles required: 48

Table A2 (Continued)

D.) Cubic

Compound: $KCr(SO_4)_2 \cdot 12H_2O$

Input Data:

h	k	ℓ	θ	χ	φ
4	0	0	6.77	335.21	45.57
8	2	0	13.87	6.95	37.74
0	6	0	10.11	56.03	322.87
0	0	6	10.03	33.31	132.48

Orientation Matrix (x 10^{-2}) - No Constraints

$b_{1x} = 5.606$ $b_{2x} = 3.705$ $b_{3x} = -4.608$
$b_{1y} = -5.719$ $b_{2y} = 2.737$ $b_{3y} = -5.033$
$b_{1z} = -1.293$ $b_{2z} = 7.066$ $b_{3z} = 4.484$

Direct Cell Constants

$a = 12.359$ Å $b = 11.875$ Å $c = 12.259$ Å
$\alpha = 90.56^\circ$ $\beta = 87.57^\circ$ $\gamma = 86.65^\circ$

Orientation Matrix (x 10^{-2}) - With Constraints

$b_{1x} = 5.73(46)$ $b_{2x} = 3.85(44)$ $b_{3x} = -4.46(41)$
$b_{1y} = -5.78(41)$ $b_{2y} = 2.44(49)$ $b_{3y} = -5.31(48)$
$b_{1z} = -1.17(38)$ $b_{2z} = 6.84(42)$ $b_{3z} = 4.40(50)$

Direct Cell Parameters

$a = 12.167$ Å $b = 12.167$ Å $c = 12.167$ Å
$\alpha = 90.03^\circ$ $\beta = 89.08^\circ$ $\gamma = 89.97^\circ$

# of cycles required: 61

Table A2 (Continued)

E.) Hexagonal

Compound: Niobium Sulfide

Input Data:

h	k	ℓ	θ	χ	ϕ
3	0	0	43.33	16.78	139.92
0	0	12	27.52	13.76	-68.37
0	3	0	43.32	-3.30	197.21

Orientation Matrix - No Constraints

$b_{1x} = -.2536$ $b_{2x} = -.3301$ $b_{3x} = -.0031$
$b_{1y} = -.2135$ $b_{2y} = .1022$ $b_{3y} = -.0203$
$b_{1z} = -.1000$ $b_{2z} = -.0199$ $b_{3z} = -.0518$

Direct Cell Constants

$a = 3.334$ Å $b = 3.335$ Å $c = 17.933$ Å
$\alpha = 90.05^{\circ}$ $\beta = 89.84^{\circ}$ $\gamma = 119.98^{\circ}$

Orientation Matrix With Constraints

$b_{1x} = -.2536(2)$ $b_{2x} = -.3302(3)$ $b_{3x} = -.0032(1)$
$b_{1y} = -.2135(3)$ $b_{2y} = .1022(3)$ $b_{3y} = -.0204(1)$
$b_{1z} = -.0997(2)$ $b_{2z} = -.0198(2)$ $b_{3z} = -.0518(1)$

Direct Cell Constants

$a = 3.335$ Å $b = 3.335$ Å $c = 17.933$ Å
$\alpha = 89.97^{\circ}$ $\beta = 89.98^{\circ}$ $\gamma = 120.00^{\circ}$

Table A2 (Continued)

F.) Trigonal

Compound: Niobium Sulfide (reindexed on trigonal cell)

Input Data:

h	k	ℓ	θ	χ	ϕ
2	$\bar{1}$	$\bar{1}$	43.33	16.78	139.92
4	4	4	27.52	13.76	-68.37
1	1	$\bar{2}$	43.32	-3.30	197.21

Orientation Matrix - No Constraints

b_{1x} = -.2566 b_{2x} = -.0797 b_{3x} = .3270
b_{1y} = -.2338 b_{2y} = .2954 b_{3y} = -.1225
b_{1z} = .0481 b_{2z} = -.1717 b_{3z} = -.0319

Direct Cell Constants

a = 6.285 Å b = 6.276 Å c = 6.279 Å
α = 30.80° β = 30.79° γ = 30.78°

Orientation Matrix With Constraints

b_{1x} = -.2568(3) b_{2x} = -.0799(4) b_{3x} = .3270(4)
b_{1y} = -.2339(4) b_{2y} = .2954(4) b_{3y} = -.1226(4)
b_{1z} = .0479(3) b_{2z} = -.1713(4) b_{3z} = -.3202(3)

Direct Cell Constants

a = 6.278 Å b = 6.279 Å c = 6.281 Å
α = 30.79° β = 30.79° γ = 30.80°

deviations serve as an indicator of the accuracy of the orientation matrix. They can also be used along with the refined matrix elements themselves to directly calculate accurate lattice constants, thus eliminating the need for any additional refinement. A further advantage over the method of Shoemaker and Bassi[79] arises from the inclusion of the constraint equations as additional observational equations. As a result the number of normal equations (9) remains unchanged. On the other hand the method of Shoemaker and Bassi involves the use of Lagrangian undetermined multipliers which leads to 9+n equations in 9+n unknowns (n = # constraints).

The major disadvantage of the constrained least-squares method arises from the approximation that the constraints are not exact. This, coupled with the dropping of the higher order terms in the Taylor series expansion, results in the necessity of running several least-squares cycles. The actual number of cycles required is dependent on the crystal class of the compound under study and the accuracy of the initial orientation matrix. In general the number is fairly high, usually ranging from 30 to 70 cycles. However as these calculations are generally carried out using a computer, this should not be a serious problem.

The constrained least-squares method has been incorporated into our data collection routine for some

time, and has been used to obtain the orientation matrix for a wide variety of compounds. In all cases the cell parameters calculated from the orientation matrix obtained by the constrained least-squares method have shown improvement over those obtained from the unconstrained refinement. In order to obtain some idea of the accuracy of these calculated lattice constants, some preliminary tests were carried out on data taken on the compound $Zr(H_2PO_2)\cdot H_2O$, which crystallizes in a monoclinic cell. A set of tuned standards were input into the constrained least-squares routine. From the orientation matrix and standard deviations which resulted, a set of lattice constants and their associated standard deviations were calculated. These were compared with lattice constants calculated from the same set of standards using a cell refinement program similar to that developed by Busing and Levy[78]. Upon comparison, the standard deviations were found to be the same order of magnitude, while the lattice constants were found to agree within the calculated error limits.

In conclusion, the constrained least-squares method has been shown to be a simple and straightforward method to obtain a more accurate crystal orientation matrix.